TECHNISCHE UNIVERSITÄT MÜNCHEN

Wissenschaftszentrum Weihenstephan für Ernährung, Landnutzung und Umwelt

Lehrstuhl für Experimentelle Genetik

REGULATION OF MYOKINES IN EXERCISING HUMAN SKELETAL MUSCLE CELLS OBTAINED FROM PHENOTYPED DONORS

Mika Scheler

Vollständiger Abdruck der von der Fakultät Wissenschaftszentrum Weihenstephan für Ernährung, Landnutzung und Umwelt der Technischen Universität München zur Erlangung des akademischen Grades eines

Doktors der Naturwissenschaften

genehmigten Dissertation.

Vorsitzender: Univ.-Prof. Dr. M. Klingenspor

Prüfer der Dissertation:
1. Univ.-Prof. Dr. M. Hrabé de Angelis
2. Univ.-Prof. Dr. J. J. Hauner

Die Dissertation wurde am 26.01.2015 bei der Technischen Universität München eingereicht und durch die Fakultät Wissenschaftszentrum Weihenstephan für Ernährung, Landnutzung und Umwelt am 20.05.2015 angenommen.

Für

Ana & Duschdala

Table of contents

Publications

Publications related to this thesis in peer reviewed journals

Scheler, M., M. Hrabé de Angelis, H. Al-Hasani, H.U. Häring, C. Weigert, and S. Lehr. 2015. Methods for proteomics based analysis of the human muscle secretome using an *in vitro* exercise model. *Methods in Molecular Biology*: in press.

Hartwig, S., S. Raschke, B. Knebel, M. Scheler, M. Irmler, W. Passlack, S. Muller, F.G. Hanisch, T. Franz, X. Li, H.D. Dicken, K. Eckardt, J. Beckers, M. Hrabé de Angelis, C. Weigert, H.U. Häring, H. Al-Hasani, D.M. Ouwens, J. Eckel, J. Kotzka, and S. Lehr. 2014. Secretome profiling of primary human skeletal muscle cells. *Biochimica et biophysica acta*. 1844:1011-1017.

Scheler, M., M. Irmler, S. Lehr, S. Hartwig, H. Staiger, H. Al-Hasani, J. Beckers, M. Hrabé de Angelis, H.U. Haring, and C. Weigert. 2013. Cytokine response of primary human myotubes in an *in vitro* exercise model. *American journal of physiology. Cell physiology*. 305:C877-886.

Wolf, M., S. Chen, X. Zhao, M. Scheler, M. Irmler, H. Staiger, J. Beckers, M. Hrabé de Angelis, A. Fritsche, H.U. Häring, E.D. Schleicher, G. Xu, R. Lehmann, and C. Weigert. 2013. Production and release of acylcarnitines by primary myotubes reflect the differences in fasting fat oxidation of the donors. *The Journal of clinical endocrinology and metabolism.* 98:E1137-1142.

Further publications in peer reviewed journals

Staiger, H., A. Böhm, M. Scheler, L. Berti, J. Machann, F. Schick, F. Machicao, A. Fritsche, N. Stefan, C. Weigert, A. Krook, H.U. Häring, and M. Hrabé de Angelis. 2013. Common genetic variation in the human FNDC5 locus, encoding novel muscle-derived 'browning' factor irisin, determines insulin sensitivity. *PloS one.* 8:e61903.

Poster and oral presentations related to this thesis

Scheler, M., M. Irmler, S. Lehr, S. Hartwig, H. Staiger, H. Al-Hasani, J. Beckers, M. Hrabé de Angelis, H.U. Häring, C. Weigert.
An *in vitro* exercise model: regulation of the transcriptome and secretome of human muscle cells.
DZD satellite workshop Tübingen 2014, poster presentation.

Scheler, M., M. Irmler, S. Lehr, S. Hartwig, H. Staiger, H. Al-Hasani, J. Beckers, M. Hrabé de Angelis, H.U. Häring, C. Weigert.
An *in vitro* exercise model: regulation of the transcriptome and secretome of human muscle cells.
IR 2013, XII International symposium on insulin receptors and insulin action, Barcelona, poster presentation.

Scheler, M., M. Irmler, S. Lehr, S. Hartwig, H. Staiger, H. Al-Hasani, J. Beckers, M. Hrabé de Angelis, H.U. Häring, C. Weigert.
Ausdauersport im Zellmodell: Regulation des Transkriptoms und Sekretoms humaner Muskelzellen.
48. Jahrestagung der Deutschen Diabetes-Gesellschaft DDG, 2013, Leipzig, oral presentation.

Scheler, M., M. Irmler, S. Lehr, J. Beckers, L. Berti, H. Staiger, H.U. Häring, M. Hrabé de Angelis, C. Weigert.
Exercising skeletal muscle cells: EPS as a model to study exercise *in vitro*.
Interact 2013, Munich, poster presentation.

Scheler, M., A. Böhm, H. Staiger, H.U. Häring, M. Hrabé de Angelis, C. Weigert.
EPS as a model to study molecular mechanisms of adaptation to exercise.
DZD satellite workshop Tübingen 2012, poster presentation.

Abbreviations

2D-DIGE	Two dimensional difference gel electrophoresis
AC	Acylcarnitine
AGPTL4	Angiopoitin like 4
Akt	RAC-alpha serine/threonine-protein kinase
AMPK	AMP-activated protein kinase
AP-1	Activator protein-1
ATP	Adenosine triphosphate
BMI	Body mass index
BSA	Bovine serum albumin
Ca^{2+}	Calcium
CaMK	Calmodulin-dependent kinase
cDNA	Complementary DNA
CK	Creatine kinase
CO_2	Carbon dioxide
COX IV	Cytochrom c oxidase IV
CPT1	Carnitine palmitoyltransferase 1
CXCL1	Growth-regulated alpha protein
CytC	Cytochrom c
DMSO	Dimethylsulfoxid
dNTPs	Desoxynucleotide
ECM	Extracellular matrix
ELISA	Enzyme-linked immunosorbent assay
EPS	Electric pulse stimulation
ERK	Extracellular-signal-regulated kinases
ERR-α	Estrogen-related receptor-α
ESI	Electrospray ionization
FBS	Fetal bovine serum
FC	Flow cytometry
FDR	False discovery rate
FFA	Free fatty acid
g	Centrifugal force
GO	Gene ontology
H_2O	Water
HIF	Hypoxia-inducible factor
HPLC	High-performance liquid chromatography
Hz	Hertz

3

IEF	Isoelectric focusing
IL	Interleukin
IMTG	Intramuscular triglycerides
IPG	Immobilized pH gradient
IR	Insulin-resistant
IS	Insulin-sensitive
ISI-MATS	ISI Matsuda index
JNK	c-Jun N-terminal kinases
LC	Lightcycler
LC	Liquid chromatography
LC	Long-chain
LDH	Lactate dehydrogenase
LIF	Leukemia inhibitory factor
LPC	Lysophosphatidylcholine
LTQ	Linear ion-trap quadrupole
MACS	Magnetic activated cell sorting
MALDI	Matrix-assisted laser desorption/ionization
MAPK	Mitogen-activated protein kinase
MC	Medium-chain
MEF2	Myocyte enhancer factor-2
MeOH	Methanol
Mg^{2+}	Magnesium
MMA	Methylmalonic aciduria
MMP	Matrix metallopeptidase
MS	Mass spectrometry
MT	Metallotheionein
MT	Myotube
mTor	Mammalian target of rapamycin
MYOD	Myoblast determination protein 1
NAD	Nicotinamide adenine dinucleotide
NAMPT	Nicotinamide phosphoribosyltransferase
NFAT	Nuclear factor of activated T cells
NFκB	Nuclear factor kappa-light-chain-enhancer of activated B cells
NP	Non-secreted protein
NRF	Nuclear-respiratory factor-1
OXPHOS	Oxidative phosphorylation
p70S6K1	Ribosomal protein S6 kinase β1
PA	Propionic aciduria
PBS	Phosphate buffered saline

PGC1α	Peroxisome proliferator-activated receptor gamma coactivator 1-alpha
PKC	Protein kinase C
PPAR	Peroxisome proliferator-activated receptor
PSMA	Proteasomal subunit A
PSMB	Proteasomal subunit B
qRT-PCR	Quantitative Real-time PCR
ROS	Reactive oxygen species
SC	Short-chain
SDS-PAGE	Sodium dodecyl sulfate polyacrylamide gel electrophoresis
SEM	Standard error of the mean
Ser	Serine
SIRT1	Sirtuin-1
SN	Supernatant
SP+	Classical protein secretion
SP-	Nonclassical protein secretion
SPARC	Secreted protein acidic and rich in cysteine
T1D	Type 1 diabetes
T2D	Type 2 diabetes
TAG	Triacylglycerol
TFAM	Transcription factor A, mitochondrial
Thr	Threonine
TUEF	Tuebingen family study
TULIP	Tuebingen lifestyle intervention program
Tyr	Tyrosine
UPLC	Ultra performance lipid chromatography
V	Voltage
VEGF	Vascular endothelial growth factor
WHO	World health organization

Summary

Skeletal muscle is a secretory organ, releasing several hundreds of proteins, the so-called myokines, which can work in hormone-like fashion, having endocrine and paracrine effects. Although the underlying molecular mechanisms are mostly unclear, it was proposed that exercise-regulated myokines play a major role in the health-promoting effects of exercise including the prevention and treatment of type 2 diabetes. However, the knowledge on myokines and their expression and release, especially upon contraction-induced activation of intramuscular signaling cascades, is scarce to date.

Electric pulse stimulation (EPS), an *in vitro* exercise model, was applied to human primary myotubes of phenotyped donors to investigate molecular adaptations of exercise in a clearly defined system.

24 h of EPS induced a metabolic switch towards higher glucose consumption. Additionally, the study of the whole genome transcriptional response revealed 183 significantly regulated transcripts with a fold change > 1.3. Changes in transcription reflect partially the *in vivo* situation in the skeletal muscle after endurance exercise, modulating pathways associated with chemokine and cytokine signaling, lipid metabolism and antioxidant defense. Targeted proteomic analysis of the supernatant by multiplex immunoassay, verified the enhanced secretion of EPS-induced cytokines, such as IL-6, IL-8, CXCL1 and LIF, as well as other myokines, e.g. ANGPTL4. Inhibitor studies and immunoblotting indicated the involvement of ERK1/2-, JNK- and NFκB-dependent pathways in the upregulation of these myokines.

Secretome profiling by untargeted proteomic analysis showed several significantly altered proteins upon 24 h of EPS in the conditioned supernatant, namely significant enrichment of pathways associated with skeletal muscle development, cell proliferation, extracellular matrix organization and disassembly. Unbiased proteomic investigation of the supernatant obtained from human myotubes derived from insulin-sensitive (IS) and resistant (IR) donors showed also differences in secretome composition whereas the enhanced release of proteasomal subunits from IR-myotubes was most strikingly.

Additionally, we developed our EPS protocol further including a recovery phase and the supplementation of physiological concentrations of fatty acids (oleic acid and palmitic acid) and applied it to IS- and IR-myotubes. Targeted metabolomic analysis of the intramyocellular acylcarnitine pattern indicated increased production of propionylcarnitine in IR-myotubes.

To conclude, the results obtained within this thesis highlight the importance of the muscle as a secretory organ. Moreover, we provide further evidence that EPS induced adaptations at least partially reflects *in vivo* exercise situation and thus could underline the importance of this *in vitro* exercise model for future studies. This might provide broader insights into contraction-induced adaptations in the skeletal muscle, which are of particular interest when investigating myotubes of donors with different phenotype, e.g. insulin resistance, type 2 diabetes or non-response to exercise intervention.

Zusammenfassung

Der Skelettmuskel ist ein sekretorisches Organ. Es wird vermutet, dass er mehrere hundert Proteine, die sogenannten Myokine, sekretiert, welche hormonähnliche Funktionen haben können und parakrin, bzw. endokrin wirken.

Es wird eine Beteiligung dieser Myokine an den durch Sport induzierten, gesundheitsförderlichen Prozessen vermutet, wie etwa bei der Prävention und Therapie von Typ 2 Diabetes. Die zugrundeliegenden molekulare Mechanismen sind jedoch weitgehend unbekannt. Ebenso ist die Regulation der Expression und Freisetzung dieser Myokine, speziell während der Muskelkontraktion, noch nicht im Detail verstanden.

Electric pulse stimulation (EPS), ein *in vitro* Sportmodell, wurde auf humane primäre Myotuben von phänotypisierten Donoren angewandt, um die durch Sport regulierten, molekularen Veränderungen in einem definierten System zu untersuchen.

24 h EP-Stimulation führte in diesem Zellkulturmodell zu einem erhöhten Energieverbrauch, messbar als vermehrter Glucosebedarf. Eine Gesamt-genomtranskriptomanalyse zeigte eine signifikante Veränderung von 183 Transkripten (Ratio > 1.3). Die erhaltenen Ergebnisse spiegelten teilweise die *in vivo* gefundenen Expressionsveränderungen nach Ausdauersport wider, da unter anderem Gene, der Cytokin und Chemokin Signaltransduktionswege, des Lipidstoffwechsels und des Antioxidationsschutzes reguliert wurden.

Eine gerichtete Proteomanalyse des Zellkulturüberstands mit Hilfe eines Multiplex Immunassays verifizierte die durch EPS induzierte, vermehrte Freisetzung von Cytokinen, wie IL-6, IL-8, CXCL1 und LIF, als auch anderer Myokine, z.B. ANGPTL4. Inhibitorstudien und Western Blot Analysen ergaben, dass die MAPK ERK 1/2 und JNK, sowie der Transkriptionsfaktor NFκB wichtige Mediatoren bei der Regulation dieser Myokine sind.

Die ungerichtete Proteomanalyse des Myotubensekretoms zeigte mehrere signifikant regulierte Proteine, die mit der Skelettmuskelentwicklung, Zellproliferation, Extrazellulärmatrixorganisation und –abbau assoziiert sind. Der Vergleich des Sekretoms von Myotuben, die von insulinsensitiven (IS), bzw. insulinresistenten (IR) Probanden gewonnen wurden, ergab auch mehrere signifikant veränderte Proteine, wobei die erhöhte Freisetzung von proteasomalen Untereinheiten durch IR-Myotuben besonders auffällig war.

Darüber hinaus wurde das EPS Protokoll weiterentwickelt und physiologische Konzentrationen von Fettsäuren (Ölsäure und Palmitinsäure) dem Medium zugesetzt, sowie nach der Stimulation eine Erholungsphase für die Zellen

angeschlossen. Dieses Protokoll wurde auf IS- und IR-Myotuben angewandt und die intrazelluläre Acylcarnitinzusammensetzung mittels LC-MS Metabolomics Analyse untersucht. Hierbei zeigte sich eine erhöhte Produktion von Propionylcarnitin in IR-Myotuben.

Zusammenfassend unterstreichen die Ergebnisse dieser Arbeit die Signifikanz des Muskels als sekretorische Einheit. Wir konnten außerdem zeigen, dass die durch EPS induzierten Veränderungen, jedenfalls teilweise, die *in vivo* Situation im Muskel während der Kontraktion widerspiegeln und damit die Wichtigkeit dieses *in vitro* Sportmodells für zukünftige Studien hervorheben. Dies könnte wichtige Erkenntnisse bezüglich der durch Kontraktion induzierten Veränderungen im Muskel liefern, welche besonders bei der Untersuchung der Myotuben von Donoren mit unterschiedlichen Phänotypen, z.B. bei Insulinresistenz, Typ 2 Diabetes oder Nonresponse auf eine Sportintervention, von großer Relevanz sein könnten.

1. Introduction

1.1 Skeletal muscle

Vertebrate muscles are divided in three different types defined by functional and structural properties: smooth, cardiac and skeletal muscle. The first one, is an involuntary and unstriated muscle found in walls of organs e.g. of the gastrointestinal tract, in blood vessels and the eye (Newsholme and Leech, 2010). Cardiac muscle, which is found exclusively in the heart propelling blood, has high endurance capacity and is also involuntary (Newsholme and Leech, 2010). The third and most common form is the skeletal muscle, a voluntarily and striated muscle type, that will be further discussed in detail in the following part.

1.1.1 Function and structure of the skeletal muscle

The human body contains approximately 600 different skeletal muscles accounting for approximately 40 % of total body mass in non-obese people, consequently being the biggest tissue in humans (Newsholme and Leech, 2010). Furthermore, it constitutes for approximately 30 % of the total metabolic rate (Zurlo et al., 1990) and is the predominant site for insulin-dependent glucose uptake (DeFronzo et al., 1981). Skeletal muscle has several functions including movement of the body, maintaining posture, storage of fuel as glycogen and triglycerides and generation of heat to maintain body temperature (Johnson et al., 2004; Newsholme and Leech, 2010; Frontera and Ochala, 2014; Rowland et al., 2014).

It is composed of muscle fibers, connective tissue, blood vessels and nerves. The complete muscle consists of several bundles of muscle fibers, which join into a tendon at each end and thus connect it to the bone (Figure 1). Each fiber has developed by the fusion of several myoblasts to long, cylindrical, multinucleated, post-mitotic myotubes and is packed with myofibrils. These consist of thousands of myofilaments, which are composed mainly of actin and myosin building up the sarcomere. This is the basic contractile unit of the skeletal muscle, whereas myosin is the main molecular motor (Newsholme and Leech, 2010).
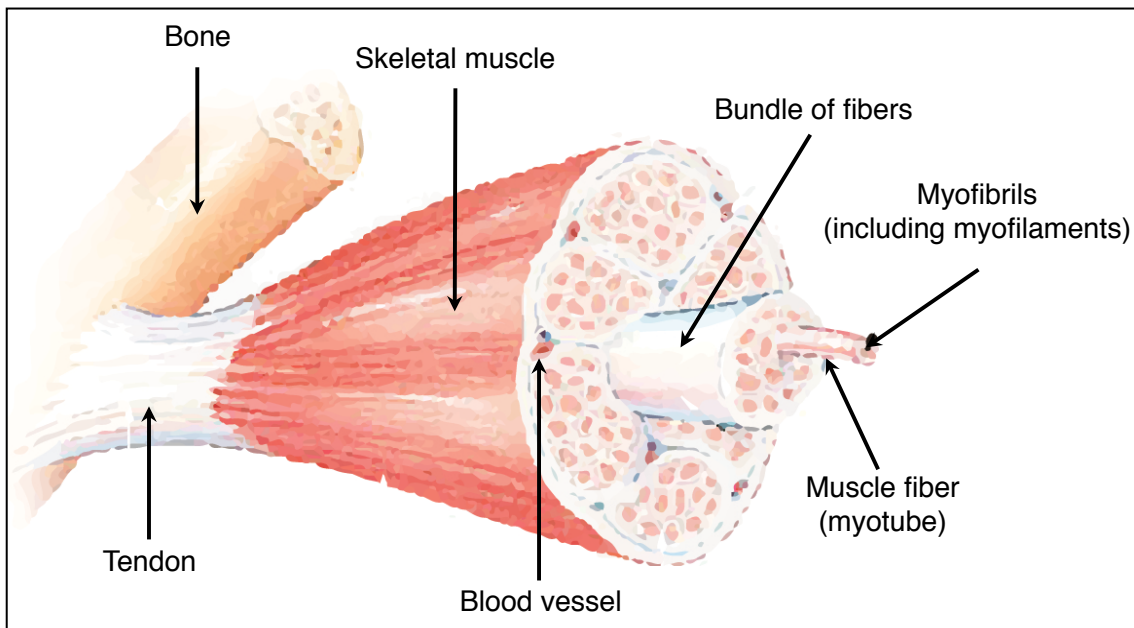
Figure 1: The arrangements of bundles, fibers and capillaries in the skeletal muscle.
Skeletal muscle consists of several bundles of fibers, which join in the tendon that is connected to the bone. See text for details. Modified from Lauritzen and Schertzer (Lauritzen and Schertzer, 2010).

The force generation and the movement of the muscle are achieved by actin sliding over myosin myofilaments to shorten sarcomeres postulated as sliding filament theory (Huxley and Niedergerke, 1954; Huxley and Hanson, 1954). The signal for contraction comes from adjacent motor neurons, passing the action potential to the muscle fiber, leading to its membrane depolarization and the induction of Ca^{2+} transients. The increased sarcoplasmic Ca^{2+} concentration activates then the sarcomeres, resulting in muscle contraction. All together, an electric signal is converted to a mechanical response called excitation-contraction coupling as recently reviewed by Rebbeck and colleagues (Rebbeck et al., 2014).

Depending on the demands of the muscle, it is capable to develop different fiber types, having diverse properties, morphology and metabolic/substrate preferences (Table 1). In humans, the predominant fiber types are: slow twitch (type I), fast/oxidative twitch (type IIA) and fast/glycolytic twitch (type IIX) fibers (Table 1). In rodents a fourth and more common fiber type than IIX, type IIB, exists. The different fiber types in mammalian skeletal muscles were recently reviewed by Schiaffino and Reggiani (Schiaffino and Reggiani, 2011).

Table 1: Contractile, metabolic and morphological properties of human skeletal muscle fibers.

	Type I	Type IIA	Type IIX
General properties			
Myosin heavy-chain isoform	MHC1	MHC2A	MHC2X
Metabolism	High oxidative	Oxidative-glycolytic	Glycolytic
Myosin ATPase Activity	Slow	Fast	Fast
Fatigue Resistance	High	Intermediate	Low
Force production (power output)	Weak	Intermediate	Strong
Endurance capacity	High	Intermediate	Low
Appearance/ myoglobin content	Red/high	Red/intermediate	White/low
Morphological properties			
Capillary density	4.2	4.0	3.2
Mitochondrial density	High	Intermediate	Low
Fiber size (cross sectional area) [a]	5310	6110	5600
Metabolic and substrate properties			
Oxidative potential	High	Intermediate-high	Low
Glycolytic potential	Low	Intermediate-high	High
[Phosphocreatine] [b]	12.6	14.5	14.8
[Glycogen] [b]	77.8	83.1	89.2
[IMTG] [b]	7.1	4.2	
Exercise-type dominance	Prolonged low, intensity	Moderate duration, high-intensity	Short duration, maximal effort

Relationship between skeletal muscle fiber type and the indicated properties. Data obtained from vastus lateralis muscle of untrained men. Adapted from Egan & Zierath and Saltin & Gollnick (Saltin and Gollnick, 1983; Egan and Zierath, 2013).
[a] μm^2
[b] mmol kg^{-1} wet weight

1.1.2 Exercise-induced adaptations

1.1.2.1 Exercise modalities

Skeletal muscle is a rather dynamic tissue, e.g. adapting during exercise either acutely as during a single bout of exercise or leading to long-term training-induced adaptations.

Two modalities of exercise are distinguished: (1) During resistance exercise (strength training; e.g. weight lifting, bodybuilding, throwing events) the skeletal muscle undergoes less repeats with a high load leading to muscle hypertrophy. Carbohydrates are the major energy source, metabolized in the glycolytic, type II fibers (Egan and Zierath, 2013). (2) A high repetition number with a low load resulting in an increased cardiovascular fitness characterizes endurance (cardiovascular or aerobic) exercise training like achieved walking, running, swimming and bicycling. This results in a fiber type switch towards more oxidative type I fibers leading to muscles with higher oxidative capacity (Egan and Zierath, 2013). The adaptations and health-promoting effects of both types of exercise training are summarized in Table 2.

Table 2: Adaptations and health-promoting effects of endurance in comparison with resistance exercise.

	Endurance exercise	Resistance exercise
Skeletal muscle morphology and exercise performance		
Muscle hypertrophy	0	+ + +
Muscle power and strength	0 -	+ + +
Muscle fiber size	0 +	+ + +
Anaerobic capacity	+	+ +
Myofibrillar protein synthesis	0 +	+ + +
Mitochondrial protein synthesis	+ +	0 +
Capillarity	+ +	0
Mitochondrial density and oxidative function	+ + +	0 +
Endurance capacity	+ + +	0 +
Whole-body and metabolic health		
Percent body fat	- -	-
Lean body mass	0	+ +
Resting insulin levels	-	-
Insulin response to glucose challenge	- -	- -
Insulin sensitivity	+ +	+ +
Inflammatory markers	- -	-
Resting heart rate	- -	0
Cardiovascular risk profile	- - -	-
Basal metabolic rate	+	+ +

Endurance exercise: exercise duration of several minutes to hours at various exercise intensities, consisting of many repetitions with low load (e.g. running, swimming and cycling); Resistance exercise: short duration exercise with high or maximal intensity (e.g. Olympic weightlifting, bodybuilding, throwing events); +: values increase, -: values decrease, 0: values remain unchanged; amount of signs: small effect (+/-), medium effect (++/--), large effect (+++/---); 0+/0-: no change or slight change. Table adapted of Egan & Zierath (Egan and Zierath, 2013).

Moreover, two types of contraction are described: (1) Isomeric, also known as static contraction, generates force without bowing joints and limbs, e.g. holding a weight in front of the body without changing level; (2) Dynamic contraction is divided in concentric contraction leading to a shortening of the muscle (e.g. bowing the elbow), and eccentric action leading to an extension of the muscle (e.g. when a weight is lifted down starting with a bowed elbow) (Frontera and Ochala, 2014).

1.1.2.2 Energy sources during exercise

Muscle contraction itself needs energy in form of adenosine triphosphate (ATP). Depending on fiber type, amount of fuel stored, transport of fuel to the muscle, availability of oxygen, intensity and duration of exercise fuel preferences differ. The muscle itself has ATP and phosphocreatine stores, which are used during short duration and high-intensity exercise. During longer periods of exercise, muscle uses either intracellular glycogen, which is metabolized to lactic acid or CO_2 or uses glucose obtained from hepatic gluconeogenesis or glycogenolysis. Moreover, muscle breaks down intramuscular triglycerides (IMTGs) to provide fatty acids for oxidation. Even more important are extramuscular long chain fatty acids obtained from lipolysis in adipose tissue (Newsholme and Leech, 2010; Egan and Zierath, 2013).

1.1.2.3 Intramuscular signaling

Muscle contraction leads to neuronal, metabolic and mechanical signals, which activate downstream sensors, modifying transcription, translation and protein modifications. This results in altered quantity, activity and localization of proteins as recently reviewed (Fluck, 2006; Hoppeler et al., 2011; Egan and Zierath, 2013). A simplified and not complete scheme of the most important signaling molecules involved in these cascades is shown in Figure 2.

During endurance exercise, the major signals are increased Ca^{2+} levels and metabolic changes as energy depletion resulting in mitochondrial biogenesis, angiogenesis and slow fiber transformation.

Elevated Ca^{2+} levels due to neuronal-induced Ca^{2+} transients activate calmodulin, initiating calmodulin-dependent kinases (CaMK) in an intensity-dependent fashion (Rose and Hargreaves, 2003; Rose et al., 2006). These serine-threonine kinases regulate amongst others transcription and activation of peroxisome proliferator-activated receptor gamma coactivator 1-alpha (PGC1α) and nuclear factor of activated T cells (NFAT). Additionally, protein kinase C (PKC) and AMP-activated protein kinase (AMPK) are activated upon elevated Ca^{2+} levels (Nielsen et al., 2003; Hoppeler et al., 2011).

Metabolic changes, like increased levels of free fatty acids (FFA) obtained from lipolysis activate peroxisome proliferator-activated receptors (PPARs) promoting the transcription of genes involved in fatty acid uptake, transport and oxidation (Fluck, 2006; Hoppeler et al., 2011). Reduced intracellular oxygen (O_2) activates hypoxia-inducible factor (HIF), a transcription factor involved in the regulation of genes involved in angiogenesis, glycolysis and energy metabolism (Ameln et al., 2005). AMPK, a multimeric serine/threonine kinase and important energy sensor, is activated upon ATP depletion, resulting in the repression of anabolic processes like

protein- and lipid biosynthesis and the stimulation of catabolic pathways, e.g. glucose and lipid uptake and its oxidation, enabling a shift of ATP towards production not usage (Fujii et al., 2000; Wojtaszewski et al., 2000; Kahn et al., 2005).

Exercise increases intramuscular reactive oxygen species (ROS) during oxidative phosphorylation in the mitochondria or by xanthine oxidase as reviewed by Sachdev and Davies (Sachdev and Davies, 2008). This results in an activation of nuclear factor kappa-light-chain-enhancer of activated B cells (NFκB), a transcription factor inducing the transcription of cytokines and ROS protective enzymes. Furthermore, mitogen-activated protein kinases (MAPK) and activator protein-1 (AP-1) have been shown to be redox-sensitive and involved in the regulation of the ROS protective system. In addition, the activation of MAPK, in particular ERK1/2, p38 MAPK and JNK, have been shown to be dependent on the intensity of the metabolic stress and the tension (Boppart et al., 1999; Widegren et al., 2000; Widegren et al., 2001; Yu et al., 2001).

During resistance exercise the increased tension is the major stimulus known so far, activating mammalian target of rapamycin (mTOR), a serine/threonine kinase involved amongst others in the regulation of cell proliferation, cell growth, differentiation, and protein synthesis. The major downstream target of mTOR is ribosomal protein S6 kinase β-1 (p70S6K1) promoting translation initiation and elongation essential for muscle hypertrophy (Dreyer et al., 2006; Terzis et al., 2008).

Overall, these signaling pathways result in exercise-induced changes including altered glucose and fatty acid metabolism, angiogenesis, mitochondrial biogenesis and muscle hypertrophy.
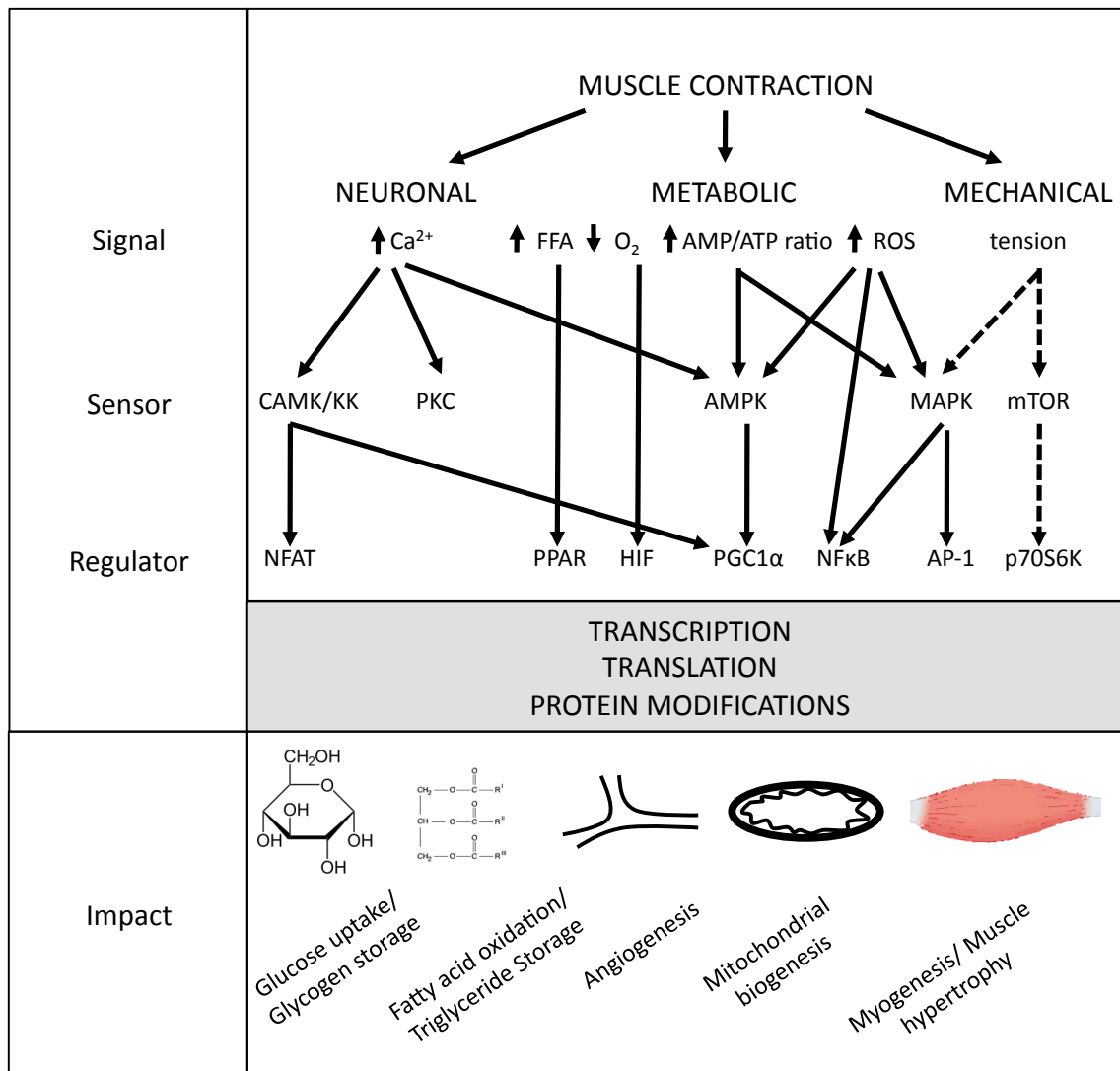
Figure 2: Exercise-induced intramuscular signaling and its impact on muscle adaptations.
Muscle contraction leads to neuronal, metabolic and mechanical signals, which activate downstream sensors. This results in altered quantity, activity and localization of regulators, modifying overall transcription, translation and protein modifications and leading to altered glucose and fatty acid metabolism, increased capillarity, mitochondrial biogenesis and muscle hypertrophy. Dashed arrows indicate signaling that occurs during resistance exercise, while continuous arrows indicate endurance exercise-induced signaling. See text for further details.

1.1.2.4 PGC1α: a major player in exercise-induced alterations

The transcriptional coregulator peroxisome proliferator-activated receptor gamma coactivator 1-alpha (PPARGC1A, also known as PGC1α) plays a major role in the exercise-induced alterations like fiber type switching (Lin et al., 2002), angiogenesis (Arany et al., 2008), improved metabolic flexibility (Michael et al., 2001) and exercise performance (Calvo et al., 2008). Moreover, PGC1α is the major player in mitochondrial biogenesis, a very complex process including the expression of genes encoded in the nucleus as well as in the mitochondria.

On the one hand, PGC1α interacts with nuclear-respiratory factor-1 (NRF-1), nuclear-respiratory factor-2 (NRF-2) and estrogen-related receptor-α (ERR-α) (Wu et al., 1999; Huss et al., 2002), all transcription factors mediating the transcription of

nuclear-encoded genes. On the other hand, PGC1α activates mitochondrial transcription factor A (TFAM), which regulates mitochondrial-encoded genes.

Exercise-increased PGC1α expression and activity is regulated by several mechanisms already introduced in section 1.1.2.3. AMPK phosphorylates histone deacetylases, leading to nuclear export and subsequent derepression of PGC1α (McGee et al., 2009). Furthermore, AMPK itself is capable to phosphorylate PGC1α (Jager et al., 2007) urgent for the SIRT1-mediated deacetylation of PGC1α and thus leading to the upregulation of PGC1α target genes like cytochrom C (CytC), cytochrom C oxidase IV (COX IV) and carnitine palmitoyltransferase 1B (CPT1B) (Canto et al., 2009). MAPK p38 is also activated during exercise and phosphorylates PGC1α (Puigserver et al., 2001) as well as myocyte enhancer factor-2 (MEF2) (Zhao et al., 1999), a transcription factor involved in the expression of PGC1α. Additionally, PGC1α also binds to MEF2 and thus improves its own expression by a feed forward regulatory loop (Handschin et al., 2003). Overall, transcriptional coactivator PGC1α seems to play an important role in the regulation and activation of exercise-induced metabolic processes and adaptations.

1.1.2.5 Extramuscular adaptations

It is well known that endurance exercise training leads to an increased oxidative degradation of fuels like glucose and fatty acids. This is accomplished on the one hand by increased mitochondrial number and density and on the other hand by an improved capillary system. The process in which new capillaries are formed from existing is called angiogenesis, which is achieved by either sprouting or splitting.

Sprouting involves endothelial cell proliferation and basement membrane disruption to form entirely new vessels from sprouts. Splitting or intussusceptive angiogenesis divides preexisting capillaries. The differences between the two types of angiogenesis were recently reviewed (Mentzer and Konerding, 2014).

Vascular endothelial growth factor (VEGF) is the major proangiogenic growth factor involved in exercise-induced angiogenesis (Gustafsson et al., 1999; Richardson et al., 2000; Olfert et al., 2010). In human skeletal muscle, increased *VEGF* mRNA (Gustafsson et al., 1999; Richardson et al., 2000) and protein levels could be measured upon endurance exercise (Gustafsson et al., 2002). The process of this exercise-mediated VEGF induction is still unclear. Recently, Chinsomboon and colleagues proposed that β-adrenergic signaling activates expression of alternative promoters, inducing expression of PGC1α isoforms, which lead to the induction of several proangiogenic factors like VEGF, PDGF-B and ANGPT2 (Chinsomboon et al., 2009).

1.1.3 Human myotubes as cell culture model

Over the last decades, investigation of the muscle itself and its exercise-induced alterations gained in importance. In humans, mechanistic *in vivo* studies are rather difficult to accomplish. Instead, a cell culture model based on human primary skeletal muscle cells has been established. Primary satellite cells, muscle progenitor cells, are isolated from human muscle biopsies, cultivated and differentiated to myotubes. Of note, these cells are still metabolically active showing insulin stimulated glycogen synthesis, glucose and fatty acid oxidation (Weigert et al., 2005; Austin et al., 2008; Wensaas et al., 2009; Bourlier et al., 2013; Wolf et al., 2013). Additionally, we and others demonstrated that myotubes reflect metabolic phenotypes of their donors (Weigert et al., 2005; Wensaas et al., 2009; Ordelheide et al., 2011; Bourlier et al., 2013; Wolf et al., 2013). This *in vitro* model enables the mechanistic study of intracellular signaling pathways, e.g. by siRNA-mediated knock down of certain proteins or the addition of selected fatty acids, in a controlled environment and in the absence of external factors (Austin et al., 2008; Wensaas et al., 2009; Broholm et al., 2011). Overall, this is a valuable tool to study muscle substrate metabolism and alterations.

Human myotubes used within this thesis were obtained from donors included in the Tuebingen lifestyle intervention program (TULIP) and the Tuebingen Family (TÜF) study, both aiming the prevention of type 2 diabetes by exercise- and diet-based lifestyle intervention.

1.2 Exercise & Diabetes

1.2.1 Diabetes mellitus type 2

Diabetes is on the rise, 380 million adults suffer from diabetes worldwide (IDF, 2013) and by the year of 2030 the World health organization (WHO) expects diabetes to become the seventh leading cause of death in the world (WHO, 2011). Diabetes is a chronic metabolic disease, which is marked by hyperglycemia induced by insufficient insulin secretion and reduced insulin sensitivity, respectively. There are two major types of diabetes: Firstly, type 1 diabetes (T1D), which goes along with complete insulin deficiency. Secondly, type 2 diabetes (T2D), which is characterized by a disturbance of insulin secretion but also by increased insulin resistance leading to relative insulin deficiency. Being the most common form of diabetes, it concerns 90% of all diabetic patients worldwide (WHO, 1999).

The importance of insulin resistance and β-cell dysfunction to the pathogenesis of type 2 diabetes was discussed for a long time: it was thought that insulin resistance occurs first and leads to the inability to secrete insulin (Reaven, 1988). Nowadays, it is known that it is most likely a feed back loop that ensures the maintenance of glucose homeostasis and preservation of glucose in a low concentration range (Kahn et al., 1993). This feed back loop depends on the communication between the insulin producing β-cells and the insulin-sensitive tissues like liver, muscle, adipose tissue and probably also the brain (Figure 3). In normal glucose tolerant people, the mechanism starts with the stimulation of the β-cells and the induction of insulin secretion. This leads to an improved uptake of glucose, fatty acids and amino acids by muscle, adipose tissue and suppression of hepatic glucose production. Consequently, insulin-sensitive tissues feed back information to the insulin producing Langerhans islets about their insulin need (Figure 3A). Beyond these peripheral effects of insulin, it has also a central effect on the brain modulating efferent neuronal outputs, which are proposed to regulate peripheral metabolism best described for hepatic glucose production as recently reviewed (Kleinridders et al., 2014).

When insulin-sensitive tissues become more and more insulin-resistant, e.g. due to obesity, β-cells increase their insulin secretion to maintain normal glucose tolerance (Figure 3B). When β-cells are not able to increase insulin output any more, glucose concentration increases, finally leading to an impaired glucose tolerance (prediabetic state) or in worst case to diabetes (Figure 3C). The whole process was recently reviewed by Kahn and colleagues (Kahn et al., 2014).
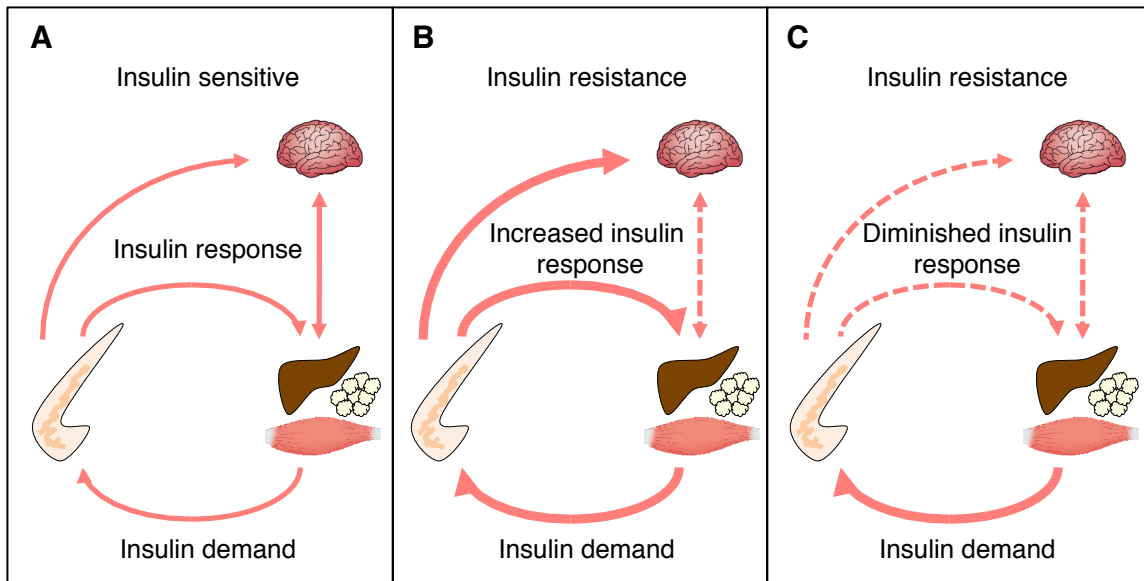
Figure 3: Communication between Langerhans islets β-cells and insulin-sensitive tissue.
(A) Insulin sensitivity is maintained through a feed back loop involving pancreatic β-cells secreting insulin, which impacts liver to suppress glucose production and muscle, adipose tissue and brain to stimulate uptake of glucose, fatty acids and amino acids. It is suggested that humoral and neuronal mechanisms feed back to the pancreas how much insulin has to be produced and secreted. (B) With the development of insulin resistance, insulin-sensitive tissues increase their feed back to the β-cells to produce more insulin and thus to maintain normal glucose tolerance. (C) The glucose concentration increases when the β-cells are unable to increase insulin output any more in the presence of insulin resistance, leading to impaired glucose tolerance. Figure is modified from Kahn and colleagues (Kahn et al., 2014).

Genetic predisposition and the environment play an important role in the development of T2D. Genome-wide association studies revealed so far 90 gene loci associated with type 2 diabetes (Grarup et al., 2014). It is rather unlikely that the altered gene pool is responsible for the tremendous increase of type 2 diabetic patients, thus environmental factors seem to play the major role in the development of this disease.

The increase in body weight due to high-fat and high-caloric intake and a sedentary lifestyle are the most important risk factors. Not least because of that, the WHO advises 30 min of moderate intensity physical activity on most days and a healthy diet (WHO, 2013). Nevertheless, there are also "nontraditional risk factors" like the in-utero environment (Guenard et al., 2013), intestinal microbiome (Diamant et al., 2011), stress (Novak et al., 2013) and environmental chemicals (Thayer et al., 2012) that might be involved in the pathogenesis of type 2 diabetes and are increasingly discussed.

1.2.2 The diseasome of physical inactivity

It is commonly known that physical inactivity not only increases the risk for T2D (Tuomilehto et al., 2001; Knowler et al., 2002) but also for certain cancers (Schmid and Leitzmann, 2014) and cardiovascular diseases (Wei et al., 2000; Hu et al., 2001). Additionally, it is involved in the development of dementia (Rovio et al., 2005) and

depression (Lawlor and Hopker, 2001; Chalder et al., 2012). Several studies have shown that these diseases are also associated between each other. For example, people with T2D have an increased risk for cardiovascular diseases (Wei et al., 2000; Hu et al., 2001; Church et al., 2004) and for developing dementia and depression (Anderson et al., 2001; Mehlig et al., 2014). In addition, type 2 diabetes is an independent risk factor for cancer development as recently reviewed by Joost (Joost, 2014). Also several other overlaps between these diseases exist, however, type 2 diabetes seems to play the major role.

Based on these findings, Bente K. Pedersen proposed the "diseasome of physical inactivity" (Figure 4), a combination of diseases, which are favored by sedentariness consisting of type 2 diabetes, cardiovascular diseases, depression, dementia and certain cancers (Pedersen, 2009; Pedersen, 2011). She proposed that physical inactivity leads to abdominal adiposity, macrophage infiltration and subsequently to chronic systemic inflammation, resulting in insulin resistance, atherosclerosis, neurodegeneration and tumor growth. Finally, this results in the manifestation of diseases included in the "diseasome of physical inactivity", diseases that are characterized by an increasing incidence worldwide (Pedersen, 2009). Thus, this model summarizes the importance of regular exercise for the overall health.
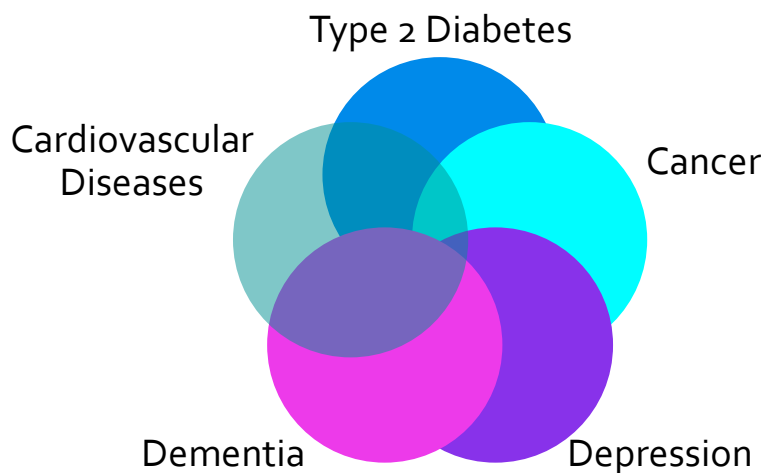
Figure 4: The diseasome of physical inactivity.
Type 2 diabetes, certain cancers, depression, dementia and cardiovascular diseases can be clustered to the "diseasome of physical inactivity", diseases that are associated with sedentariness. Figure modified from Pedersen (Pedersen, 2009).

1.2.3 The myokine concept

Even short periods of sedentary lifestyle lead to metabolic variations like decreased insulin sensitivity, reduction of cardiovascular fitness, loss of muscle mass and accumulation of visceral adipose tissue (Olsen et al., 2008; Krogh-Madsen et al., 2010). For a long time, it was hypothesized that the exercising muscle produces and releases circulating factors, facilitating the communication between the energy-demanding muscle and the energy-supplying organs like liver and adipose tissue (Goldstein, 1961) and might directly or indirectly influence their function. Interleukin-6 (IL-6) was the first discovered "exercise factor", secreted from the muscle into the blood stream upon muscle contraction (Steensberg et al., 2000; Pedersen et al., 2003).

In 2003 Pedersen and colleagues defined cytokines and peptides that are produced, expressed and released by the muscle, acting in endocrine or paracrine fashion, as myokines (Pedersen et al., 2003). Henceforward, the muscle gained in importance as an endocrine organ. By now, the muscle is supposed to secrete several hundreds of proteins and peptides (Bortoluzzi et al., 2006; Yoon et al., 2009; Henningsen et al., 2010). Numerous examples are presented in Figure 5 and will be further discussed in detail in the following part.
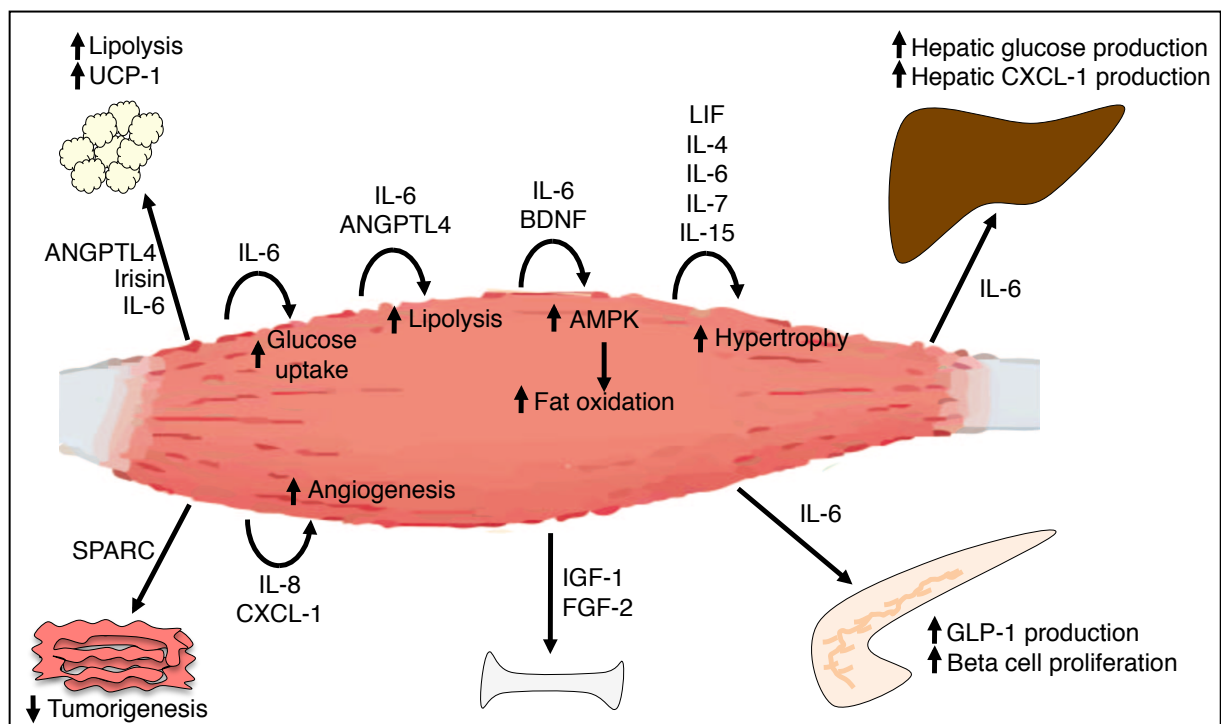
Figure 5: Skeletal muscle as a secretory organ and the impact on other tissues.
Skeletal muscle is capable to secrete proteins and peptides, the so-called myokines, that act in autocrine and paracrine fashion on the muscle itself and in endocrine fashion on other tissues like adipose tissue, liver, colon, bone and pancreas. Several more myokines are known so far, the figure shows only a selection of these. See text for more details. Figure adapted from (Pedersen and Febbraio, 2012) and Eckardt et al. (Eckardt et al., 2014).

IL-6 is the best-studied myokine. Following exhausting exercise, plasma IL-6 concentration increases up to 100 fold, with less pronounced increases after moderate intense physical activity (Fischer, 2006; Pedersen and Fischer, 2007). Importantly, the contracting muscle per se appears to be the major source of IL-6 as intracellular RNA concentration as well as protein concentration increase (Steensberg et al., 2000; Keller et al., 2001; Steensberg et al., 2002). Plasma concentration increases rather in an exponential manner (Ostrowski et al., 1998; Steensberg et al., 2000; Fischer et al., 2004), whereas maximum is reached at the end or directly after end of exercise followed by a rapid decrease to basic value (Ostrowski et al., 1998; Fischer et al., 2004). By now, it is known that the combination of mode, intensity and duration of exercise influence the increase of IL-6 plasma concentration as reviewed by Fischer (Fischer, 2006). Additionally, low intramuscular glycogen leads to an increased expression and release of IL-6 (Keller et al., 2001; Steensberg et al., 2001), which suggests a role as an energy sensor (Hoene and Weigert, 2008; Pedersen, 2012). This myokine is important for tissue hypertrophy, satellite cell proliferation and myotube formation (Serrano et al., 2008; Hoene et al., 2013; Zhang et al., 2013). Via autocrine and paracrine signaling, it can stimulate glucose uptake, lipolysis and fat oxidation in the muscle (Bruce and Dyck, 2004; Petersen et al., 2005; Carey et al., 2006), whereas endocrine signaling is suggested to increase lipolysis in adipose tissue and hepatic glucose production (Stouthard et al., 1995; Febbraio and Pedersen, 2002; Trujillo et al., 2004).

Another exercise-induced myokine is interleukin-8 (IL-8), belonging to the CXC family of chemokines. During exhausting eccentric exercise like a marathon run increased plasma IL-8 levels were measured (Nieman et al., 2001; Ostrowski et al., 2001), whereas shorter concentric cycling sessions increased only *IL-8* mRNA expression (Chan et al., 2004; Nieman et al., 2005). Since the muscle is an important source for IL-8 (Haugen et al., 2010) and only low amounts of the cytokine are secreted upon contraction, it seems to perform rather in a paracrine or autocrine fashion. This myokine induces angiogenesis and thus might support exercise-induced vascularization and oxygen supply (Pedersen, 2011). Further exercise-dependent functions of IL-8 are still unclear and have to be further investigated.

In 2012, irisin, a myokine that affects white adipose tissue and induces browning, was discovered (Bostrom et al., 2012). Exercise-induced PGC1α expression was shown to increase *FNDC5* expression in muscle, which encodes a membrane protein that is cleaved and secreted as irisin (Bostrom et al., 2012). The health-promoting effects and the exercise-induced secretion of irisin in humans are controversially discussed and its relevance in humans is still unclear (Timmons et al., 2012; Raschke et al., 2013b; Staiger et al., 2013; Huh et al., 2014).

Secreted protein acidic and rich in cysteine (SPARC) is a recently discovered exercise-regulated myokine, which is suggested to inhibit colon tumorigenesis by inducing apoptosis (Aoi et al., 2013). Aoi and colleagues showed that a single bout of exercise increased expression and secretion of SPARC in mice and humans (Aoi et al., 2013).

Altogether, more and more exercise-induced myokines are described. Nevertheless, function and health-promoting effects are often unclear and have to be further investigated in future.

1.3 Electric pulse stimulation

Over the last years many attempts have been made to gain insights into contraction-induced intramuscular molecular mechanisms ongoing during exercise and myokine secretion. Nevertheless, knowledge about this issue is still very limited. One major problem is the fact that other endocrine organs might also be stimulated upon exercise, e.g. liver and adipose tissue and thus influence exercise-induced signaling in the muscle. Additionally, it is very difficult to determine whether increased plasma myokine levels are due to the secretion of the muscle cell itself or due to the release of other tissues e.g. adipose tissue or liver.

To overcome this problem an *in vitro* exercise model, Electric pulse stimulation (EPS), has been established for skeletal muscle cell culture during the last decade (Figure 6). Therefore, the *in vivo* motor nerve is simulated by electric impulses generated by electrodes. This leads to Ca^{2+} influx into the muscle cells, finally resulting in *de novo* sarcomere formation and contraction. Investigations with C2C12 cells, a mouse muscle cell line, showed a delayed contraction start upon EPS because the sarcomere structure has first been built up (Fujita et al., 2007). Additionally, several exercise-induced properties known from the *in vivo* system were observed in murine myotubes upon EPS: upregulation of *PPARGC1A* and mitochondrial *OXPHOS* genes, increased energy expenditure and activation of AMPK, the induction of stress activated MAPK signaling, improved insulin-dependent and independent glucose uptake with increased conversion and glycogen synthesis and secretion of several exercise-induced cytokines, e.g. IL-6, CXCL-1, CXCL-5 (Nedachi et al., 2008; Nedachi et al., 2009; Burch et al., 2010). Moreover, IL-6 expression and secretion is influenced in C2C12 myotubes by glucose supply and glycogen stores (Farmawati et al., 2013). Furthermore, it was proposed that IL-6 expression is mediated by extracellular ATP and nucleotide receptors activating IP_3-dependent Ca^{2+} signaling, resulting in transcription activation (Bustamante et al., 2014).

In summary, EPS is a suitable model for studying exercise-induced molecular mechanisms and myokine secretion in muscle cells *in vitro*.
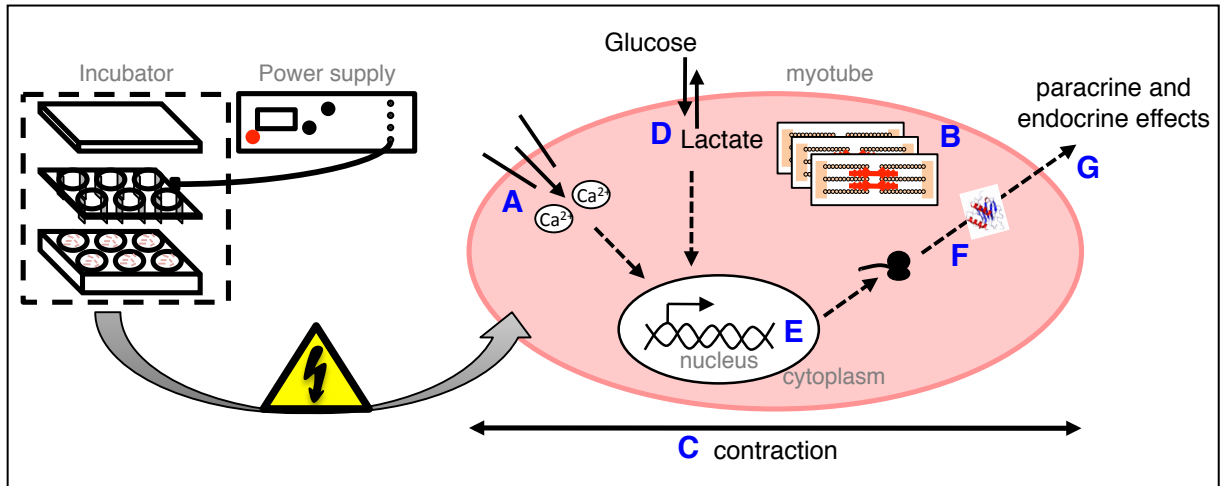
Figure 6: Electric pulse stimulation: an *in vitro* exercise model.
Electric pulse stimulation (EPS) is applied to differentiated myotubes. In this *in vitro* exercise model the *in vivo* motor nerve activation is replaced by electric impulses, leading to (A) Ca^{2+} transients that result in (B) *de novo* sarcomere formation and (C) contraction. (D) To meet the energy demand, myotubes increase their glucose uptake and oxidation leading to release of lactate. (E) Metabolic and mechanical stimuli lead to the regulation and modification of several signaling cascades, resulting (E) in altered gene expression, (F) protein translation and (G) myokine release.

1.4 Aims of this thesis

Several studies proposed that the skeletal muscle is a secretory organ, releasing several hundreds of proteins, called myokines, which work in a hormone-like fashion, having paracrine and endocrine effects. Although molecular mechanisms are mostly unclear, it was suggested that exercise-regulated myokines play a major role in the health-promoting effects of exercise including the treatment and prevention of type 2 diabetes. Nevertheless, the knowledge on myokines and their expression and release, especially upon contraction-induced activation of intramuscular signaling cascades, is scarce.

Electric pulse stimulation, an *in vitro* exercise model, enables the investigation of contraction-induced intramuscular alterations in differentiated myotubes in a well-defined system without any disturbing factors.

One aim of this thesis was the optimization and validation of EPS for human primary myotubes. The EPS protocol was then used to gain further insights into contraction-induced metabolic alterations, gene regulation and signaling pathways and compare these findings to the *in vivo* exercise response. Moreover, we aimed to identify novel exercise-induced myokines either by targeted or untargeted proteomic analysis of the supernatant.

In a second approach human primary myotubes obtained from insulin-sensitive and resistant donors were EP-stimulated with an extended EPS protocol covering also a recovery phase. We aimed to find novel markers of insulin sensitivity and resistance, respectively. Furthermore, we intended to identify pathomechanistic alterations, e.g. changes in lipid metabolism and myokine release, due to insulin resistance during basal and exercise conditions.

2. Materials and methods

2.1 Materials

2.1.1 Chemicals, consumables and laboratory equipment

Standard chemicals were obtained from Sigma-Aldrich (Munich, Germany), Merck (Darmstadt, Germany), Roth (Karlsruhe, Germany) or AppliChem (Darmstadt, Germany) unless stated otherwise. Cell culture media and supplements were from Lonza (Basel, Switzerland), chicken embryo extract was from Seralab (West Sussex, UK) and FBS was obtained from Biochrom (Berlin, Germany). All chemicals were p.a. or higher quality.

Table 3: Consumables and kits.

Consumables/ kits	Company
6-well cell culture dish	Greiner Bio One, Kremsmünster, Austria
Cell culture dish 15 cm	TPP, Trusadingen, Switzerland
Protein concentrator 4 mL and 15 mL (3 kDa cutoff)	Merck Millipore, Darmstadt, Germany
MACS LS columns	Miltenyi Biotech, Bergisch Gladbach, Germany
QIAshredder	Qiagen, Hilden, Germany
MinElute PCR Purification Kit	Qiagen, Hilden, Germany
RNeasy Mini Kit	Qiagen, Hilden, Germany
First Strand cDNA Synthesis Kit	Roche Diagnostics, Mannheim, Germany
QuantiFast SYBR Green PCR Kit	Qiagen, Hilden, Germany
XTT cell proliferation Kit	AppliChem, Darmstadt, Germany
Trans AM NFκB p65 Kit	Active Motif, Carlsbad, CA
20S/26S Proteasome ELISA Kit	Enzo Life Sciences, Farmingdale, NY
Bio-Plex Pro multiplex bead-based immunoassay	Bio-Rad, Hercules, CA
ANGPTL4 ELISA	BioVendor, Heidelberg, Germany
Bradford Protein Assay	Bio-Rad, Hercules, CA
Ambion WT Expression Kit	Affymetrix, Santa Clara, CA
WT Terminal Labeling Kit	Affymetrix, Santa Clara, CA
Human Gene 1.0 ST Array	Affymetrix, Santa Clara, CA

Table 4: Laboratory equipment.

Laboratory equipment	Company
C-Dish electrodes	IonOptix, Dublin, Ireland
C-Pace EP Culture Pacer	IonOptix, Dublin, Ireland
Quadro MACS	Miltenyi Biotech, Bergisch Gladbach, Germany
LightCycler 480 Instrument II	Roche, Mannheim, Germany
Bio-Plex 200 suspension array system	Bio-Rad, Hercules, CA
2100 Bioanalyzer Instrument	Agilent Technologies, Santa Clara, CA
Maxigel	Biometra, Goettingen, Germany
Fastblot B43/B44	Biometra, Goettingen, Germany

2.1.2 Primers

For qRT-PCR commercially available QuantiTect Primer Assays (Qiagen, Hilden, Germany) were used.

Table 5: QuantiTect Primer Assays used for qRT-PCR.

Gene symbol	Assay name (Catalogue Number)
ANGPTL4	Hs_ANGPTL4_1_SG (QT00003661)
IL-6	Hs_IL6_1_SG (QT00083720)
IL-8	Hs_IL8_1_SG (QT00000322)
MYOD1	Hs_MYOD_1_SG (QT00209713)
NAMPT	Hs_NAMPT_1_SG (QT00087920)
PPARGC1A	Hs_PPARGC1A_1_SG (QT00095578)
TBP	Hs_TBP_1_SG (QT00000721)

2.1.3 Antibodies

Table 6: Primary antibodies for western blot.

Antibody	Dilution	Donor	Manufacturer
Akt	1:1000	rabbit	Cell Signaling Technology, Frankfurt, Germany
ERK1/2	1:1000	rabbit	Cell Signaling Technology, Frankfurt, Germany
ERK5	1:500	rabbit	Cell Signaling Technology, Frankfurt, Germany
JNK	1:500	mouse	BD Biosciences, San Jose, CA
p38 MAPK	1:1000	rabbit	Cell Signaling Technology, Frankfurt, Germany
P70S6 kinase	1:500	rabbit	Cell Signaling Technology, Frankfurt, Germany
p-Ser473 Akt	1:1000	rabbit	Cell Signaling Technology, Frankfurt, Germany
p-Thr202/p-Tyr204 ERK1/2	1:1000	rabbit	Cell Signaling Technology, Frankfurt, Germany
p-Thr218/p-Tyr220 ERK5	1:500	rabbit	Cell Signaling Technology, Frankfurt, Germany
p-Thr183/p-Tyr185 JNK	1:1000	rabbit	Cell Signaling Technology, Frankfurt, Germany
p-Thr180/Tyr182 p38 MAPK	1:1000	rabbit	Cell Signaling Technology, Frankfurt, Germany
p-p70S6 kinase	1:1000	rabbit	Cell Signaling Technology, Frankfurt, Germany

Table 7: Secondary antibodies for western blot.

Antibody	Dilution	Donor	Manufacturer
anti-rabbit IgG-HRP	1:500-1:3000	goat	Santa Cruz Biotechnology, Dallas, Tx
anti-mouse IgG-HRP	1:2500	goat	Santa Cruz Biotechnology, Dallas, Tx

Table 8: Antibodies for flow cytometry.

Antibody	Dilution	Manufacturer
5.1H11 (CD56 Antibody)	1:10	Developmental Studies Hybridoma Bank, Iowa City, IA
Purified Mouse IgG1, κ Isotype Ctrl (CD56 Isotype)	1:10	BioLegend, San Diego, CA
FITC RAT Anti-Mouse IgG1	1:500	BD Biosciences, San Jose, CA

Table 9: Antibodies for immunostaining.

Antibody	Dilution	Manufacturer
MyHCII	1:100	Sigma-Aldrich, Munich, Germany
TO-PRO3	1:1000	Invitrogen, Karlsruhe, Germany
Alexa Fluor 488 Goat Anti-Mouse IgG	1:200	Invitrogen, Karlsruhe, Germany

2.1.4 Inhibitors

Table 10: Inhibitors used in cell culture.

Name	Solvent	Manufacturer
Bay 11-7082	DMSO	InvivoGen, San Diego, CA
JNK Inhibitor VIII	DMSO	Merck Millipore, Darmstadt, Germany
U0126	DMSO	Cell Signaling Technology, Frankfurt, Germany

2.2 Methods

2.2.1 Cell culture methods

2.2.1.1 Primary muscle cell culture

Primary skeletal muscle cells were obtained from percutaneous needle biopsies performed on the lateral portion of quadriceps fermoris (vastus lateralis) muscle of subjects participating in the Tuebingen lifestyle intervention program (TULIP) and the Tuebingen family (TÜF) study. The donors gave informed written consent to the study, and the protocol was approved by the Ethics Committee of the University of Tuebingen.

Experiments were performed on the first and second passages of subcultured cells, since more passages decreased proliferation and differentiation behavior (lab intern observation, data not shown). Cells were proliferated in Cloning medium, a 1:1 mixture of Ham´s F12 (No. F0815, Biochrom, Berlin, Germany) and α-MEM (No. BE12-169F, Lonza, Basel, Switzerland) supplemented with 20 % FBS (No. 0615, Biochrom, Berlin, Germany), 1 % chicken embryo extract, 100 U/mL penicillin, 100 μg/mL streptomycin, and 0.5 μg/mL amphotericin B until 80 % confluence in an incubator at 37 °C with 5 % CO_2. Fusion and differentiation of myoblasts to myotubes was achieved by Fusion medium consisting of α-MEM containing 5.5 mM glucose supplemented with 2 % FBS, 2 mM glutamine, 100 U/mL penicillin, 100 μg/mL streptomycin, and 0.5 μg/mL amphotericin B within 6-7 days.

Usually uncoated cell culture dishes were used. Nevertheless, for some experiments, Matrigel (Corning, Tewksbury, MA) coated dishes were used. Therefore, Matrigel was thawed on ice, diluted 1:100 in α-MEM and 750 μL added to each well. Matrigel was polymerized for 3 h at 37 °C and remaining liquid removed afterwards. Myoblasts were then proliferated and differentiated to myotubes as described above.

2.2.1.2 Magnetic activated cell sorting

Magnetic activated cell sorting (MACS; Miltenyi Biotech, Bergisch Gladbach, Germany) was included for cell separation and enrichment of the myoblast fraction for some experiments. The method uses 50 nm superparamagnetic beads, which are conjugated to a highly specific antibody directed against an antigen on the cell surface. The beads bind specifically to the cells. Suspension is then loaded on a column containing a matrix comprised of ferromagnetic spheres. The column is attached to a strong magnet, and MicroBead bound cells are retained in the column during washing. Cells are eluted by removal of the column from the magnet and a further washing step. For human primary myoblasts human CD56 MicroBeads

(Myltenyi Biotech, Bergisch Gladbach, Germany) were used (de Luna et al., 2006; Stadler et al., 2011).

In detail myoblasts were seeded on six 15 cm cell culture dishes and proliferated as described in section 2.2.1.1. When 80 % confluence was reached, myoblasts were washed with PBS and trypsinated of the culture dish (Trypsin-EDTA, 10 min, 37 °C). Cells were harvested by centrifugation (8 min, 800 g, 4 °C) and the pellet properly resuspended in 1 mL Cloning media (1:1 mixture of Ham´s F12 and α-MEM, 20 % FBS, 1 % chicken embryo extract, 100 U/mL penicillin, 100 μg/mL streptomycin, 0.5 μg/mL amphotericin B). The single cell suspension was transferred to an 1.5 mL Eppendorf cup and spun down with 300 g for 10 min at 4 °C. After removal of the supernatant, cell pellet was resuspended in 70 μL MACS buffer (PBS pH 7.2, 0.5 % BSA, 2 mM EDTA; degassed and cold) and 30 μL CD56 MicroBeads were added. After proper mixing, the Eppendorf cup was stored for 15 min at 4-8 °C. Subsequently, 1.3 mL of MACS buffer were added and MicroBead-bound cells spun down (300 g, 10 min, 4 °C). Supernatant was removed and pellet resuspended in 1 mL MACS buffer. The magnetic cell separation was performed in LS columns attached to a magnet (QuadroMACS; Miltenyi Biotech, Bergisch Gladbach, Germany). The columns are suitable for positive separation and can be used with up to 10^8 magnetically labeled cells. The column was equilibrated with 5 mL MACS buffer and the cell suspension applied. During 3 washing steps with 3 mL MACS buffer each, unlabeled cells passed through the column. The column was removed off the magnetic adapter and CD56 containing myoblasts were eluted within 5 mL MACS buffer by applying the plunger supplied with the columns and flushing them out. Purified myoblasts were then seeded in 6-well dishes and proliferated and differentiated as described in section 2.2.1.1. Additionally, samples of myoblasts before magnetic labeling and after MACS were frozen in cryo media (90 % FBS, 10 % DMSO) in liquid nitrogen to determine enrichment efficiency of the different myoblasts via flow cytometry.

2.2.1.3 Flow cytometry

Myoblast cell culture purity was determined by fluorescence based flow cytometry (FC), which was performed with the help and under supervision of Heike Runge at the University hospital in Tuebingen (group: Pathobiochemistry of insulin signaling and energy metabolism; head: Prof. Cora Weigert).

In detail, myoblasts were proliferated on a 15 cm cell culture dish until 80 % confluence, washed with PBS and trypsinated (10 min, 37 °C with Trypsin-EDTA) of the culture dish. Cell number was determined with a C-Chip Neubauer improved haemocytometer (CarlRoth, Karlsruhe, Germany) and suspension adjusted to 1x10^5

cells/mL with FC buffer (PBS supplemented with 2 % FBS). $1x10^5$ cells were transferred to FC vials (BD 352052, BD Falcon, Franklin Lakes, NJ). After two washings with 500 μL FC buffer and centrifugation with 800 g at 4 °C for 3 min in between, cells were incubated with 100 μL FC buffer containing 1st antibody (1:10 diluted) for 30 min at 4 °C in the dark. Cells were washed again (3 times) and treated with 100 μL 2nd antibody (1:500 diluted in FC buffer) for 30 min at 4 °C in the dark. Subsequent washing (3 times), labeled cells were resuspended in 300 μL FC buffer and analyzed on a flow cytometer (FACSCalibur, Becton Dickinson, Franklin Lakes, NJ). Simultaneously, an isotype control and an unstained control was prepared. Analysis of the raw data was done with FCS-Express software (Denovo, Glendale, CA).

2.2.1.4 Immunostaining

For immunostaining, myoblasts were seeded on a 12-well plate on cover slips and differentiated to myotubes as described in section 2.2.1.1.

Myotubes were washed twice with PBS and fixed in PBS containing 4 % paraformaldehyde (pH 7.4) for 20 min. After two further washings with PBS, fixation was quenched with 150 mM glycine in PBS for 10 min and myotubes washed twice with PBS. In the next step, the nucleus was permeabilized with 0.1 % Triton-X100 in PBS for 10 min. After further washing (2x with PBS) unspecific antibody binding was blocked with blocking solution (5 % normal goat serum, 0.05 % Tween-20 in PBS) for 30 min. Cover slips were incubated with an antibody recognizing fast-type skeletal myosin MyHC II diluted 1:100 in blocking solution for 1 h, washed 3 times with PBS and subsequently incubated with the Alexa 488-labeled secondary antibody (1:200 dilution in blocking solution) for 2 h and washed again (3 times with PBS). Nuclei were stained using TO-PRO3 diluted 1:1000 in PBS for 1 h before being mounted with PermaFluor. Pictures were taken with a Leica TCS confocal microscope (Leica, Wetzlar, Germany). Simultaneously, unstained controls were performed.

2.2.1.5 Electric pulse stimulation

Electric pulse stimulation, an *in vitro* exercise model, was applied to differentiated myotubes in 6-well dishes using C-Pace EP system (IonOptix, Dublin, Ireland). Directly before starting the electric stimulation, medium was changed (2 mL/well). Usually Fusion medium (α-MEM containing 5.5 mM glucose, 2 % FBS, 2 mM glutamine, 100 U/mL penicillin, 100 μg/mL streptomycin, 0.5 μg/mL amphotericin B) was used.

In case of the inhibitor studies, 10 μM U0126 (Cell Signaling, Danvers, MA), 10 μM JNK inhibitor VIII (Calbiochem, Darmstadt, Germany) or 5μM Bay 11-7082 (Sigma-Aldrich, St.Louis, MO) was added. For untargeted proteomic profiling of the supernatant, Fusion medium without phenol red and FBS was used. In other studies respective amounts of fatty acids and L-carnitine were supplemented as indicated in the figure legends.

Myotubes were stimulated for a given time with 14 V, 5 Hz and 2 ms in the basic mode unless otherwise stated. Finally, electrodes were removed of the dishes, soaked in double distilled water to remove any electrophoretic byproducts that might have formed on the carbon electrode and heat sterilized before reuse.

2.2.2 Gene expression analysis

2.2.2.1 RNA preparation

Total RNA was isolated with RNeasy Mini kit (Qiagen, Hilden, Germany). First cells were washed once with PBS and lysed with 350 μL RLT buffer including proper amount of β-mercaptoethanol per well. Cell lysate was homogenized by QIAshredder (Qiagen, Hilden, Germany) and stored at -80 °C until RNA isolation. This was done according to the manufacturer's instructions including digestion of remaining genomic DNA. RNA concentration and quality was evaluated by measuring the absorption at 260 nm and 280 nm with a NanoDrop (Thermo Scientific, Idstein, Germany). RNA was stored at -80 °C until usage.

2.2.2.2 Reverse transcription

For reverse transcription Transcriptor First Strand cDNA synthesis kit was used (Roche, Mannheim, Germany). To dissolve any secondary structure, 500 ng-1 μg RNA was filled up to 11 μL with H_2O and was incubated for 10 min at 65 °C.

Afterwards, a mastermix containing random hexamer primer, the reverse transcriptase and dNTPs was added to the preincubation mix and reverse transcription started as follows:

Reverse Transcription

Preincubation mix	11 μL
5 x Buffer	4 μL
Random Hexamer Primer	2 μL
dNTPs	2 μL
Reverse Transcriptase	0.05 μL
RNase Inhibitor	0.05 μL
Activation	10 min, 25 °C
Reverse Transcription	30 min, 55 °C
Inactivation Step	5 min, 85 °C

The cDNA samples were aliquoted and stored at -20 °C until use.

2.2.2.3 Quantitative realtime polymerase chain reaction

Quantitative realtime polymerase chain reaction (qRT-PCR) allows the quantification of cDNA. The method uses a standard PCR for amplification and simultaneously enables to follow the increase of cDNA by a fluorescence signal after each amplification cycle. Therefore, SYBR green, a fluorescent dye that emits a signal of a defined wavelength upon intercalation into double stranded DNA fragments, is added to each PCR mix. The fluorescence signal, which is detected by the LightCycler, increases proportional to the amount of PCR product. After the run has been completed, the cycle number is determined at which the amplification curve crosses a defined threshold in a log-linear ratio (C_p value), which is used to calculate the quantitative value of cDNA. Two types of quantification are commonly used: relative quantification based on the relative expression of a target mRNA to a reference mRNA and absolute quantification, which uses a standard curve for quantification and was used in the experiments of this thesis.

Firstly, standard stocks were prepared by purification of amplified cDNA fragments obtained in a previous run with the Mini Elute PCR purification kit (Qiagen, Hilden, Germany) as described in the manufacturer's manual. cDNA concentration were determined and concentration adjusted to 5 ng/µL. Aliquots of this stock were stored at -20 °C.

For qRT-PCR standard dilutions were prepared for each pair of primers. The stock solution (5 ng/µL) was nine times serially diluted 1:10 (0.5 ng/µL, 0.05 ng/µL, 5×10^{-3} ng/µL,…, 5×10^{-9} ng/µL). Only dilutions 4 to 9 (5×10^{-3} ng/µL to 5×10^{-9} ng/µL) were used in the LightCycler run.

For the qRT-PCR QuantiTect primer assays, consisting of forward and reverse primer, in combination with QuantiFast SYBR Green PCR kit (Qiagen, Hilden, Germany), including HotStarTaq Plus DNA Polymerase, QuantiFast SYBR Green PCR Buffer, dNTP mix, SYBR Green and ROX passive reference dye, was used. For each sample the following mix was prepared:

Component	Amount
cDNA	1 μL
H_2O	3 μL
QuantiTect primer assay Mix	1 μL
QuantiFAST SYBR Green Mix	5 μL

Amplification of the cDNA and detection of the SYBR Green fluorescent signal was done with a LightCycler 480 II (Roche, Mannheim, Germany). The following table summarizes the amplification conditions:

Step	Time	Temperature	
Initial activation step	5 min	95 °C	
Amplification			
Denaturation	10 s	95 °C	40 cycles
Combined annealing/extension	30 s	60 °C	
Melting			
Denaturation	10 s	95 °C	
Start Melting	5 s	62 °C	
Gradually increase	continuous		

Resulting cDNA amounts were then normalized to the housekeeping gene TBP.

2.2.2.4 Whole genome transcriptome analysis

Microarray analysis and data analysis was performed by Dr. Martin Irmler of the Institute of Experimental Genetics at the Helmholtz Center Munich (head of the group "Gene Regulation": Prof. Johannes Beckers). After RNA quality was analyzed by Agilent 2100 Bioanalyzer (Agilent Technologies, Santa Clara, CA), only high-quality RNA (RIN > 8) was used for microarray analysis. Total RNA (150 ng) was amplified using the Ambion WT Expression Kit and the WT Terminal Labeling Kit (Affymetrix, Santa Clara, CA). Amplified cDNA was hybridized on Affymetrix Human Gene 1.0 ST arrays containing approximately 28000 probe sets. Details about the protocol were recently published (Scheler et al., 2013).

Statistical analysis of the raw data was done with the statistical programming environment R (R Foundation for Statistical Computing, Vienna, Austria) included in

CARMAweb (Rainer et al., 2006). The paired limma t-test in combination with the Benjamini Hochberg multiple testing correction (false discovery rate (FDR) < 10%) was used for the genewise testing for differential expression. Heatmaps were generated with CARMAweb and gene ontology (GO) term and pathway enrichment analyses (p < 0.01; adj. p < 0.05) were done with GePS (Genomatix) or Inguinity software (p < 0.05).

Array data was submitted to Gene Expression Omnibus (GEO) with the accession number GSE44051.

2.2.3 Protein analysis

2.2.3.1 Protein lysate

Protein lysates were generated for subsequent SDS-PAGE and western blot analysis.

Immediately after end of stimulation, myotubes were washed once with cold PBS and incubated with 100 μL cold Protein lysis buffer (50 mM HEPES, 150 mM NaCl, 1.5 mM MgCl$_2$, 1 mM EGTA, 10 % (v/v) glycerol, 1 % (v/v) Triton-X100, pH 7.5) including freshly added 1x phosphatase inhibitor (10x: 100 mM NaF, 50 mM Na$_4$P$_2$O$_7$, 100 mM Na$_3$VO$_4$, 100 mM β-glycerolphosphat) per well on a rocker at 4 °C for 15 min. Afterwards, lysates were scrapped off the cell culture dish and transferred to an Eppendorf cup which was incubated on ice for further 10 min. Remaining cell debris were spun down with 13000 rpm for 4 min at 4 °C and supernatant was aliquoted and stored at -80 °C until use.

2.2.3.2 Bradford Protein Assay

Protein concentration of cell lysates was determined by Bradford Protein Assay (Bio-Rad, Hercules, CA) (Bradford, 1976).

Therefore, Bradford reagent concentrate was mixed 1:5 with deionized water and filtered through a Whatman filter paper. Additionally, protein lysates were diluted 1:5 with deionized water to be in the standard range of this assay. A mixture of 10 μL of diluted samples with 200 μL diluted Bradford reagent was prepared and extinction measured at 595 nm against a blank. BSA solutions ranging from 500 ng/μL to 31.3 ng/μL were used as protein concentration standards and enabled thus the calculation of the concentration of the samples.

2.2.3.3 SDS-PAGE

Proteins can be separated according to their molecular weight using discontinuous sodiumdodecylsulfate polyacrylamide gel electrophoresis (SDS-PAGE). Therefore, first a separating gel was cast and covered with a layer of isopropanol. After complete polymerization, isopropanol was decanted and stacking gel was cast.

Table 11: Composition of stacking and separating gel for SDS-PAGE.

	Stacking gel	Separating gel (7.5 %)
SDS Stacking gel buffer	3.4 mL	-
SDS Separating gel buffer	-	10 mL
H_2O	9.4 mL	20 mL
Acrylamide 30%	1.8 mL	9.9 mL
10% APS	150 μL	270 μL
TEMED	20 μL	66 μL

10 % APS: 10% (w/v) ammonium persulfate; SDS separating gel buffer: 1.5 M Tris, 2 % (w/v) SDS, pH 8.8; SDS Stacking gel buffer: 0.5 M Tris, 2 % (w/v) SDS, pH 6.8.

For the separation the Maxigel equipment (Biometra, Goettingen, Germany) was used. Respective amounts of 5x sample loading buffer (1 M Tris-HCl pH 6.8, 50 % (v/v) glycerol, 10 % (w/v) SDS, 0.5 % β-mercaptoethanol, 1 % (w/v) bromophenol blue) were added to 50-100 μg protein lysate and the mixtures were heated for 3 min at 95 °C to denature the proteins. The gel chamber was filled with 1x SDS running buffer (2.5 mM Tris, 20 mM glycine, 0.1 % (w/v) SDS) and samples loaded onto the gels next to 15 µL of protein standard (Precision Plus Protein Standards Dual Color; Bio-Rad, Hercules, CA).

The electrophoretic separation was carried out with 100 V until the dye front reached separating gel. Voltage was then either raised to 200 V when running the gel during the day or turned down to 40 V when running over night. In either case the separation was stopped when the bromophenol blue dye front ran out of the gel.

2.2.3.4 Western Blot

For western blot analysis, proteins separated by SDS-PAGE were transferred to a nitrocellulose membrane by semidry blotting using Fastblot B43/B44 (Biometra, Goettingen, Germany). First, nitrocellulose membrane and whatman papers were incubated in 1x Blotting buffer (48 mM Tris, 39 mM glycine, 0.4 % (w/v) SDS, 20 % (v/v) MeOH). Afterwards a sandwich composed of 2 whatman paper, nitrocellulose membrane, polyacrylamide gel and further 2 whatman paper was assembled on the anode. The transfer occurred within 45 min with the appropriate

current at 4 °C. The current was calculated based on the size of the gel (length x width x 4 mA).

The protein transfer was checked by reversible Ponceau S (0.1 % (w/v) Ponceau S, 1% (v/v) glacial acetic acid) staining. Next, the membrane was washed 3 times for 20 min with NET-G (150 mM NaCl, 5 mM EDTA, 50 mM Tris, 0.05 % (v/v) Triton-X100, 2.5 % (w/v) gelatine, pH 7.4). Upon blocking, the membrane was incubated with the first antibody, diluted in NET-G, overnight at 4 °C on a rocker. After three further washing steps with NET-G the HRP-conjugated second antibody, diluted in NET-G, was incubated for 45 min at room temperature. The membrane was washed as before and antibody detected protein bands were visualized by using the HRPO luminescent substrate included in the Western Lightning Plus-ECL Kit (Perkin Elmer, Waltham, MA) and subsequent exposure of a X-ray film for an appropriate time. Usually, first phospho-antibodies were incubated with the membranes and signal visualized. To determine signal of the corresponding protein, phospho-antibodies were stripped of the membrane before further incubation as follows: membranes were washed twice for 20 min with NET-G, incubated with Stripping buffer (66 mM Tris pH 6.8, 0.5 % (v/v) β-mercaptoethanol, 2 % (w/v) SDS, pH 6.8) for exactly 30 min at 56 °C and again washed three times for 20 min with NET-G. Afterwards, membrane was reprobed with an antibody directed against the corresponding protein as described above.

Densiometric analysis of western blots was performed with Image Studio Lite (LI-COR, Lincoln, NE). The resulting values are shown as arbitrary units. Phosphorylation intensities were related to the amount of the corresponding protein.

2.2.3.5 Targeted proteomic analysis of the supernatant

The targeted proteomic profiling of the supernatant was performed by Bio-Plex Multiplex Immunoassay (Bio-Rad, Hercules, CA) in cooperation with the Proteome Analysis Unit at the German Diabetes Center (DDZ) in Duesseldorf (head: Dr. Stefan Lehr). The assay was performed with the help and under supervision of the technician Waltraud Passlack and Dr. Sonja Hartwig.

Conditioned medium was collected after end of stimulation and put on ice until further processing. The supernatant was then spun down with 2700 g for 4 min at 4 °C to remove detached cells, transferred to a new tube and frozen at -80 °C until analysis in Duesseldorf. There, it was thawed on ice and secreted proteins were analyzed using a Bioplex 200 suspension array system (Bio-Rad, Hercules, CA) as described in the manufacturer's instructions. Since antibodies might cross-react with proteins of FBS it is important to analyze a sample of unconditioned reference medium. For the analytes measured in this thesis neat samples were used and results obtained were

in the assay working range. Protein concentrations of the analytes were calculated from the appropriate optimized standard curve by Bio-Plex Data Pro Software and then normalized to total protein amount per well.

The amount of ANGPTL4 in the supernatant was determined by ELISA (from BioVendor, Heidelberg, Germany) according to the instructions in the manual.

2.2.3.6 Untargeted proteomic analysis of the supernatant

For untargeted proteomic analysis of the cell supernatant, a gel-based (two dimensional difference gel electrophoresis; 2D-DIGE) and gel-free separation (liquid chromatography; LC) was used. Subsequent protein analysis was MS-based. For both techniques, the sample preparation was equal and will be described in the nascent part.

During stimulation, Fusion medium (α-MEM containing 5.5 mM glucose, 2 mM glutamine, 100 U/mL penicillin, 100 μg/mL streptomycin, and 0.5 μg/mL amphotericin B) without phenolred and FBS was used. To decrease any serum carryovers cells were washed twice with PBS containing Ca^{2+}/Mg^{2+} and once with standard PBS before medium was changed. Stimulation was performed according to section 2.2.1.5. Directly after stimulation end, supernatant was removed and spun down with 800 g for 5 min at 4°C to remove any cell debris. During subsequent high speed centrifugation (45000 g, 5 min, 4 °C in SS34 rotor) insoluble material was removed. Supernatant was frozen at -80 °C until further proceeding. To obtain a protein concentration sufficient for analysis (1-3 mg/mL), supernatant was spin-concentrated at 4 °C (concentrator with 3 kDa cutoff). Afterwards, it was aliquoted, stored at -80 °C and sent to Duesseldorf for further analysis.

2.2.3.6.1 Untargeted proteomic analysis via 2D-DIGE and MALDI-MS

Analysis of myotube secretome using 2D-DIGE and subsequent protein identification was performed by Dr. Sonja Hartwig of the Proteome Analysis Unit at the German Diabetes Center (DDZ) in Duesseldorf (head: Dr. Stefan Lehr).

Concentrated supernatant, produced as described in section 2.2.3.6, was diluted in lysis buffer (25 mM Tris, 4 % CHAPS (w/v), 7 M urea, 2 M thiourea). Samples were labeled with cyanine-dyes (GE Healthcare, Chalfont St Giles, UK) using the minimal dye labeling method according to the description by Lehr and colleagues (Lehr et al., 2005). Briefly, 50 μg of proteins per gel of either sample, which was supposed to be compared, was labeled with 400 pmol of Cy3 or Cy5. Additionally, a pool of all 12 samples (25 μg each) was labeled with Cy2, functioning as internal standard on each gel. To exclude any dye-specific alterations, dye-swap protocol was used for EPS and control samples. For each gel, the labeled samples (Cy3 and Cy5) and internal

standard (Cy2) were separated in first dimension by isoelectric focusing (IEF) using pH 4-7 and pH 6-9 linear IPG strips (MultiPhor II electrophoresis unit, GE Healthcare, Freiburg, Germany). In the second dimension proteins were separated according to their molecular weight by SDS-PAGE (12% gels; Ettan DaltTwelve Electrophoresis system, GE Healthcare, Chalfont St Giles, UK).

Subsequent electrophoretic separation, protein patterns were visualized by laser scanning on a Typhoon 9400 (GE Healthcare, Chalfont St Giles, UK). Detection of protein spots and calculation of relative spots was carried out automatically using Proteomweaver 4.0 image analysis software (Bio-Rad, Hercules, CA). Regulated spots with a fold change > 1.5 fold and a p-value < 0.05 in any comparison were selected for protein identification by MALDI-MS. Spot picking, in gel digestion, MALDI-MS and prediction/annotation of proteins was performed as recently described (Lehr et al., 2012).

To determine secretory properties of the identified proteins, sequences were analyzed by SignalP 4.1 (Petersen et al., 2011) and SecretomeP 2.0 (Bendtsen et al., 2004). Statistical analysis of the identified protein spots was performed by student's t'test.

2.2.3.6.2 Untargeted proteomic analysis via LC-MS/MS

Analysis of the myotube secretome using liquid chromatography-electrospray ionization (LC-ESI) mass spectrometry and data analysis including statistics was done by Dr. Gereon Poschmann at the Molecular Proteomics Laboratory (head: Prof. Kai Stühler) at the Heinrich-Heine-University in Duesseldorf.

Concentrated supernatant, produced as described in section 2.2.3.6, was analyzed via LC-MS/MS as recently described (Hartwig et al., 2014a). In detail, 5 μg of sample was focused on a 4-12 % polyacrylamide bis-tris gel (Life Technologies, Darmstadt, Germany) and the gel subjected to silver staining. Protein bands were cut out, destained (15 mM $Na_2S_2O_3$, 50 mM $K_3[FE(CN)_6]$), reduced (10 mM DTT, 50 mM $(NH_4)HCO_3$), alkylated (50 mM C_2H_4INO, 50 mM NH_4HCO_3) and proteins were digested overnight (0.1 μg trypsin, 50 mM NH_4HCO_3). For LC-MS/MS analysis, peptides were extracted from the gel with 1:1 (v/v) 0.1 % TFA/acetonitrile and subsequently the acetonitrile was removed by vacuum concentration. 500 ng peptides were separated by liquid chromatography (UltiMate 3000 Rapid Separation LC System, Dionex/Thermo Scientific, Idstein, Germany). Mass spectrometry was carried out with an Orbitrap Elite high resolution instrument (Thermo Scientific, Bremen, Germany) operated in positive mode and equipped with a nano ESI-source. Raw data were analyzed with MaxQuant (version 1.4.1.2, Max Planck Institute for Biochemistry, Munich, Germany) for protein and peptide identification and

quantification with preset parameters. For peptide and protein acceptance, the false discovery rate was set to 1 %, only proteins with at least two identified peptides were used for protein assembly. The label free quantification algorithm implemented in MaxQuant was used for quantification. A two way ANOVA was calculated on logarithmic transformed normalized intensity values for proteins with at least two quantitative values in each group and p values adjusted for multiple testing by the method of Benjamini Hochberg. Statistical analysis was done using the R environment (R Foundation for Statistical Computing, Vienna, Austria).

To determine secretory properties of the identified proteins, sequences were analyzed by SignalP 4.1 (Petersen et al., 2011) and SecretomeP 2.0 (Bendtsen et al., 2004). Pathway enrichment analyses ($p < 0.05$) were done with InCroMAP (Wrzodek et al., 2012).

2.2.4 Acylcarnitine analysis

MS-based metabolome analysis was used for the investigation of intracellular acylcarnitines.

Therefore, Fusion media (α-MEM containing 5.5 mM glucose, 2 % FBS, 2 mM glutamine, 100 U/mL penicillin, 100 μg/mL streptomycin, 0.5 μg/mL amphotericin B) was supplemented with 100 μM L-carnitine, 125 μM oleate and 125 μM ^{13}C labeled palmitate ($^{13}C_{16}$, 99 atom % ^{13}C; all purchased from Sigma-Aldrich, Munich, Germany) during stimulation. Directly, after end of stimulation, medium was removed, and cells washed twice with cold saline (9 g/L NaCl) and subsequently lysed in 300 μL cold 80 % MeOH (MeOH LC-MS Chromasolv and H_2O for HPLC, Sigma-Aldrich, Munich, Germany). Lysed cells were scraped off the cell culture dish, lysates of 6 wells pooled and frozen at -20 °C until further usage.

Samples were thawed and a combination of standards was added (Table 12). For acylcarnitine determination only carnitine standards are relevant. Nevertheless, a standard mixture including carnitines, acylcarnitines (AC), free fatty acids (FFA), amino acids and lysophosphatidylcholine (LPC) was added to each sample since they were used also for further lipidome analyses.

Table 12: Internal standards added to samples for metabolomic analysis.

Internal standard	ng/sample	Stock solution (mg/mL)	Solvent/diluent
d3-carnitine	50	1	MeOH/MeOH
d3-C2 carnitine	50	1	MeOH/MeOH
d3-C4 carnitine	10	0.1	MeOH/MeOH
d3-C10-carnitine	0.5	0.01	MeOH/MeOH
d3-C16-carnitine	1	0.01	MeOH/MeOH
d4-C16:0-FFA	200	1	MeOH/MeOH
d4-C22:0-FFA	10	0.1	$CHCl_3$:MeOH (2:1)/MeOH
d3-leucine	500	1	H_2O/MeOH
d5-phenylalanine	25	0.1	H_2O/MeOH
LPC (19:0)	300	1	$CHCl_3$:MeOH (2:1)/MeOH

For further lysis, cells were then sonicated in a cooled ultrasonic bath (twice for 5 min each). Myotube lysates were then vortexed for 2 min with 2500 rpm in the pulse modus and spun down for 20 min with 13000 rpm at 4 °C. Supernatant was divided in 4 aliquots (350 μL each) and lyophilized in a speed-vac.

Analysis of the acylcarnitines was performed by Xinjie Zhao at the Dalian Institute of Chemical Physics (Dalian, China; head: Prof. Guowang Xu). There, samples were reconstituted in 60 μL acetonitril/water (2:8) and analyzed by Acquity ultra performance lipid chromatography system (UPLC; Waters, Milford; MA) coupled with a linear ion-trap quadrupole (LTQ) orbitrap hybrid mass spectrometer (Thermo Fisher, Waltham, MA). The peaks were extracted by Thermo Xcalibur Quan Browser 2.2 (Thermo Fisher, Waltham, MA). The concentrations of the carnitines were calibrated with one of the internal standards (Table 13).

Table 13: Internal standards used for calibration of the different determined carnitines

Internal standard	Measured acylcarnitine (AC)
d3-carnitine	L-carnitine
d3-C2 carnitine	C2-AC, [$^{13}C_2$] C2-AC, C3-AC
d3-C4 carnitine	C4-AC, [$^{13}C_4$] C4-AC, C5-AC
d3-C10-carnitine	C6-AC, [$^{13}C_6$] C6-AC, C8-AC, [$^{13}C_8$] C8-AC, C10-AC, [$^{13}C_{10}$] C10-AC, C12-AC, [$^{13}C_{12}$] C12-AC, C14:1-AC, C14-AC, [$^{13}C_{14}$] C14-AC
d3-C16-carnitine	C16:1-AC, [$^{13}C_{16}$] C16:1-AC, C16-AC, [$^{13}C_{16}$] C16-AC

2.2.5 ELISA and commercial Assays

2.2.5.1 TransAM NFκB p65 Transcription factor assay kit

The TransAM NFκB p65 Transcription factor assay kit (Active Motif, Carlsbad, CA) was used to determine NFκB transcription factor activity. The Rel homology domain of NFκB, a conserved 300 amino acid sequence, which is located in the N-terminal region of NFκB, is responsible for DNA binding, protein dimerization and nuclear localization of this transcription factor. For the assay an oligonucleotide that contains an NFκB consensus binding site (5´-GGGACTTTCC-3´) is immobilized on a 96-well plate. The active, dimeric form of NFκB binds specifically to this oligomer. Afterwards the primary antibody recognizes an epitope of p65, a subunit of NFκB, which is only accessible when the protein is in its active conformation. The HRP-conjugated second antibody enables a sensitive colorimetric readout by spectrometry.

First, nuclear extracts were prepared. Therefore, medium was removed and 6-well plates washed with 1 mL cold PBS. The cells were scraped off the plastic and transferred to a cold Eppendorf cup. 3 wells were pooled to achieve proper amount of starting material. The remaining cells were rinsed with 400 μL PBS supplemented with 20 μL Phosphatase inhibitor buffer (125 mM NaF, 250 mM β-glycerophosphate, 250 mM p-nitrophenyl phosphate, 25 mM NaVO₃) out of the wells and transferred to the Eppendorf cup. The cells were harvested by centrifugation (1 min, 13000 rpm, 4 °C) and supernatant discarded. The pellet was resuspended in 0.5 mL cold Hypotonic buffer (HB buffer: 20 mM HEPES pH 7.5, 5 mM NaF, 10 μM Na_2MoO_4, 0.1 mM EDTA, adjusted to pH 7.5 with NaOH) and incubated for 15 min on ice. After 25 μL 10 % NP-40 (diluted in HB buffer) was added, lysed cell suspension was mixed and spun down for 30 s with 13000 rpm at 4 °C. After discarding the supernatant, the pellet was resuspended in 25 μL Complete lysis buffer (included in the kit) and incubated on ice for 30 min. Cell debris were spun down (5 min, 13000 rpm, 4 °C) and aliquots of the supernatant containing the nuclear extract frozen at -80 °C.

For the assay, which was performed according to manufacturer's instructions, 2 μg of nuclear extract were applied. The absorbance at 450 nm and the reference wavelength of 655 nm was measured at a spectrophotometer and the relative amount of NFκB, reflecting the relative activity, in the samples calculated through the absorption of the positive control.

2.2.5.2 20S/26S Proteasome ELISA

The quantity of 20S core proteasome in cell lysates and in cell culture supernatant was analyzed by 20S/26S Proteasome ELISA Kit (Enzo Life Sciences, Farmingdale, NY) as described in the manufacturer's instructions.

For the analysis of the intracellular proteasome amount, the protein concentrations of the cell lysates were determined by Bradford assay (see section 2.2.3.2) and adjusted to 1 mg/mL. For the assay this stock was diluted 1:400 to give results within the detection limit of the proteasome ELISA kit (upper limit: 1.6 μg/mL).

Since the Fusion medium of the analyzed samples contained phenol red, which disturbs Bradford assay, no protein determination could be performed and supernatant was diluted 1:2 for the assay. For analysis of these raw data, values were normalized to protein amount per well.

2.2.5.3 Cell proliferation assay

A XTT cell proliferation kit (AppliChem, Darmstadt, Germany) was used to check the cell viability of the EP-stimulated myotubes. This assay uses 2,3-Bis-(2-methoxy-4-nitro-5-sulfophenyl)-2H-tetrazolium-5-carboxanilide salt (XTT), which can be only reduced in mitochondria of living cells by succinate dehydrogenase system. In the end orange colored formazan is generated whose concentration is proportional to the amount of metabolically active cells.

For this assay, human myotubes were grown in the 6-well format. Right before start of EP-stimulation Fusion medium (α-MEM containing 5.5 mM glucose, 2 % FBS, 2 mM glutamine, 100 U/mL penicillin, 100 μg/mL streptomycin, 0.5 μg/mL amphotericin B) was changed (2 mL per well). After 24 h of EPS XTT assay was started. Therefore, 10 μL of Activation solution was diluted with 1 mL XTT reagent and 1 mL of this mix was added to the 2 mL media in the well. The cell culture dish was incubated for 1.5-2 h in the incubator until color has changed noticeable. The dish was agitated gently before 150 μL of the supernatant were transferred to a 24-well dish for measurement of the absorbance against a blank with a spectrophotometer at 450 nm and background control at 650 nm. For this assay it is essential to have a similar treated medium control since albumin in the serum leads to an increased signal.

47

2.2.5.4 Triglyceride-determination

For intracellular triglyceride determination, cells were washed once with PBS and lysed with 50 μL of 1 % Triton-X100 diluted in PBS per well for 30 min at 4 °C on a rocker. After lysates were scraped off the dishes and transferred into Eppendorf cups, they were frozen at -80 °C until further analysis in Tuebingen.

The quantification of total-triglyceride content including mono- and diglycerides as well as glycerol was performed with buffers included in the ADVIA 1800 chemistry system (Siemens Healthcare Diagnostics, Fernwals, Germany). Shortly, samples were thawed, vortexed and 10 μL transferred to a microtiter plate. 100 μL of a 1:1 mixture of buffer Reagent1 and buffer R1-Mix were added, incubated for 5 min and absorption measured at 490 nm. As reference wavelength 655 nm was used.

2.2.5.5 Determination of glucose, lactate, CK and LDH

Glucose and lactate concentrations as well as creatine kinase (CK) and lactate dehydrogenase (LDH) enzyme activities were measured in the cell supernatant. Medium was removed of the cells and spun down for 4 min with 13000 rpm at 4 °C to remove any detached cells. In case of glucose and lactate, aliquots could be stored at -20 °C. For CK and LDH measurement, enzyme activity was inactivated while freezing at -20 °C thus aliquots were stored at 4 °C until measurement. Concentration and enzyme activity were analyzed with the ADVIA 1800 clinical chemical analyzer (Siemens Healthcare Diagnostics, Fernwald, Germany) in Tuebingen, respectively.

2.2.6 Statistical analysis

Unless otherwise noted, values are shown as means ± SEM and groups of data were compared using two-sided Student's t-test. The statistical significance was set at $p < 0.05$.

3. Results

3.1 EPS: an *in vitro* exercise model

In the beginning of this thesis, Electric pulse stimulation was only reported for murine myotube cell culture systems (Fujita et al., 2007; Nedachi et al., 2008; Nedachi et al., 2009; Burch et al., 2010). Thus, an EPS protocol suitable for human primary myotubes had to be established, which induces a metabolic shift towards higher energy consumption and shows activation of intracellular signaling pathways and gene expression patterns comparable with the response in the contracting skeletal muscle *in vivo*.

Parts of the data shown in this section have been already published (Scheler et al., 2013; Scheler et al., 2015).

3.1.1 EPS for 24 h induced glucose consumption and lactate production

In the beginning an EPS protocol that shifts myotubes metabolism to higher glucose consumption and higher lactate production, a state that simulates physiological endurance exercise, had to be established. A time-dependent stimulation of human myotubes showed that glucose consumption was strongly induced after 24 h of EPS, which was in concordance with increased lactate production at this time point (Figure 7).
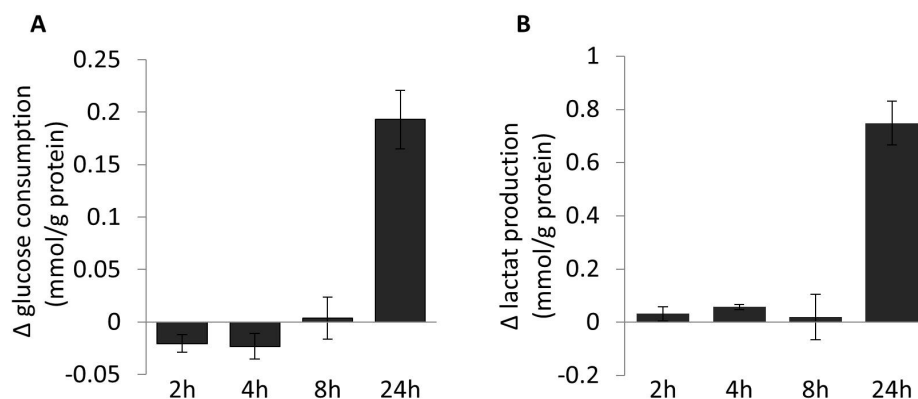
Figure 7: Electric pulse stimulation for 24 h increases glucose consumption and lactate production.
Human myotubes were EP-stimulated for 2, 4, 8, 24 h with 14 V, 5 Hz, 2 ms. Glucose (A) and lactate concentration (B) were measured in the supernatant and are shown as difference from EPS to control. Values are shown as mmol/g protein (means ± SEM; n = 8). Figures from (Scheler et al., 2013).

3.1.2 EPS does not influence cell viability

Next, EP-stimulated myotubes were analyzed for cell damage and cell viability. Myotubes integrity was verified by quantification of secreted cytosolic or mitochondrial localized proteins. Therefore, creatine kinase (CK) and lactate dehydrogenase (LDH), both markers for muscle fiber damage (Fernandez-Gonzalo et

al., 2014), were analyzed in the supernatant and in total cell lysate by measurement of their enzymatic activities (Figure 8).
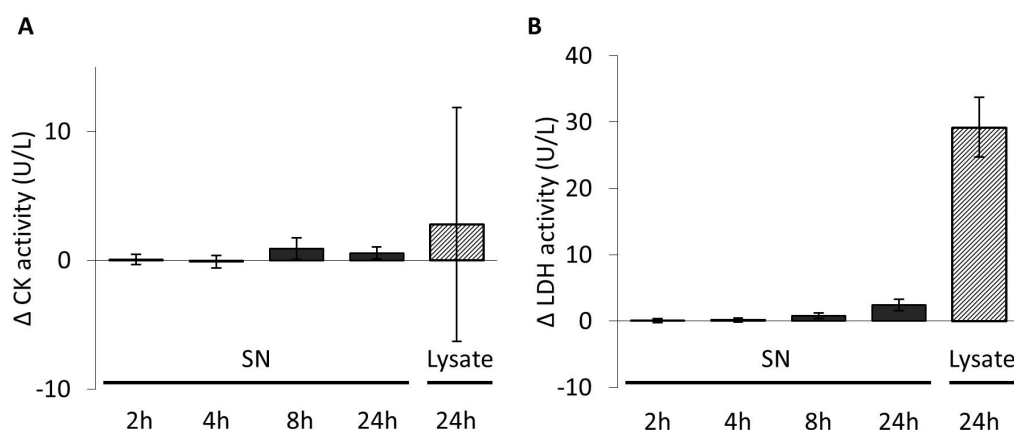
Figure 8: EPS does not increase creatine kinase (CK) and lactate dehydrogenase (LDH) activity.
(A) CK and (B) LDH activity was measured in the supernatant of EP-stimulated myotubes after 2, 4, 8, 24 h of EPS with 14 V, 5 Hz, 2 ms (filled bars) and in Triton-X100 lysates of the cells after 24 h EPS (striped bars). Values are shown as difference of EPS to control (means ± SEM; n = 5-8). Figures from (Scheler et al., 2013).

Activity of CK was not increased in the supernatant after 24 h of EPS (Figure 8A, filled bars) while activity of LDH was slightly increased after 24 h treatment (Figure 8B, filled bars). Since the enzymatic activity of total LDH in the cell lysate was also elevated (striped bar) this might explain the increased LDH activity determined in the supernatant of cells treated for 24 h with EPS.

To exclude any effect on cell viability, XTT proliferation assay was performed. This assay measures the reduction of tetrazolium salts into colored formazan compounds accomplished by mitochondrial enzymes in living cells. These enzymes are inactivated shortly after cell death, thus the assay enables the determination of cell viability. The absorbance of the orange formazan compounds was determined by spectrophotometer at 450 nm, showing similar results between con-myotubes and EPS-myotubes after 24 h of EPS (Figure 9).
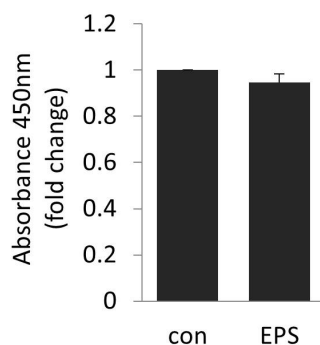
Figure 9: EPS does not influence cell viability.
Cell viability was measured by XTT cell viability assay. Human myotubes were stimulated for 24 h with 14 V, 5 Hz, 2 ms and XTT assay performed subsequent. Measured absorbencies at 450 nm are shown as fold change of EPS vs. control (con) supernatants (means ± SEM; n = 5). Figure from (Scheler et al., 2015).

Summing up, EPS conditions of 14 V, 5 Hz, 2 ms do not induce cytotoxicity but increase glucose consumption and lactate production and thus provide conditions that are indeed suitable to mimic exercise *in vitro*.

3.1.3 EPS with different intensities

The EPS device offers different setting possibilities. Amongst voltage and pulse duration also intensity can be adjusted. Higher voltages and longer pulse durations than 14 V and 2 ms over 24 h of EPS led to cell lesion and cell death (Mika Scheler, unpublished observation). When applying a higher frequency to the myotubes (30 Hz instead of 5 Hz) for 4 h, an increased phosphorylation of ribosomal protein S6 kinase β-1 (p70S6K1) could be observed (Figure 10A). Additionally, mRNA expression of *MYOD*, a myogenic regulator, was increased during higher intensity (Figure 10B). The data indicate that high-intensity EPS mimics resistance exercise training shown as the activation of signal transduction pathways leading to the muscle protein synthesis and muscle hypertrophy.
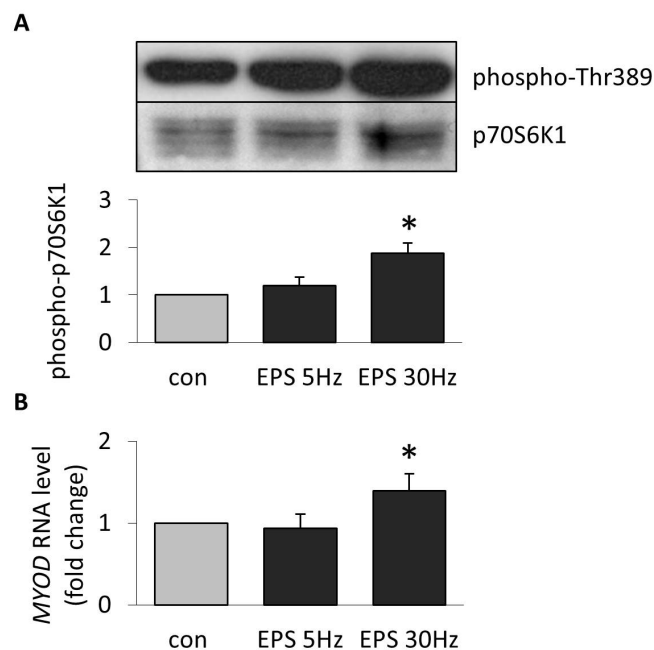
Figure 10: High frequency EPS simulates resistance exercise.
Human myotubes were either stimulated with 5 Hz or 30 Hz for 4 h (14 V, 2 ms). (A) Phosphorylation of p70S6K1 was detected by immunoblotting of myotube cell lysate obtained after different EPS conditions. Membrane was reprobed for p70S6K1 protein. Histogram shows the result of the densitometric quantification (means ± SEM; n = 3-5; * $p < 0.05$ vs. EPS with 5 Hz). (B) Relative expression levels of myogenic differentiation 1 (MYOD) were measured in human myotubes that were EP-stimulated with either 5 Hz or 30Hz for 4 h. RNA was isolated after EPS and qRT-PCR was performed. Values are normalized to housekeeping gene TBP and shown as fold change to control cells (means ± SEM; n = 4). Statistical analysis was performed between mRNA expression levels of the myotubes stimulated with different intensities (* $p < 0.05$). Figures from (Scheler et al., 2013).

For further experiments the low frequency protocol with 14 V, 5 Hz, 2 ms was applied to human myotubes, since the focus of the project was rather on endurance exercise than resistance exercise.

3.1.4 EPS-induced changes in gene expression

Next, the transcriptional changes induced by EPS were investigated in human primary myotubes. Therefore, mRNA expression of the known myokines *IL-6* and *IL-8* and of an exercise-regulated transcriptional coactivator, peroxisome proliferator-activated receptor gamma coactivator 1-alpha (*PPARGC1A*), was measured in RNA lysates of human myotubes obtained after different EPS durations. Significantly increased RNA expression of *IL-6* and *IL-8* was already apparent after 2 h and 4 h (Figure 11A, B), respectively. Longer duration led to an accumulation of the mRNA. *PPARGC1A* showed only a significantly increased expression after 24 h of EPS (Figure 11C).
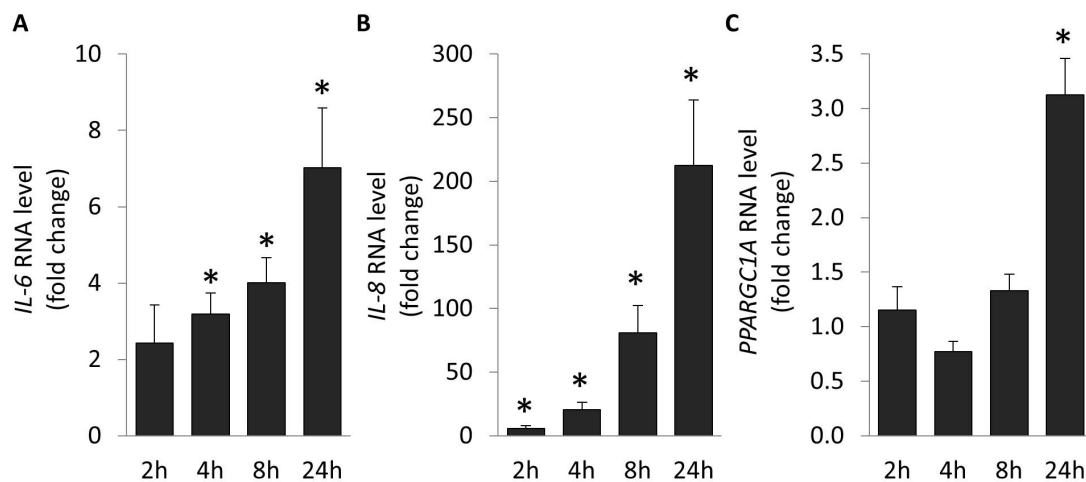
Figure 11: Electric pulse stimulation for 24 h leads to an increased expression of *IL-6, IL-8* and *PPARGC1A.*
(A) *IL-6*, (B) *IL-8* and (C) peroxisome proliferator-activated receptor gamma coactivator 1-alpha (*PPARGC1A*) mRNA expression was measured in myotubes that were EP-stimulated for 2, 4, 8, 24 h with 14 V, 5 Hz, 2 ms. After EPS, RNA was isolated and mRNA level determined by qRT-PCR. Values are normalized to levels of housekeeping gene TBP and are shown as fold increase to control cells (means ± SEM; n = 8). Statistical analysis was performed between levels in control and EPS cells (*p < 0.05 significant increase). Figures from (Scheler et al., 2013).

In summary, 24 h of EPS with 14 V, 5 Hz, 2 ms induced most significant transcriptional changes in the studied genes. In concordance with a metabolic shift of glucose consumption and lactate production after 24 h of EPS (see section 3.1.1) for the following genome-wide transcriptome analysis 24 h of EPS were applied to human myotubes.

3.1.5 Genome-wide transcriptional response to EPS

For further characterization of the model, we used genome-wide transcriptome analysis to gain an overall view over EPS-induced gene regulation and to identify novel contraction-induced targeted genes.

Therefore, human primary myotubes of 12 different donors were stimulated for 24 h and gene regulation was analyzed by microarray analysis on Affymetrix Gene 1.0 ST arrays. Donors were young, lean and insulin-sensitive (Table 14).

Table 14: Characteristics of the myotubes donors used for genome-wide transcriptome analysis.

Characteristics	Values
Gender (m/f)	9/3
Age (y)	25.6 ± 4.4
BMI	22.7 ± 2.1
Fasting glucose (mM)	4.8 ± 0.4
2 h glucose (mM)	5.3 ± 1.1
Fasting insulin (pM)	32.2 ± 9.7
2 h insulin (pM)	175.5 ± 62.1
ISI-MATS	25.0 ± 7.1

M: male; f: female; BMI: body mass index; ISI-MATS: ISI Matsuda index indicating insulin sensitivity; Values are shown as means ± SEM.

The expression data clustered samples mainly according to the donors and not according to the treatment (data not shown). Thus, for statistical analysis a paired approach was used. In total 2,200 significantly regulated probe sets (FDR < 10 %), according to approximately 2,118 genes, were observed. The majority of the 2,200 probe sets showed only small expression changes between EPS and control. Genes were down- as well as upregulated by EPS (961 up, 1,259 down). A fold change > 1.2 times was observed in 368 probe sets (268 up, 100 down) and only 183 probe sets remained with a factor > 1.3 fold (153 up, 30 down). A heatmap showing the gene regulation upon the 183 probe sets is in the appendix (Supplementary Figure I). The top 20 upregulated genes of this subset are listed in Table 15. Amongst these, increased genes were *IL-8* (13.5 times), *CXCL1* (6.7 times), and *IL-6* (2.7 times). Further EPS-induced chemokines and cytokines were *IL-1B* (5.5 times) and *CXCL6* (5.6 times). Of note, several metallothioneins and matrix metallopeptidases were also upregulated by EPS. The expression of PPARG coactivators was either elevated at expression level (*PPARGC1A*, 1.3 times) or was predicted to be activated by Ingenuity software (*PPARGC1B*, data not shown).

Table 15: 20 most significantly upregulated genes upon EPS.

Gene ID	Gene description	Ratio > 1.3 (183), FDR < 10 %
IL-8	Interleukin-8	13.54
CXCL1	Chemokine (C-X-C motif) ligand 1	6.70
CXCL6	Chemokine (C-X-C motif) ligand 6	5.56
IL-1B	Interleukin-1, beta	5.49
MT1F	Metallothionein 1F	5.37
MMP1	Matrix metallopeptidase 1	5.18
MT1M	Metallothionein 1M	4.60
CLDN1	Claudin 1	4.53
TFPI2	Tissue factor pathway inhibitor 2	4.46
MMP3	Matrix metallopeptidase 3	4.12
MT1G	Metallothionein 1G	3.92
MT1X	Metallothionein 1X	3.64
SLC7A11	Solute carrier family 7	3.36
TRPA1	Transient receptor potential cation channel, subfamily A, member 1	3.28
CXCL10	Chemokine (C-X-C motif) ligand 10	3.04
ICAM1	Intercellular adhesion molecule 1	2.90
SOD2	Superoxide dismutase 2, mitochondrial	2.69
IL-6	Interleukin-6	2.67
CXCL2	C-X-C motif chemokine 2	2.65
MT1P3	Metallothionein 1 Pseudogene 3	2.58

Human myotubes obtained from 12 different donors were EP-stimulated for 24 h (14 V, 5 Hz, 2 ms). Afterwards, RNA was isolated and a whole genome transcriptome analysis (Affymetrix Gene 1.0 ST Array) performed. The table shows the 20 most upregulated genes that have a fold change > 1.3 times (total 183 significantly regulated probe sets) and a false discovery rate (FDR) < 10 %.

To assess the biological function of the regulated transcripts it was sought for enriched GO terms and enriched pathways connected with the observed transcriptional changes. The 183 probe sets with highest ratios were analyzed and a significant enrichment ($p < 0.01$; adj. $p > 0.05$) of terms and pathways related to inflammation, leukocyte migration, lipid metabolism, adaption of smooth muscle cell proliferation and signaling by NFκB, interleukins, chemokines, PPARG and metalloproteinases was found (Table 16).

Table 16: GO term and pathway analysis of the whole genome transcriptome analysis.

GO term or pathway association	GO term ID	p-value	Genes observed	Gene symbols of observed genes
Inflammatory response	GO:0006954	4.66E-10	20	CCL2, CCL5, C3, CXCL6, IL8, VCAM1, NFKBIZ, TNFAIP6, IRAK2, CCL11, IL1B, HMOX1, CXCL10, CXCL1, CXCL2, BDKRB1, TNFAIP3, CEBPB, AGTR1, IL6
Leukocyte migration	GO:0050900	6.16E-10	15	CCL2, CCL5, IL8, VCAM1, ANGPT1, SLC7A11, EDNRB, CCL11, IL1B, HMOX1, CMKLR1, MMP1, ICAM1, BDKRB1, IL6
Lipid metabolic process	GO:0006629	3.20E-06	26	LDLR, LPIN1, AKR1C2, ME1, CYP7B1, INSIG1, ABCC3, ELOVL2, SCD, FADS1, FADS2, FASN, ANGPTL4, DHCR7, IL1B, NPC1, PLIN2, LRP8, ABCA1, *CRABP2*, HSD11B1, TXNRD1, AKR1B10, AKR1C3, AGTR1, PTGES
Regulation of smooth muscle cell proliferation	GO:0048660	1.19E-04	5	CCL5, IGF1, HMOX1, TNFAIP3, IL6
Negative regulation of muscle cell apoptosis	GO:0010656	2.62E-03	2	*IGF1*, *NRG1*
NF KAPPA B		1.40E-11	27	CCL2, CCL5, CXCL6, IL8, VCAM1, NFKBIZ, NAMPT, SPP1, IRAK2, NFKBIA, CCL11, *ID1*, SOD2, IL1B, HMOX1, IER3, NFKB2, BIRC3, MMP1, CXCL10, CXCL1, CXCL2, ICAM1, TNFAIP3, CEBPB, IKBKE, IL6
INTERLEUKIN 1		1.52E-10	17	CCL2, LIF, MMP3, IL8, VCAM1, IRAK3, IRAK2, NFKBIA, SOD2, IL1B, MMP1, ZC3H12A, CXCL10, ICAM1, BDKRB1, IL6, PTGES
CHEMOKINE (C C MOTIF) LIGAND 2		2.98E-09	12	CCL2, CCL5, IL8, VCAM1, NAMPT, IL1B, ZC3H12A, CXCL10, CXCL1, CXCL2, ICAM1, IL6
PEROXISOME PROLIFERATOR ACTIVATED RECEPTOR GAMMA		1.64E-08	12	LPIN1, SCD, NAMPT, FADS2, FASN, NFKBIA, PLIN2, CXCL10, ABCA1, CEBPB, AGTR1, PTGES
MATRIX METALLO-PROTEINASE		5.58E-06	12	CCL2, CCL5, MMP3, IL8, TIMP4, NAMPT, SPP1, SOD2, IL1B, MMP1, CXCL10, PTGES

Shown are selected significantly ($p < 0.01$; adj. $p < 0.05$) enriched gene ontology (GO) terms and pathways associated with the subset of 183 significantly regulated probe sets, which were changed > 1.3 fold upon EPS vs. con. Genes that were down regulated are shown in italics, while all other genes were upregulated. Adapted from (Scheler et al., 2013).

3.1.6 EPS-induced secretion of cytokines

The whole genome transcriptome analysis showed among the 183 significantly regulated probe sets 35 that were supposed to be secreted as protein and among the top 10 regulated genes even 7. The translation of this transcriptional response into changes in the myotube secretome was investigated by targeted proteomic profiling of the supernatant.

A multiplex immunoassay was used to measure the secretion of selected proteins in supernatants of human primary myotubes obtained from the 12 different donors after 24 h of EPS (Table 17). Candidate proteins were selected based on the results of the array (see section 3.1.5). The secretion with highest fold increase compared to control was observed for IL-8 (44 ± 9 vs. 2 ± 0.3 pg/μg total protein). CXCL1 secretion was also remarkable increased upon 24 h of EPS (43 ± 9 vs. 5 ± 1 pg/μg total protein), same for IL-6 (72 ± 19 vs. 19 ± 3 pg/μg total protein). Increased protein secretion, which correlated to elevated RNA expression in the array, was also found for LIF, IL-1B and CCL2. Interleukins IL-2, IL-4, IL-13, IL-17A, TNF-α and CSF3 showed an increased protein secretion that was not in concordance with an increased RNA expression. The secretion of IL-5, IL-7, IL-10, IL-12, interferon-γ (INFG) and VEGF was not induced by EPS. Other proteins were below the detection limit of the multiplex immunoassay as IL1-RA, IL-15, IL-33 and CCL4. CSF2 secretion was below the concentration found in the control medium.

Table 17: Overview of secreted proteins detected by multiplex immunoassays in cell culture supernatant of myotubes after 24 h of EPS and their corresponding microarray expression data.

Analyte	Protein amount (pg analyte/µg protein) con	EPS	p-value	Fold change protein (EPS vs. con)	Linear ratio RNA (EPS vs. con)
IL-8	1.93 ± 0.29	43.9 ± 11.9	0.0019 *	20.8 ± 3.5	13.5
CXCL1	4.73 ± 1.21	42.7 ± 8.57	0.0002 *	10.4 ± 1.7	6.7
IL-6	18.9 ± 3.47	72.2 ± 19.3	0.0126 *	3.8 ± 0.6	2.7
LIF	0.15 ± 0.03	0.36 ± 0.05	0.0019 *	3.8 ± 1.1	2.2
IL-4	0.02 ± 0.01	0.03 ± 0.01	0.0350 *	1.7 ± 0.1	ns
IL-13	0.02 ± 0.01	0.04 ± 0.01	0.0025 *	1.7 ± 0.2	ns
IL-17A	0.11 ± 0.01	0.20 ± 0.03	0.0138 *	2.3 ± 0.3	ns
IL-1B	0.008 ± 0.001	0.015 ± 0.002	0.0256 *	1.8 ± 0.1	5.5
CSF3	0.25 ± 0.04	1.19 ± 0.42	0.0389 *	4.8 ± 1.2	ns
TNF	0.17 ± 0.03	0.27 ± 0.04	0.0294 *	1.8 ± 0.1	ns
CCL2	19.5 ± 2.28	25.3 ± 1.28	0.0369 *	1.5 ± 0.1	1.6
IL-2	[#]	0.04 ± 0.01	[#]	[#]	ns
IL-5	0.009 ± 0.001	0.012 ± 0.002	0.1907	ns	ns
IL-7	0.027 ± 0.004	0.033 ± 0.004	0.3290	ns	ns
IL-12	0.11 ± 0.02	0.13 ± 0.02	0.4519	ns	ns
IFNG	0.96 ± 0.13	1.27 ± 0.13	0.0989	ns	ns
IL-10	0.018 ± 0.003	0.021 ± 0.002	0.3480	ns	ns
VEGFA	7.83 ± 0.82	9.35 ± 0.86	0.2128	ns	ns
IL-1RA	nd	nd			ns
IL-15	nd	nd			ns
IL-33	nd	nd			ns
CCL4	nd	nd			ns
NAMPT	nd	nd			1.8
CSF2	[##]	[##]			ns

Table shows absolute protein amount in the supernatant of EPS and control (con) cells normalized to total cell protein amount (means ± SEM) with corresponding p value (* p < 0.05). The fold change of the protein secreted by EPS cells to control cells is shown as means ± SEM. Significantly regulated RNA expression is shown as linear ratio (results of array analysis, ratio > 1.3 times, false discovery rate < 10 %). # IL-2 could not be detected in the supernatant of control cells but in 9 of 12 EPS-supernatants. ## CSF2 concentration in the reference medium was higher as in samples. nd: not detectable, below limit of detection; ns: not significant; Table adapted from (Scheler et al., 2013).

Interestingly, the myotubes of the 12 different donors showed a wide range of cytokine release. This is exemplarily demonstrated for IL-8, CXCL-1 and IL-6, the three secreted proteins that are reaching the highest concentration in the supernatant (Figure 12 A-C). The fold change of their secretion reveals a strong correlation with the ratio of their gene transcripts after 24 h of EPS (Figure 12 D-F).
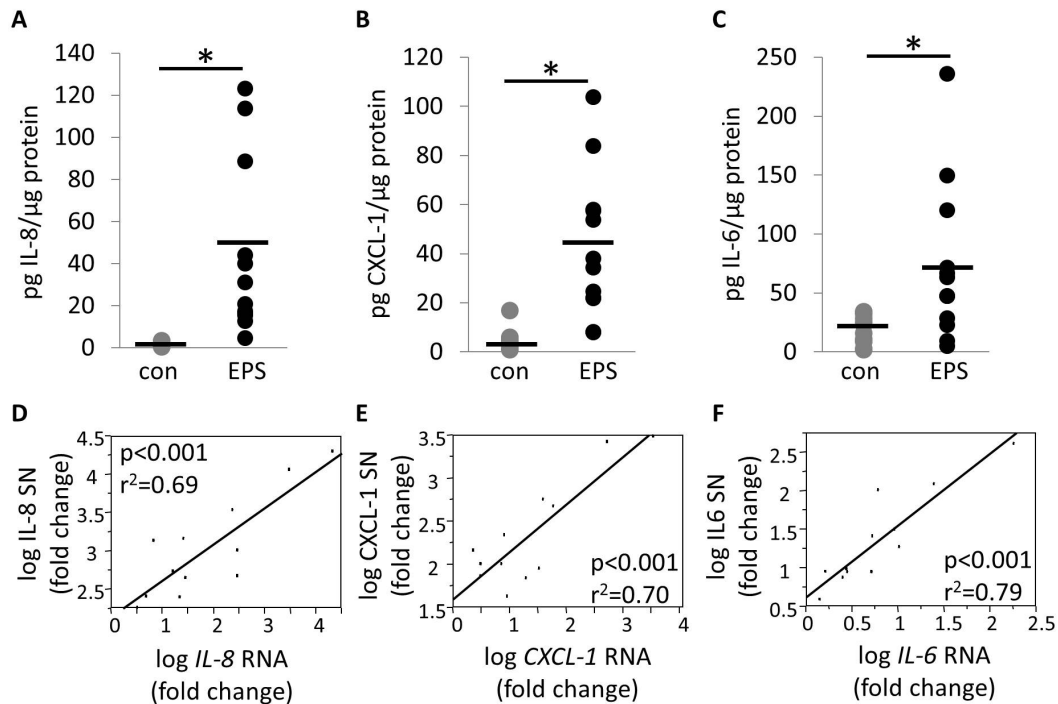
Figure 12: Myotubes of different donors reveal a wide range of cytokine secretion.
(A-C) Supernatants of 12 human myotubes were analyzed for IL-8, CXCL-1 and IL-6 secretion after 24 h of EPS. The dots show the individual secretion value of the myotubes as pg analyte/µg protein, the mean value is indicated by the black line (means ± SEM as depicted in Table 17). Statistical analysis was done between supernatant of EPS and control cells (*p < 0.05). (D-F) Correlation of the secreted protein (SN as fold change to control cells) with mRNA level (RNA level as fold change to control cells) for IL-8, CXCL-1 and IL-6 after 24 h of EPS (n = 12). Figures from (Scheler et al., 2013).

To ensure that this finding is not influenced by the individual myotube formation and differentiation, the fusion index, a measure for myotube differentiation, was calculated. Therefore, the human myotubes were divided in two groups: myotubes with a high *IL-8* expression and IL-8 secretion after 24 h of EPS and myotubes with lower expression and secretion (further called high and low IL-8 responder, Figure 13A, B). The fusion index showed no difference between these two groups, which implies similar myotube formation (Figure 13C). Additionally, the RNA expression of several differentiation markers, CKM, MYH2 and MYH7, did not correlate with the upregulated *IL-8* RNA expression (Figure 13 D-F). In summary, data indicate that the altered secretion pattern between myotubes obtained from different donors is not caused by variable myotube formation and differentiation.
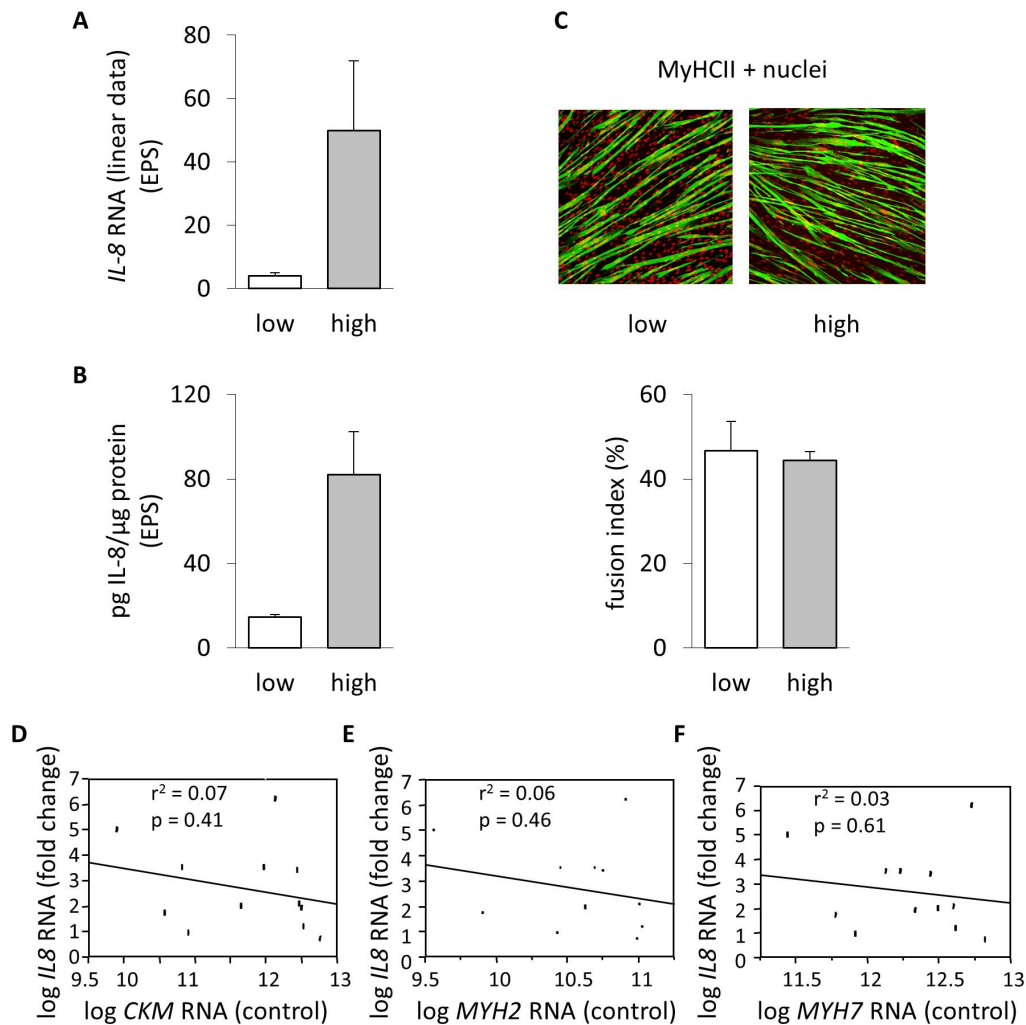
Figure 13: Cytokine secretion of myotubes obtained from different donors is independent of myotube formation and differentiation.
(A-C) Immunostaining of MyHCII protein (C, 10x magnification, in green) in human myotubes showing a low or high *IL-8* RNA expression (A) or IL-8 protein secretion (B) upon 24 h of EPS (values are shown as means ± SEM, n = 3 per group). Nuclei are shown in red. Fusion index was calculated by dividing nuclei of MyHCII positive myotubes by the total number of nuclei counted. (D-F) Correlation of RNA levels in control cells (basal expression) of CKM, MYH2 or MYH7 with EPS-induced *IL8* RNA expression (RNA level as fold change to control cells) after 24 h of EPS (n = 12). Figures from (Scheler et al., 2013).

Since the individual *IL-8* mRNA expression and secretion could not be clarified by the fusion index, we searched for further candidates and signaling pathways that might induce the individual response. Therefore, the data obtained from the genome-wide transcriptome analysis were investigated for significantly regulated probe sets (p < 0.01) that had a different basal expression when grouping myotubes with a low *IL-8 / IL-6* response to EPS and comparing them to myotubes with high response. This revealed 443 significantly regulated probe sets. A heatmap showing the top 45 regulated genes is shown in the appendix (Supplementary Figure II).

3.1.7 Different expression kinetics of cytokines, PPARGC1A, NAMPT and ANGPTL4

The genome-wide transcriptome analysis demonstrated a significant increase in angiopoietin-like 4 (*ANGPTL4*; 1.6 fold) and nicotinamide phophoribosyltransferase (*NAMPT*; 1.8 fold) mRNA expression. The study of the kinetic of these new EPS targets showed that *NAMPT* behaves similar to *IL-6* expression (Figure 11). It is significantly enriched after 8 h of EPS and further accumulates when stimulating for 24 h (Figure 14A). *ANGPTL4* mRNA expression peaks the maximum after 4 h of EPS (Figure 14B). This is in accordance with an increased secretion of ANGPTL4 after 8 h of EPS (1.8 ± 0.3 ng/mL vs. 1.1 ± 0.2 ng/mL) from myotubes into the supernatant while NAMPT protein could not be detected because the level was under the limit of detection. The different RNA expression kinetics of *IL-6*, *IL-8*, *PPARGC1A* (Figure 11), *NAMPT* and *ANGPTL4* (Figure 14) in EP-stimulated myotubes suggests that different signal transduction pathways are activated during EPS that mediate transcriptional responses of different sets of genes.
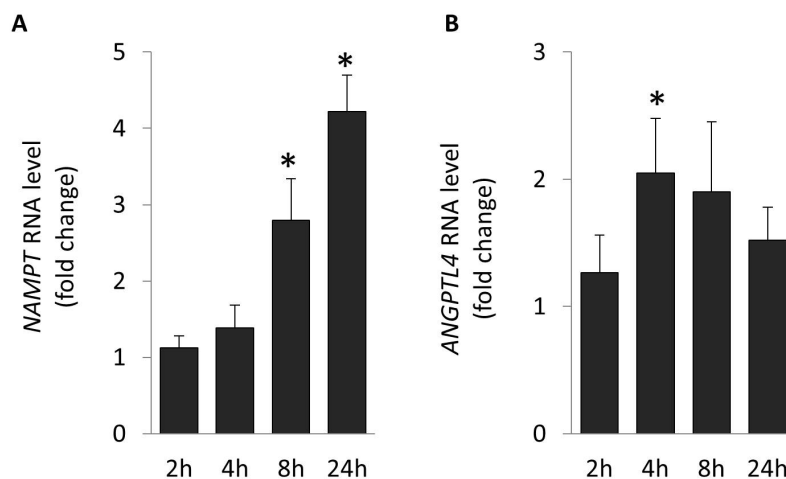
Figure 14: EPS increases the RNA expression of nicotinamide phosphoribosyltransferase (NAMPT) and angiopoietin-like 4 (ANGPTL4).
(A) NAMPT and (B) ANGPTL4 mRNA expression were measured in myotubes that were EP-stimulated for 2, 4, 8, 24 h with 14 V, 5 Hz, 2 ms. After EPS, RNA was isolated and mRNA level determined by qRT-PCR. Values are normalized to levels of housekeeping gene TBP and are shown as fold increase to control cells (means ± SEM; n = 8). Statistical analysis was performed between levels in control and EPS cells (* $p < 0.05$ significant increase). Figures from (Scheler et al., 2013).

3.1.8 Cytokine secretion and its effect on insulin sensitivity of myotubes

To investigate whether cytokine secretion during EPS has any impact on insulin sensitivity of the human myotubes and thus influences insulin signaling, conditioned medium of myotubes EP-stimulated for 24 h was incubated on so far untreated cells for 4 h. Afterwards cells were stimulated with insulin for 10 min and Akt phosphorylation (Ser473) was analyzed by immunoblotting (Figure 15). Medium without FBS was included to expose any putative effects of FBS components on insulin signal transduction. Insulin stimulation showed a dose-dependent increase in

Akt phosphorylation with no further effect of the conditioned medium with or without FBS. It seems, that the EPS-induced secretion of several cytokines does not influence insulin sensitivity of human myotubes treated with the conditioned medium.
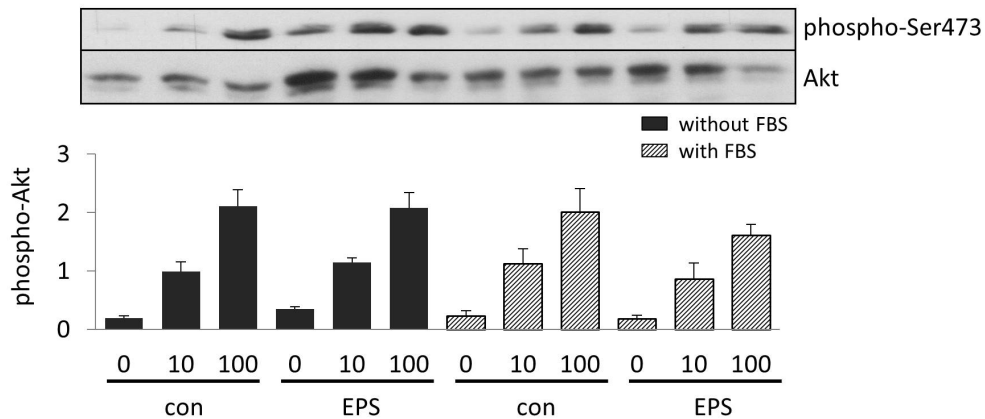
Figure 15: EPS-induced secretion of cytokines does not influence insulin sensitivity of human myotubes. Myotubes were EP-stimulated for 24 h with 14 V, 5 Hz and 2 ms in fusion medium with or without FBS. Conditioned medium was transferred to untreated myotubes. After 4 h, medium was changed to α-MEM and cells stimulated with 0, 10 or 100 nM insulin for 10 min. Ser473 phosphorylation of Akt was detected by immunoblotting of myotube cell lysates. Membrane was reprobed for Akt protein. Histogram shows the result of the densitometric quantification as means ± SEM (n = 3-4).

3.1.9 EPS activates MAPK signaling and NFκB

Former studies showed that EPS leads to increased phosphorylation and activation of the MAPK, ERK1/2 and JNK (Nedachi et al., 2008; Lambernd et al., 2012). Here, we wanted to verify that these findings can be further confirmed with our EPS model. Human myotubes EP-stimulated with 14 V, 5 Hz and 2 ms revealed an increased ERK1/2 and JNK phosphorylation after 2 and 4 h, respectively (Figure 16A, B), which decreased with longer stimulation. MAP-kinases ERK5 and p38 showed no EPS-induced phosphorylation at any time point (Figure 16C, D).
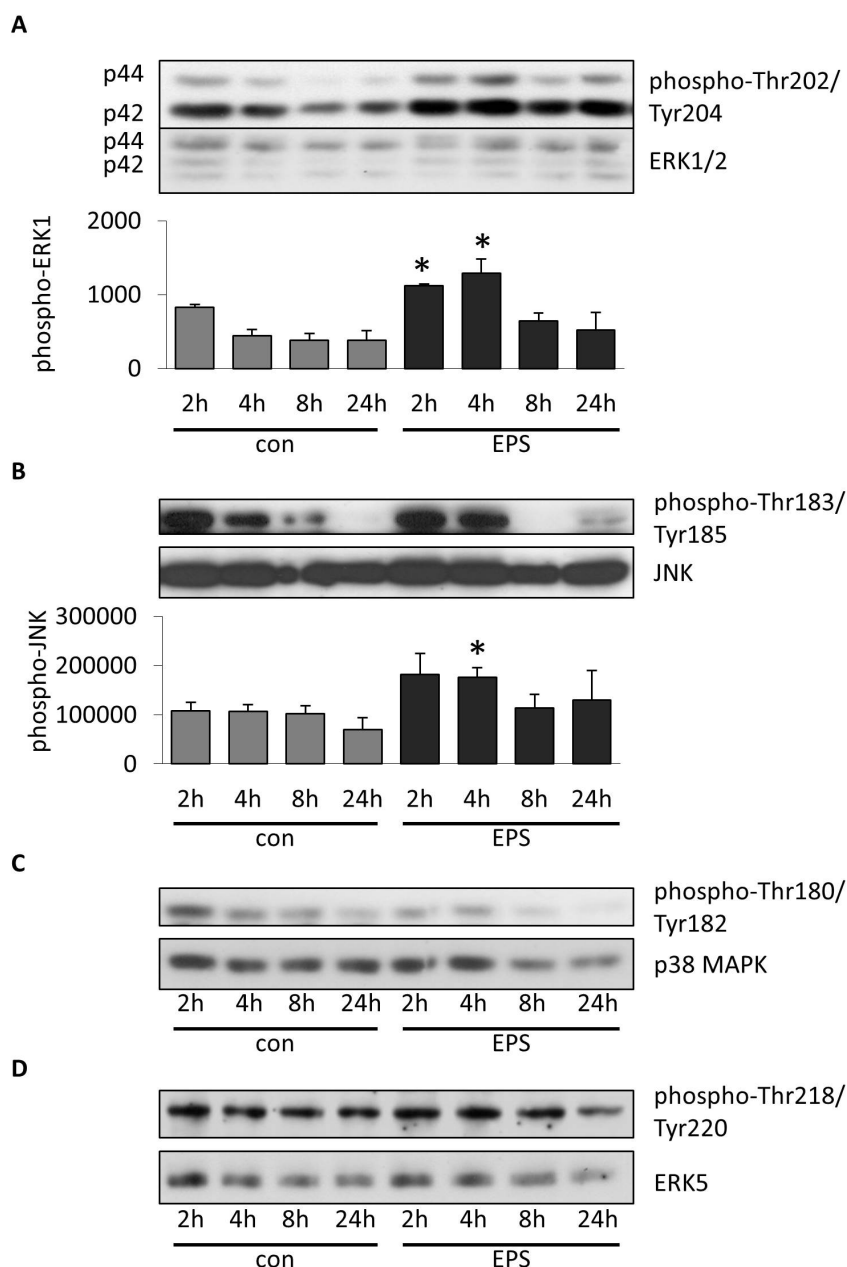
Figure 16: Activation of MAPK signaling in response to EPS in human myotubes.
(A) Phosphorylation of ERK1/2 and (B) JNK was detected by immunoblotting of cell lysates from EP-stimulated myotubes (2, 4, 8 or 24 h of EPS). Membrane was reprobed for ERK1/2 or JNK protein, respectively. Histogram shows the densiometric quantification (means ± SEM, n = 3; * p < 0.05 vs. control cells). (C) Phosphorylation of p38 MAPK and (D) ERK5 was detected by immunoblotting of cell lysates obtained after a certain time of EPS. Membranes were reprobed for p38 MAPK protein or ERK5 protein, respectively. Figures from (Scheler et al., 2013).

The analysis of the genome-wide transcriptome analysis resulted in a significant enrichment of genes associated with NFκB (Table 16). Subsequently, the connection between MAPK signaling or NFκB, respectively, and its influence on gene expression was analyzed. Therefore, myotubes were treated with inhibitors directed against MEK1/2 (U0126), JNK (JNK VIII) or NFκB (BAY11-7082) during either 4 h or 24 h of EP-stimulation. Exemplarily, gene expression of *IL-8*, *PPARGC1A* and *ANGPTL4* was studied, all transcripts that are increased by EPS but are supposed to be

regulated by different pathways due to their different kinetics of expression (Figure 17 A-C). Inhibition of MEK1/2 regulated *IL-8*, *PPARGC1A* expression (after 4 h and 24 h) and early induction of *ANGPTL4* (after 4 h). Inhibition of JNK resulted in decreased *IL-8* (after 4 h) and *PPARGC1A* expression (after 24 h) and had no effect on *ANGPTL4* expression. Inhibition of NFκB affected only *IL-8* upregulation after 24 h of EPS. Interestingly, MEK1/2 inhibitor U0126 also inhibited EPS-induced NFκB activation, proposing a role for ERK1/2 in the EPS-induced activation of NFκB (Figure 17 D).
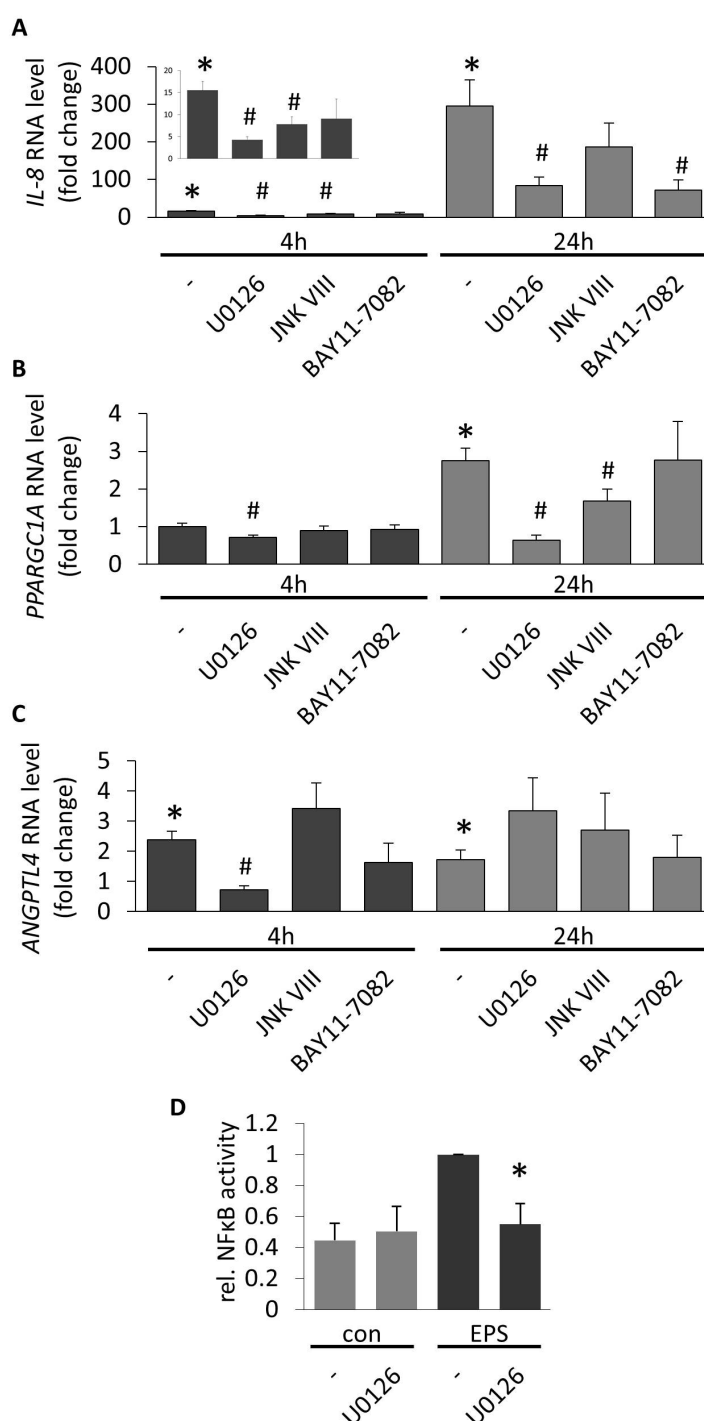
Figure 17: ERK1/2, JNK an NFκB signaling influence EPS-induced expression of IL-8, PPARGC1A und ANGPTL4.
(A) *IL-8,* (B) *PPARGC1A* and (C) *ANGPTL4* mRNA levels were measured in human myotubes that were EP-stimulated for either 4 h or 24 h and simultaneously treated without inhibitor, MEK1/2 inhibitor (U0126; 10 μM), JNK inhibitor (JNK VIII; 10 μM) or NFκB inhibitor (BAY11-7082; 5 μM). Values are normalized to levels of housekeeping gene TBP and shown as fold change to control mRNA level without inhibitor (means ± SEM, n = 8-12). Statistical analysis was performed between RNA levels of EP-stimulated and control cells without inhibitor (* p < 0.05 significant increase) and between EP-stimulated cells with and without inhibitor of respective EPS duration (# p < 0.05 significant decrease). (D) NFκB activity was measured by TransAM NFκB p65 assay in nuclear extracts of human myotubes that had been EP-stimulated for 24 h in the absence or presence of 10 μM ERK1/2 inhibitor (U0126). EPS-treated samples were set as 1. Values are shown as means ± SEM (n = 6; *p < 0.05 vs. EPS treated cells without inhibitor). Figures from (Scheler et al., 2013).

3.1.10 EPS-induced IMTG storage

Intramuscular triglycerides (IMTG) are important energy sources for the muscle during exercise training and recovery phase (Phillips et al., 1996; Kiens and Richter, 1998). Prolonged exercise training leads to an increase in IMTGs (Pruchnic et al., 2004; Shaw et al., 2012). Here, we aimed to investigate IMTG storage in human myotubes and its regulation by repetitive EP-stimulating exercise training. Therefore, over 4 days myotubes were either incubated with oleic acid alone, with a mixture of oleic acid and insulin to induce triglyceride storage or were EP-stimulated for 4 h per day and simultaneously incubated with oleic acid. Since oleic acid was linked to BSA, myotubes treated with BSA were used as control. Intracellular triglycerides were elevated with the addition of oleic acid and further tended to increase with the supplementation of insulin or the application of EPS (Figure 18). Thus, EPS over several days can mimic the effect of prolonged exercise training on IMTG storage in human myotubes.
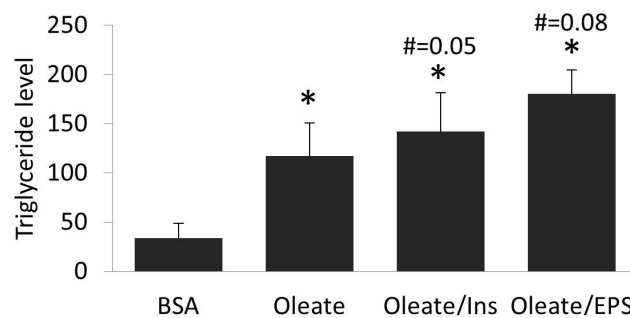
Figure 18: EPS-induced intramuscular triglyceride storage.
Myotubes were treated for 4 days either with BSA, 250 mM oleate, 250 mM oleate/ 100 nm insulin (Ins) or with 250 mM oleate and EPS for 4 h per day (14 V, 5 Hz, 2 ms). Medium including supplements was changed daily. 24 h after last stimulation, cells were harvested and triglyceride content determined by an enzyme coupled assay measuring glycerol. Absolute values are shown in μg Triglyceride/ mg protein (means ± SEM; n = 4; *p < 0.05 to BSA; #p-value to oleate).

65

3.2 EPS of myotubes obtained from different donors

In the first part of this thesis, it was shown that myotubes obtained from different donors show an individual response to EPS. In the second part, myotubes from insulin-sensitive (IS-myotubes) and insulin-resistant donors (IR-myotubes) were investigated to find novel markers for insulin sensitivity and resistance, respectively. Furthermore, we intended to identify pathomechanistic alterations, e.g. changes in lipid metabolism during basal and exercise conditions.

3.2.1 Further improvement of the EPS protocol

For this study, the EPS protocol was further optimized. On the one hand, Magnetic activated cell sorting (MACS) was included enabling the enrichment of myoblasts by the purification via magnetically labeled beads detecting CD56 cell surface marker (de Luna et al., 2006; Stadler et al., 2011).

On the other hand, Matrigel (gelatinous protein mixture containing structural proteins, as laminin, entactin, collagens and heparan sulfate, and growth factors) coating was implemented to provide the myoblasts and myotubes, which are surrounded by extracellular matrix *in vivo*, a more physiological surrounding (Funanage et al., 1992). Moreover, the stimulation time was shortened to 8 h and a recovery phase of 16 h was included afterwards since it is suggested that many exercise-induced transcriptional adaptations, e.g. *PPARGC1A*, in the skeletal muscle occur during recovery phase (Mahoney et al., 2005; Leick et al., 2010; Neubauer et al., 2014).

It is known that during acute exercise adipose tissue lipolysis is increased, resulting in elevated levels of free fatty acids (FFA) in plasma (Catoire et al., 2014). To establish a more physiological environment, FFA (125 μM palmitic acid and 125 μM oleic acid) and 100 μM L-carnitine, required for the transport of fatty acids into mitochondria, was supplemented to the medium during stimulation. Pre-experiments showed an increased *IL-6* mRNA expression directly after end of 8 h stimulation, which decreased during recovery time (Figure 19A). In contrast, *PPARGC1A* showed a clear trend towards an elevated mRNA level upon EPS after recovery phase (Figure 19B).
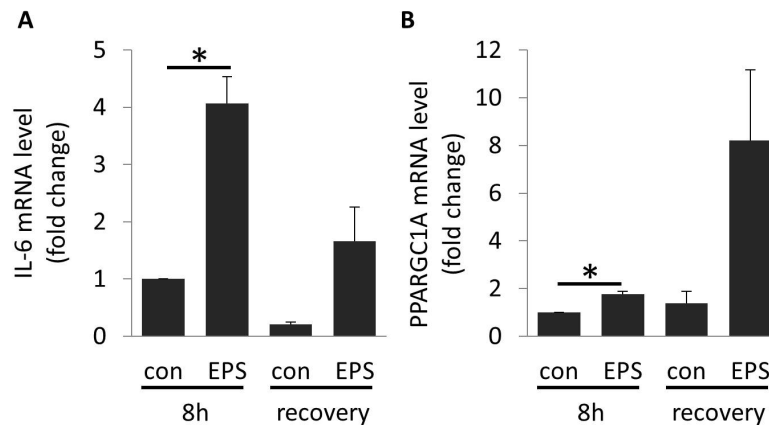
Figure 19: Recovery phase affects PPARGC1A mRNA expression but not IL-6 mRNA expression.
Magnetic activated cell sorted myoblasts were seeded on Matrigel coated cell culture dishes and differentiated to myotubes. (A) *IL-6* and (B) *PPARGC1A* mRNA expression was measured in myotubes that were EP-stimulated for 8 h with 14 V, 5 Hz, 2 ms and either harvested directly after end of stimulation or after 16 h of recovery phase. During stimulation medium was supplemented with 100 µM L-carnitine, 125 µM palmitate, 125 µM oleate. RNA was isolated and mRNA level determined by qRT-PCR. Values are normalized to levels of housekeeping gene TBP and are shown as fold change to con, 8 h (means ± SEM; n = 3). Statistical analysis was performed between levels in control and EPS cells of the respective time point (* $p < 0.05$).

3.2.2 Acylcarnitine profiling

Fatty acids are an important energy source during prolonged exercise and once inside the cell are activated by esterification to CoA. The breakdown of fatty acids, called β-oxidation, occurs in the mitochondria. To pass the mitochondria membrane, acyl-CoAs are converted to acylcarnitines by carnitine palmitoyltransferase 1 (CPT1). However, breakdown might occur only partially and intermediates might be shuttled out of the mitochondria as acylcarnitines.

Earlier studies revealed that exercise leads to increased plasma acylcarnitine levels, which might influence muscle metabolism (Lehmann et al., 2010). Additionally, plasma acylcarnitines are elevated in obese and T2D patients (Newgard et al., 2009; Mihalik et al., 2010). Less is known about the acylcarnitine production in the skeletal muscle. Here, we investigated intracellular acylcarnitine production in human myotubes obtained from donors that differed in ISI Matsuda index (ISI-MATS) and thus in insulin sensitivity (Table 18) and searched for acylcarnitines that were changed between the two groups upon EPS or after recovery phase.

Table 18: Characteristics of the myotube donors used in this study.

Characteristics	Insulin-sensitive IS	Insulin-resistant IR	p-val
Gender (m/f)	6 (5/1)	6 (5/1)	
Age (y)	31.8 ± 7.0	34.8 ± 7.0	0.474
BMI	24.3 ± 4.1	27.8 ± 4.2	0.177
Fasting glucose (mM)	4.8 ± 0.2	5.4 ± 0.5	0.015*
2 h glucose (mM)	5.4 ± 0.7	6.5 ± 1.2	0.080
Fasting insulin (pM)	25.0 ± 12.3	69.3 ± 33.0	0.012*
2 h insulin (pM)	126.7 ± 60.5	421.5 ± 121.1	< 0.001*
ISI-MATS	30.5 ± 8.5	8.9 ± 2.7	< 0.001*

M: male; f: female; BMI: body mass index; ISI-MATS: ISI Matsuda index indicating insulin sensitivity; *p < 0.05 significant difference between insulin-sensitive donors and insulin-resistant donors.

Differentiated myotubes were EP-stimulated for 8 h and harvested directly afterwards or after 16 h of recovery. During EPS 100 μM L-carnitine, 125 μM ^{13}C-palmitate and 125 μM oleate were supplemented to the medium. Cell lysates were analyzed by stable isotope dilution-based metabolomic analysis using ultra performance lipid chromatography system coupled with linear ion-trap quadrupole orbitrap hybrid mass spectrometer to investigate the production of acylcarnitines. In total, 12 unlabeled and 9 ^{13}C-labeled acylcarnitines were detected among them acetylcarnitine (C2), short-chain (C3-C5), medium-chain (C6-C12) and long-chain acylcarnitines ($> $C12) (Figure 20). Three unsaturated acylcarnitines were identified but no hydroxylated or branched-chain acylcarnitines. Figure 20 depicts that myotubes obtained from donors with different insulin sensitivity reveal no significant changes in intracellular acylcarnitine production. Nevertheless, in both groups intracellular acylcarnitine levels increased with recovery phase.

Additionally, myotubes from insulin-sensitive donors show a trend towards decreased acetylcarnitine to free carnitine ratio (C2-AC/C0), demonstrating a lower β-oxidation rate after 8 h of EPS (Figure 21A, B). The propionylcarnitine to carnitine (C3-AC/C0) ratio was increased in all myotubes obtained from insulin-resistant donors during all four conditions (Figure 21C, D). Propionylcarnitine emerge from breakdown of amino acids and odd-numbered long-chain fatty acids.
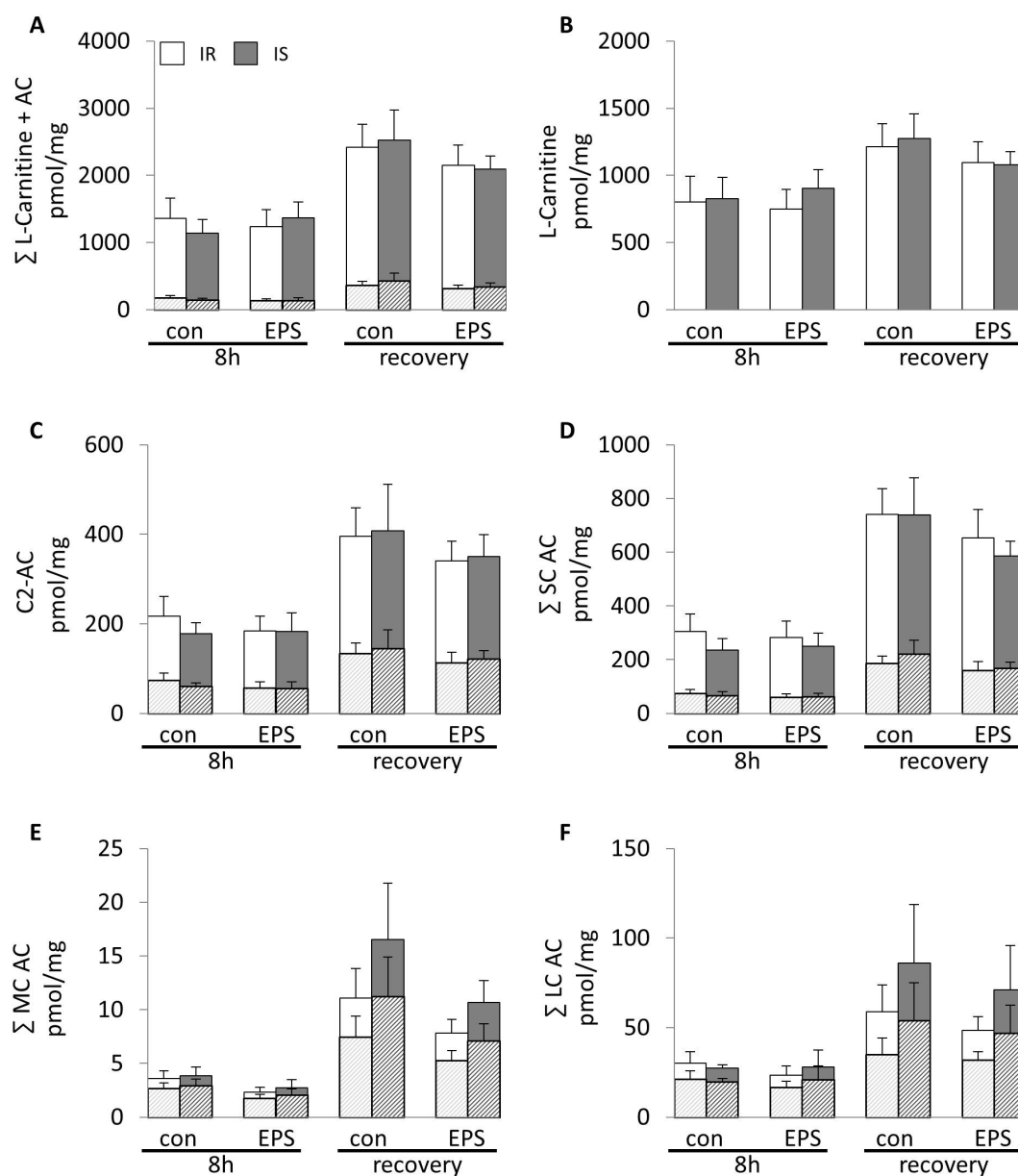
Figure 20: Intracellular acylcarnitine and L-carnitine content is not different in myotubes obtained from donors with different insulin sensitivity.
(A-F) Intracellular acylcarnitines (AC) and free L-carnitine contents were investigated in myotubes of insulin-resistant (IR; light columns) and sensitive donors (IS; dark columns), which were EP-stimulated for 8 h and harvested directly at the end of stimulation or after 16 h of recovery. Control cells (con) were treated equally. During stimulation, medium was supplemented with 100 μM L-carnitine, 125 μM ^{13}C-palmitic acid and 125 μM oleic acid and cell lysates analyzed by ultra performance lipid chromatography system coupled with linear ion-trap quadrupole orbitrap hybrid mass spectrometer. The sum of the ^{12}C and ^{13}C acylcarnitines is shown as plain column, whereas ^{13}C-labeled species are shown as hatched columns. Values are shown as pmol/mg dry weight (mean ± SEM; n = 5-6). C2-AC: acetylcarnitine; SC AC: short-chain acylcarnitines (C3-C5); MC AC: medium-chain acylcarnitines (C6-C12); LC AC: long-chain acylcarnitines (> C12).
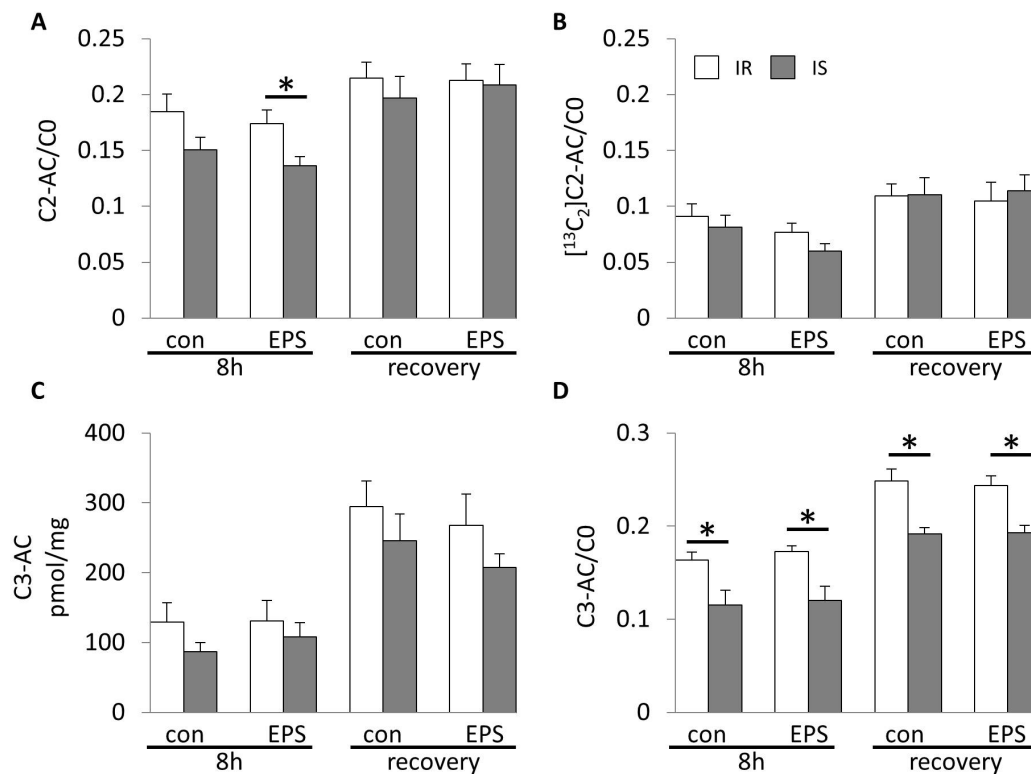
Figure 21: Myotubes obtained from donors with different insulin sensitivity show different C3-AC/C0 ratio.
(A-B) Ratio of intracellular unlabeled or ^{13}C-labeled acetylcarnitine (C2-AC) to free L-carnitine and (C-D) propionylcarnitine (C3-AC) level and ratio to free L-carnitine (C3-AC/C0) investigated in myotubes of insulin-resistant (IR; white columns) and sensitive donors (IS; grey columns), which were EP-stimulated for 8 h and harvested directly at the end of stimulation or after 16 h of recovery. Control cells (con) were treated equally. During stimulation, medium was supplemented with 100 μM L-carnitine, 125 μM ^{13}C-palmitic acid and 125 μM oleic acid and cell lysates analyzed by ultra performance lipid chromatography system coupled with linear ion-trap quadrupole orbitrap hybrid mass spectrometer for acylcarnitines. Values are shown as means ± SEM (n = 5-6). C3-AC level is indicated as pmol/mg dry weight.

There are no significant differences between the IR-myotubes and IS-myotubes in C16 acylcarnitine to carnitine ratio (Figure 22), indicating no difference in carnitine palmitoyltransferase 1 activity (Fingerhut et al., 2001).
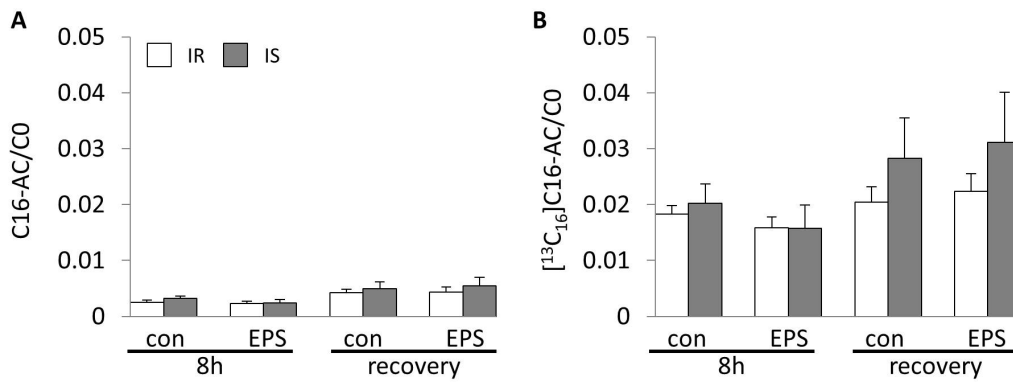
Figure 22: Myotubes obtained from donors with different insulin sensitivity show no difference in carnitine palmitoyltransferase 1 activity.
(A) Ratio of intracellular unlabeled or (B) ^{13}C-labeled palmitoylcarnitine (C16-AC) to free L-carnitine investigated in myotubes of insulin-resistant (IR; white columns) and sensitive donors (IS; grey columns), which were EP-stimulated for 8 h and harvested directly at the end of stimulation or after 16 h of recovery. Control cells (con) were treated equally. During stimulation, medium was supplemented with 100 μM L-carnitine, 125 μM ^{13}C-palmitic acid and 125 μM oleic acid and cell lysates analyzed by ultra performance lipid chromatography system coupled with linear ion-trap quadrupole orbitrap hybrid mass spectrometer for acylcarnitines. Values are shown as mean ± SEM (n = 5-6).

In summary, thus far intramyocellular propionylcarnitine levels seems to be a major difference in acylcarnitine metabolism between IS-myotubes and IR-myotubes.

3.3 Search for new myokines

Proteins produced and secreted by the muscle are supposed to play a major role in the health-promoting effects of exercise. We used an untargeted proteomic profiling approach to discover new contraction-induced myokines and myokines that are differently regulated in human myotubes obtained from insulin-sensitive and resistant donors.

The protein profile of the supernatant of EP-stimulated human primary myotubes was analyzed by a gel-based (2D-DIGE and spot identification via MALDI-MS) and gel-free separation technique (LC-MS/MS). The myotubes originated of six different donors and were separated according to their ISI Matsuda index (ISI-MATS) and their body mass index (BMI) in two groups (Table 19): a rather insulin-sensitive and lean group (IS) and a rather insulin-resistant and moderately obese group (IR). Medium without FBS was used in this study because serum is one of the most complex proteomes, spanning a concentration range of at least 10 magnitudes (Issaq et al., 2007) and thus disturbs untargeted proteomic analysis.

Table 19: Characteristics of the myotube donors used for the search of new myokines.

Characteristics	Total	Insulin-sensitive (IS)	Insulin-resistant (IR)	p-val
Gender (m/f)	5/1	2/1	3/0	-
Age (y)	28.3 ± 2.0	24.0 ± 1.7	32.7 ± 0.3	0.001*
BMI	26.3 ± 2.0	22.2 ± 1.4	30.4 ± 0.8	0.007*
ISI-MATS	20.0 ± 5.7	31.4 ± 5.3	8.7 ± 2.0	0.016*
Fasting glucose (mM)	5.3 ± 0.2	4.9 ± 0.2	5.7 ± 0.3	0.070
2 h glucose (mM)	6.1 ± 0.5	5.3 ± 0.3	6.9 ± 0.7	0.112
Fasting insulin (pM)	47.8 ± 16.9	22.7 ± 4.1	73.0 ± 28.0	0.150
2 h insulin (pM)	306.0 ± 87.2	134 ± 55.6	478.0 ± 73.2	0.020*

M: male; F: female; BMI: body mass index; ISI-MATS: Matsuda-Index; IS: myotubes obtained from 3 insulin-sensitive and lean donors; IR: myotubes obtained from 3 insulin-resistant, moderately obese donors. *p < 0.05 significant difference between insulin-sensitive donors and insulin-resistant donors.

3.3.1 Proteomic profile of the muscle secretome by LC-MS/MS

In a first approach 5 µg protein of the concentrated supernatants obtained from the human myotubes was analyzed by LC-MS/MS and data investigated for differences upon EPS and insulin sensitivity of myotubes donor (basal secretion). Additionally, we wanted to find differences between myotubes of insulin-sensitive and resistant donors upon EP-stimulation.

3.3.1.1 Differences induced by Electric pulse stimulation

To find novel EPS-induced myokines the control and EPS-supernatant of human myotubes was analyzed by LC-MS/MS. In total, 170 proteins that revealed altered extracellular levels upon EPS were found ($p < 0.05$; increased in EPS-supernatant: 85, decreased in EPS-supernatant: 85). A complete list of these proteins is shown in the appendix (Supplementary Table I). Of note, EPS-myotubes show a decreased extracellular level of seven identified collagens: COL4A1 (0.63 fold), COL5A3 (0.60 fold), COL5A2 (0.56 fold), COL1A1 (0.53 fold), COL1A2 (0.51 fold), COL3A1 (0.46 fold) and COL8A1 (0.46 fold).

To gain a general idea about the biological function of all significantly changed proteins upon EPS a GO term pathway analysis was performed. Several interesting pathways associated with extracellular matrix organization and disassembly, cell matrix adhesion, collagen catabolic process and cell proliferation were enriched (Table 20).

Table 20: GO term analysis EPS vs. con of the LC MS/MS results.

Name	ID	P-value	Proteins observed	Protein symbols of observed proteins
extracellular matrix organization	GO:0030198	3.97E-36	23	*MFAP5, PXDN, COL3A1, CTSL1, LAMA1,* PPIB, LGALS3, CTSB, *COL5A3, POSTN, COL1A2, NCAM1, COL8A1, COL1A1, COL5A2, OLFML2A, COL4A1, ABI3BP, BMP1,* CCDC80, *ELN, LAMA2, ITGB1*
extracellular matrix disassembly	GO:0022617	1.19E-17	11	*COL1A2, COL8A1, COL1A1, COL5A2, COL4A1, COL3A1,* CTSL1, *BMP1, ELN,* CTSB, *COL5A3*
collagen catabolic process	GO:0030574	8.73E-18	9	*COL1A2, COL8A1, COL1A1, COL5A2, COL4A1, COL3A1,* CTSL1, CTSB, *COL5A3*
skeletal muscle development	GO:0001501	7.66E-11	8	*COL1A2, COL1A1, COL5A2, COL3A1, BMP1, IGFBP4, LGALS3, POSTN*
cell proliferation	GO:0008283	2.12E-07	8	LRP1, UCHL1, BCAT1, *RAC1, IGFBP4, UBE2V2, ELN,* TXN
cell-matrix adhesion	GO:0007160	3.01E-08	6	*COL3A1, RAC1, THBS3, BCAM, ITGB1, COL5A3*
inflammatory response	GO:0006954	1.01E-04	6	ANXA1, PRDX5, LTA4 h, *RAC1, IGFBP4, RARRES2*

Shown are selected enriched gene ontology (GO) terms associated with the 170 proteins that had an altered secretion upon EPS ($p < 0.05$; only proteins that are predicted to be secreted via classical or non-classical pathway). Proteins that were less secreted upon EPS are shown in italics, all others are higher secreted upon EPS.

When including proteins that were declared as non-secreted (NP) by SignalP and SecretomeP database (Bendtsen et al., 2004; Petersen et al., 2011) the number of proteins increased to 228 ($p < 0.05$; increased in EPS-supernatant: 125; decreased

in EPS-supernatant in EPS: 103). In general, EPS seems to have highest impact on proteins involved in extracellular matrix remodeling.

3.3.1.2 Differences among insulin sensitivity

Next, the basal protein release of myotubes obtained from insulin-sensitive and resistant donors was investigated by LC-MS/MS analysis. Comparing the protein profile of the control supernatant obtained from IR-myotubes with IS-myotubes, 115 proteins were significantly different ($p < 0.05$), whereas 62 proteins were increased in IR supernatant and 53 decreased (appendix, Supplementary Table II). GO term analysis revealed a significant enrichment of terms associated with extracellular matrix organization, disassembly and structural constituent, as well as cell matrix adhesion (Table 21). Interestingly, several terms associated with the 20S core proteasome complex emerged, amongst others RNA metabolic process, proteasome core complex and protein polyubiquitination.

Table 21: GO term analysis of proteins significantly regulated between IR-myotubes and IS-myotubes in the control supernatants by LC-MS/MS analysis.

Name	ID	P-value	Proteins observed	Protein symbols of observed proteins
extracellular matrix organization	GO:0030198	1.02E-36	20	*COL12A1*, OLFML2B, COL18A1, *LAMA1, FBLN1, EFEMP1, SERPINH1,* COL5A3, *VCAN, NCAM1,* COL15A1, *COL8A1, COL5A2,* OLFML2A, PLOD1, *LOX, LAMA2, FBN1, FMOD,* MMP1
extracellular matrix disassembly	GO:0022617	1.13E-12	8	*COL12A1*, COL8A1, *COL5A2,* COL18A1, COL5A3, *FBN1,* MMP1
RNA metabolic process	GO:0016070	5.53E-10	8	PSMA2, RPS12, PSMB4, HSPA8, RPL12, PSMA6, PSMB5, PSMB6
extracellular matrix structural constituent	GO:0005201	2.27E-10	6	COL15A1*, COL5A2, LAMA1, FBLN1,* COL5A3, *FBN1*
proteasome core complex	GO:0005839	3.43E-10	5	PSMA2, PSMB4, PSMA6, PSMB5, PSMB6
protein polyubiquitination	GO:0000209	3.54E-06	5	PSMA2, PSMB4, PSMA6, PSMB5, PSMB6
cell-matrix adhesion	GO:0007160	6.70E-05	4	RAC1, *THBS3, EPDR1,* COL5A3

Shown are selected enriched gene ontology (GO) terms associated with the 115 proteins that were significantly altered in the control supernatant of IR- and IS-myotubes (p < 0.05; only proteins that are secreted by classical or non-classical secretion pathway). Proteins that were less secreted in the supernatant of IR-myotubes are shown in italics, all others are higher secreted in the supernatant of IR-myotubes.

Six proteins belonging to the standard core proteasome were significantly enriched in the supernatant of IR-myotubes: PSMA2 (2.13 fold), PSMA4 (1.83 fold), PSMA6 (1.77 fold), PSMB4 (2.45 fold), PSMB5 (1.73 fold) and PSMB6 (1.76 fold). All these proteasomal subunits are predicted to be secreted by the non-classical, i.e. not signal peptide triggered, pathway (SP-)(Bendtsen et al., 2004).

Including the proteins predicted as not-secreted by SignalP and SecretomeP database (NP) (Bendtsen et al., 2004; Petersen et al., 2011), the number of significantly changed proteins increased to 142 (86 proteins increased in IR-supernatant, 56 proteins decreased in IR-supernatant). This subset included five additional proteasomal subunit proteins: PSMA1 (1.86 fold), PSMA7 (1.81 fold), PSMA3 (2.24 fold), PSMB1 (1.86 fold) and PSMB2 (1.57 fold). Thus, including NPs, there are 11 of the 14 proteins of the 20S proteasome core complex significantly increased in the supernatant of IR-myotubes. A table revealing all significantly secreted proteins that differ in the supernatant of IR-myotubes vs. IS-myotubes is in the appendix (Supplementary Table II).

The overall increased extracellular level of proteasomal subunits of myotubes obtained from insulin-resistant donors leads to the suggestion that IR-myotubes have in general more intracellular proteasomes and thus are capable to release more proteasome or proteasomal subunits. Therefore, a proteasome ELISA was used for

the quantification of the 20S proteasome core-complex level in cell lysates and supernatant of IS- and IR-myotubes. The myotubes were incubated for 24 h either with medium containing FBS or not since the medium analyzed by LC-MS/MS did not contain FBS and we wanted to exclude that findings are due to FBS removal. It seems that myotubes obtained from insulin-sensitive donors have less 20S core-proteasome. The decrease is more pronounced in cells incubated without FBS (Figure 23A) but it is still only a trend (p = 0.07 IS vs. IR). Investigating the quantity of the 20S proteasome in the supernatant of these cells, no significant difference could be detected (Figure 23B).
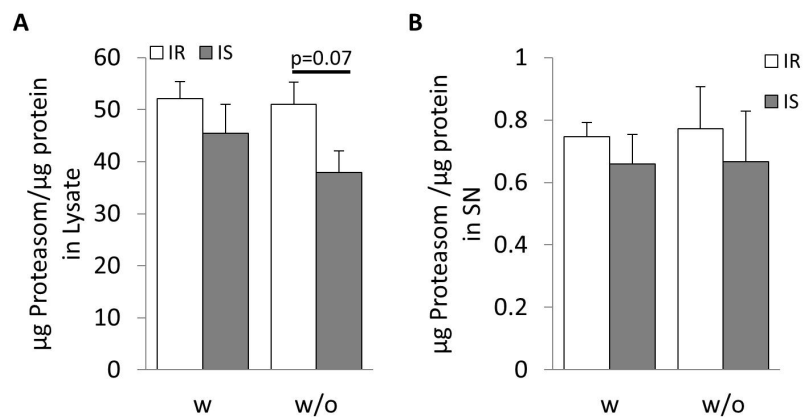
Figure 23: Myotubes of insulin-sensitive donors have reduced intracellular 20S core proteasome quantity and secrete less core proteasome compared to myotubes obtained from insulin-resistant donors.
Myotubes obtained from insulin-resistant (IR) or insulin-sensitive (IS) donors were either incubated with Fusion medium containing FBS (w) or without FBS (w/o) for 24 h. (A) 20S Proteasome ELISA was performed with a defined amount of cell lysates (105 ng, 1:400 diluted). The amount of 20S proteasome was determined by reading the absorption at 450 nm and calculating the proper amount by interpolation. Values are shown as means ± SEM in μg/mL (n = 4). (B) The amount of 20S proteasome was determined in the supernatant (SN; diluted 1:2) by reading the absorption at 450 nm and calculating the proper amount by interpolation. The values were then normalized to protein content per well. Values are shown in means ± SEM in μg proteasome/ μg total protein (n = 3).

3.3.1.3 Differences in protein profile induced by EPS and insulin sensitivity

Analysis of released proteins with regard to the influence of EPS and insulin sensitivity revealed 38 proteins that were significantly different between IR-myotubes and IS-myotubes upon EPS (17 proteins higher in IR-myotubes, 21 higher in IS-myotubes). Protein number increased when including proteins that were predicted as not-secreted by SignalP and SecretomeP (NP) (Bendtsen et al., 2004; Petersen et al., 2011) to 49, whereas 17 were higher in the supernatant of EP-stimulated IR-myotubes and 32 lower. A table including all proteins that were secreted differently (p < 0.05) is shown in the appendix (Supplementary Table III).

3.3.2 Proteomic profile of the muscle secretome by 2D-DIGE MALDI-MS

In a second approach the secretome of the human myotubes obtained from different donors was analyzed by 2D-DIGE MALDI-MS and data investigated for differences upon EPS and upon insulin sensitivity of myotubes donor (basal secretion). Additionally, we wanted to find differences between myotubes of insulin-sensitive and resistant donors upon EP-stimulation. For the first dimension separation via isoelectric focusing (IEF), strips with two different pH scales were used (pH 4-7 and pH 6-9) to unravel as many proteins as possible.

3.3.2.1 Differences induced by Electric pulse stimulation

Comparing EPS with control supernatant, in total 165 protein spots with a ratio > 1.5 fold were significantly changed ($p < 0.05$). Therefrom, 52 were increased and 113 were decreased in the EPS-supernatant. Up to now, only 76 spots are identified by MALDI-MS. A table showing all so far annotated proteins is in the appendix (Supplementary Table IV).

In concordance with the LC-MS secretome analysis, two type I collagens, COL1A1 (0.44 fold) and COL1A2 (0.52 fold) were significantly altered by EPS. Additionally, IGF-binding protein IGFBP4 was significantly decreased in EPS-supernatant (0.56 fold), as well as the myokines SPARC (0.60 fold), FSTL1 (0.53 fold) and RARRES2 (0.49 fold). Expectedly, some proteins were identified by several individual spots, e.g. as COL1A1 (13 individual spots) and COL1A2 (10 individual spots), revealing posttranslational modifications. Additionally, some proteins showed spots regulated in different directions, e.g. POSTN.

Figure 24 shows exemplarily the scan of two gels demonstrating protein spots that are significantly different in EPS-supernatant and control-supernatant.
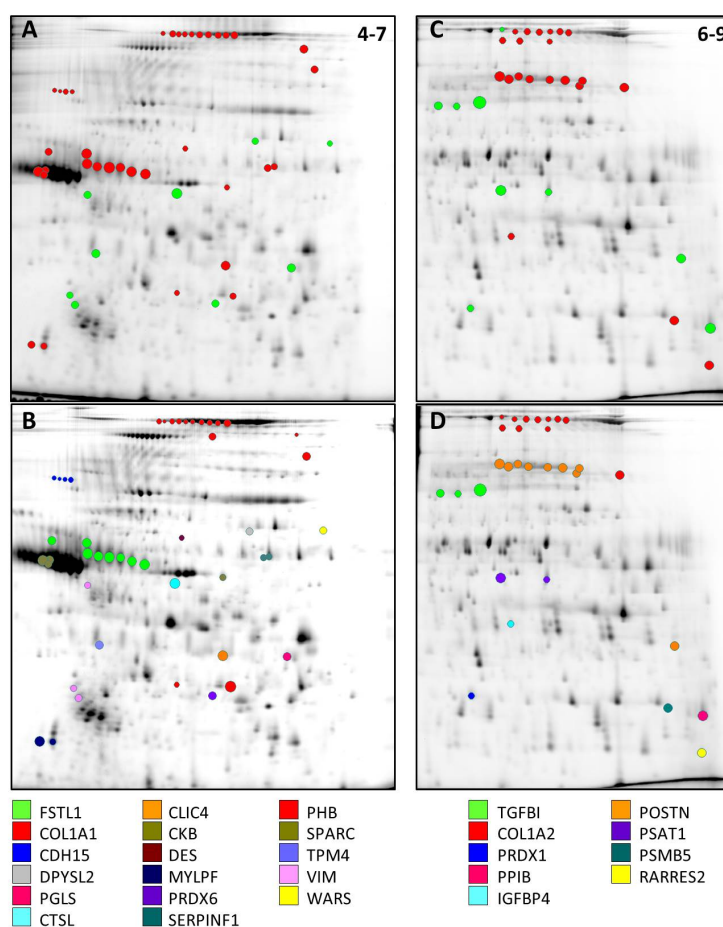
Figure 24: Scan of 2D-gels demonstrating significantly regulated proteins upon EPS.
The supernatant of EP-stimulated and control myotubes was separated by 2D-DIGE and altered protein spots identified by MALDI-MS and subsequent database search. For first dimension separation via isoelectric focusing either (A-B) pH 4-7 or (C-D) pH 6-9 strips were used. Red dots in A and C indicate proteins that were decreased, whereas green dots show proteins that are increased in the EPS-supernatant compared to control supernatant (FC > 1.5; p < 0.05). The colored dots in figure B and D indicate the annotated proteins as shown below that were significantly different in A and C. Figure A/B and C/D are scans of the same gel.

3.3.2.2 Differences among insulin sensitivity

The comparison of the basal secretion of myotubes obtained from insulin-sensitive and resistant donors revealed 53 protein spots, which were different (ratio > 1.5; 30 spots increased and 34 spots decreased in the control supernatant of IR-myotubes). By now, only 21 spot are identified, which are shown in the appendix (Supplementary Table V).

Of note, two proteasomal subunits were increased in the supernatant of the IR-myotubes, PSMA2 (1.67 fold) and PSMA7 (1.56 fold). Since only two gels (pH 6-9) were available with samples of IS-myotubes no significance could be calculated here. In the 2D-gels obtained with pH 4-7, COL1A1 (0.67 fold) just as intermediate filament VIM (1.55 fold) were significantly (p < 0.05) regulated.

3.3.2.3 Differences in protein profile induced by EPS and insulin sensitivity

By comparing secreted proteins that were influenced by EPS and insulin sensitivity, in total 12 proteins were significantly regulated ($p < 0.05$, 8 increased in IR-supernatant upon EPS, 4 decreased in IR-supernatant upon EPS). So far, only two proteins are annotated: transitional endoplasmatic reticulum ATPase (TERA; 0.66 fold) and collagen COL1A2 (2.19 fold) but only latter one is predicted to be secreted (classical secretion, SP+) by SignalP and SecretomeP database (Bendtsen et al., 2004; Petersen et al., 2011).

4. Discussion

4.1 Validation of EPS as *in vitro* exercise model

Physical exercise has been shown to have several health-promoting effects in humans (Pedersen, 2009). However, the knowledge on metabolic adaptations and different molecular signaling pathways occurring in the working muscle is limited. During the last decade, EPS, an *in vitro* exercise model, has been accomplished to study the molecular changes in the contracting muscle cell *in vitro.*

In the beginning of this thesis, the model was only established for murine myotubes (Silveira et al., 2006; Park et al., 2008; Nedachi et al., 2009; Burch et al., 2010), whereas two studies using human myotubes (Lambernd et al., 2012; Nikolic et al., 2012) were published during our own study.

4.1.1 EPS-induced alterations in glucose and fatty acid metabolism

It is well accepted that the contracting muscle is dependent on the breakdown of adenosine triphosphate (ATP). Since the intramyocellular ATP stores are rather small, ATP is resynthesized by creatine kinase, glycolysis and mitochondrial oxidation (Baker et al., 2010). Based on the intensity and duration of the exercise bout, all three energy sources contribute to different degrees to the refilling of ATP (Baker et al., 2010).

In the present study, we aimed to establish an EPS protocol that induces a metabolic shift in human myotubes towards higher energy consumption. After 24 h of EPS (14 V, 5 Hz and 2 ms) glucose consumption of human myotubes was increased, well in concordance with observations in other studies predicting enhanced glucose uptake and glucose oxidation in human myotubes upon EPS (Lambernd et al., 2012; Nikolic et al., 2012). However, the two predominant glucose transporters in skeletal muscle, GLUT1 and GLUT4 (Ebeling et al., 1998) were not induced upon EPS in human myotubes (present study and (Lambernd et al., 2012; Nikolic et al., 2012)), suggesting that EPS rather affects glucose transporter localization than enhances expression of the glucose transporter.

Of note, in response to 24 h of EPS, we and others observed an increase in *MYHI* mRNA expression, predicting a fiber switch towards oxidative type I fibers (Lambernd et al., 2012; Nikolic et al., 2012). However, we detected no increased expression of genes involved in oxidative phosphorylation or encoding key enzymes in fatty acid import and oxidation, as carnitine palmitoyltransferase 1B (*CPT1B*) and medium chain acyl-CoA dehydrogenase (*MCAD*) after 24 h of EPS. Mitochondrial content was not determined in EPS-treated myotubes in our study. Well in accordance, no

EPS-induced increase in fatty acid uptake or oxidation in the human myotubes was observed after 24 h of EPS (Lambernd et al., 2012; Nikolic et al., 2012). It is known that human myotubes have a rather glycolytic metabolism (Aas et al., 2011), which might explain the minor adaptations of the mitochondrial metabolism upon EPS. However, Nikolic and colleagues were able to show an increased oxidation of glucose and oleic acid in response to 48 h of EPS in human myotubes indicating that these cells are capable to adopt their metabolism towards oxidative respiration in this *in vitro* exercise model (Nikolic et al., 2012).

The increased lactate release after 24 h of EPS indicates that glucose is only partially broken down or oxidized as known from *in vivo* high-intensity exercise studies (Balsom et al., 1994). In this case, glucose is catabolized to pyruvate at rates that exceed mitochondrial uptake capacity. To prevent product inhibition of glycolysis and reduced ATP resynthesis, most of the pyruvate in the cytosol is then converted to lactate via lactate dehydrogenase. Additionally, NAD^+ is regenerated from $NADH/H^+$ (Baker et al., 2010). Altogether, this further proposes that during *in vitro* exercise human myotubes mostly metabolize glucose for ATP generation under the respective conditions.

One possible limitation of our study is that we have not performed functional test of oxidative capacity e.g. determination of substrate oxidation. Future studies should address a switch towards more oxidative metabolism in human myotubes during EPS, since this is especially in long-duration endurance exercise the *in vivo* situation (Turcotte et al., 1992; Coggan et al., 2000).

In vivo, exercise training leads to the accumulation of intramuscular triglycerides (IMTGs), which are a major energy source during contraction (Hurley et al., 1986; Krssak et al., 2000; Goodpaster et al., 2001). Additionally, an exercise-mimicking approach induced by pharmacological treatment (combination of forskolin and ionomycin) in human myotubes over 3 days revealed increased triacylglycerol (TAG) storage and oxidative capacity (Sparks et al., 2011). Similar results were obtained in our study by applying a long-term EPS protocol consisting of stimulation on 4 consecutive days for 4 h per day with a simultaneous addition of oleate, which significantly increased IMTG storage in EPS-myotubes compared to muscle cells that were only treated with oleate. However, we have not checked whether these EPS-myotubes have an increased oxidative capacity or fuel preference. Additionally, other training-induced effects, e.g. mitochondrial content, known from *in vivo* studies should be addressed.

In summary, an EPS protocol for human primary myotubes could be established, which induces a metabolic shift towards higher glucose consumption and thus mimics exercise *in vivo*.

4.1.2 EPS-induced gene expression

Muscle contraction leads to rapidly induced changes in skeletal muscle activity of key enzymes and transporters involved in glucose and fatty acid metabolism to overcome the increasing demand for ATP, oxygen and fuels. This is on the one hand enabled by allosteric regulation and phosphorylation of rate-limiting enzymes and on the other hand by transcriptional regulation. One aim of this project was to get an overview of EPS-induced gene regulation in human primary myotubes. Therefore, a whole genome transcriptome analysis was used, which has been shown to be a valuable tool for the investigation of endurance exercise-induced alterations in the skeletal muscle *in vivo* (Mahoney et al., 2005; Schmutz et al., 2006; Catoire et al., 2012; Neubauer et al., 2014). Since our first EPS experiments revealed a significant increase of the mRNA level of the myokines *IL-6* and *IL-8*, as well as the transcriptional coregulator *PPARGC1A* after 24 h of EPS, this duration was used for the microarray analysis.

Similar to the findings obtained from the *in vivo* microarray analysis (Mahoney et al., 2005; Catoire et al., 2012; Neubauer et al., 2014), most of the significantly regulated genes (FDR < 10%; fold change > 1.3) were upregulated upon EPS (153), whereas less genes (30) were repressed by EPS, suggesting that transcription is rather induced than inhibited by contraction.

Of note, among the top 20 upregulated genes, 4 metallothioneins (MT; in particular *MT1F*, *MT1M, MT1G* and *MT1X*), enzymes with antioxidant activity, were significantly upregulated. The other 5 metallothioneins of the isoform 1, as well as *MT2A* were also significantly enriched upon EPS. This is largely in concordance with results obtained after a high-intensity cycling exercise for 75 min *in vivo* (Mahoney et al., 2005) and proposes that the rapid and coordinate upregulation of MTs represents an important antioxidant response to the oxygen free radicals that are generated during exercise. It is so far not clear how MTs act as antioxidants. However, they might capture harmful oxidative radicals (Thornalley and Vasak, 1985) or upregulate mitochondrial superoxide dismutase (SOD2) (Mahoney et al., 2005), another important antioxidant enzyme. Concordantly, *SOD2* was also significantly induced by our EPS protocol. Another enzyme involved in anti-oxidant defense is heme oxygenase 1 (*HMOX1*), which was also induced by 24 h of EPS as well as after 60-90 min exhaustive one-legged knee extensor exercise (Pilegaard et al., 2000) or 2 h of endurance exercise *in vivo* (Neubauer et al., 2014).

Additionally, we found several chemokines and cytokines induced by EPS, e.g. *IL-6*, *IL-8* and *CXCL1* which are also known to be increased in an exercise-dependent fashion *in vivo* (Pedersen and Febbraio, 2012) and will be discussed in detail in section 4.1.3.

A comparison of *in vivo* muscle transcriptome analysis either of mice that underwent one hour of treadmill exercise (Hoene et al., 2009) or of humans who cycled for 1 hour (J. Hansen, P. Plomgaard, M. Irmler, M. Scheler, J. Beckers, M. Hrabé de Angelis, C. Weigert, unpublished data) with the *in vitro* gene regulation partly overlapped (Table 22).

This proposes, also including the similarities discussed above, that EPS is indeed capable to induce alterations in gene regulation that mimic the *in vivo* response. However, transcriptional activation of several genes induced in humans have not been changed significantly in the microarray analysis of the human myotubes upon 24 h of EPS, e.g. encoding key enzymes involved in metabolism (*PDK4, FOXO1*) (Mahoney et al., 2005; Catoire et al., 2012), which can have various reasons. First of all, most of the *in vivo* exercise studies used several post-exercise time points for muscle biopsies and included recovery phase in their investigations. We analyzed by transcriptomics only the gene expression directly after the end of 24 h of EP-stimulation and thus missed further transcriptional alterations occurring during earlier time points and recovery phase. Therefore, future experiments should also analyze alterations occurring in the recovery phase. Additionally, Catoire and colleagues showed that endurance exercise also changes gene expression in non-exercising muscle through plasma FFA (Catoire et al., 2014). In this *in vitro* exercise model no changes in gene regulation initiated through systemic factors, including FFA or hormones, can be investigated. Moreover, muscle fibers are surrounded by connective tissue and extracellular matrix (ECM), which can further influence the transcriptional response. Hence, it might be useful to supplement media with respective systemic factors during EPS and/or use ECM-coated cell culture dishes and analyze the impact on the transcriptional response, as has been done in the developed EPS protocol, which will be further discussed in section 4.1.5.

Summing up, the transcriptional changes induced through EPS reflect at least partially transcriptional response during exercise *in vivo*.

Table 22: Comparison of exercise-induced changes in muscle gene expression of *in vivo* exercise studies to *in vitro* EPS.

Symbol or ID	Human muscle biopsy		Mice	Human MT	Human MT
	1 h exercise	3 h recovery	1 h treadmill	24 h EPS	Verification by qRT-PCR
C8orf4	3.42	-	-	1.14	-
PPP1R15A	1.35	-	-	1.21	-
KLF4	3.09	-	5.36	-	-
EGR1	2.89	-	2.11	-	2 h
ADAMTS1	2.73	-	2.08	0.90	-
NR4A3	2.47	2.21	5.08	-	8 h, 24 h
CXCL2	2.30	-	-	2.65	-
ACTA2	2.12	2.37	-	-	-
ID1	1.94	-	-	0.76	-
HSPH1	1.89	-	-	1.09	-
HES1	1.74	-1.40	-	0.88	-
DNAJB1	1.72	-	4.42	-	-
CCL2	1.62	-	-	1.58	-
HMOX1	1.61	2.00	-	2.40	-
ARRDC3	1.50	-	-	0.93	-
JUNB	1.48	-	3.15	-	-
JUN	1.44	-	2.10	-	-
ID2	1.42	-	-	1.24	-
SLC2A3	1.40	-	-	1.18	-
SPRY4	1.39	-	2.19	-	-
SLC25A25	1.38	-	5.79	-	-
KLF2	1.34	-	2.40	-	-
TMEM140	1.34	1.51	-	1.30	-
BCL2L1	1.27	-	-	1.10	-
CLDN12	1.27	-	-	1.15	-
NFIL3	-	2.00	2.24	-	-
NR1D2	-	-1.40	2.09	-	-
NRBF2	-	1.37	3.80	-	-
PER1	-	-1.36	2.15	-	-
PPARGC1A	-	2.39	-	1.30	24 h

Values are shown as fold increase to basal expression obtained with whole genome transcriptome analysis. For the human exercise study (Human muscle biopsy), subjects completed 60 min of bicycle ergometer exercise at approx. 50 % of their individual VO_2max. Muscle biopsies were taken from the vastus lateralis immediately prior exercise bout, immediately post-exercise and after 3 h of recovery (n = 16). The mRNA was isolated and gene expression determined by microarray analysis. For the mice exercise study, 12-week-old-mice ran 60 min at 5 m min-1 (n = 8) and mRNA isolated afterwards from soleus muscle for analysis. *In vitro*, activation of genes was investigated after 24 h of EPS (14 V, 5 Hz, 2 ms; n = 12) in human primary myotubes (human MT). Here, some genes were verified by qRT-PCR, whereas EPS duration that induced significant changes is indicated (p < 0.05; n = 8).

4.1.3 EPS-induced cytokine pattern

One aim of this study was the investigation of the transcriptional response of human primary myotubes upon EPS with a special focus on potentially secreted peptides and proteins and to determine the release of these myokines. Of note, among the 153 significantly upregulated genes (fold change > 1.3) are 35 encoding secreted proteins. Additionally, 7 of the 10 genes with the highest fold increase upon EPS are supposed to be secreted as protein, in detail IL-8, CXCL1, CXCL6, IL-1B, tissue factor pathway inhibitor (TFPI2), matrix metallopeptidase 1 (MMP1) and MMP3. In a

targeted proteomic analysis of the supernatant we could verify the functional importance of the changed transcriptome as significant increase of chemokines and cytokines in the supernatant of EP-stimulated myotubes. In particular, interleukins IL-1B, IL-2, IL-4, IL-6, IL-8, IL-13, IL-17A and CXCL1, LIF, CSF3, TNF and CCL2 were identified as EPS-induced human myokines. In accordance, Raschke and colleagues determined an enhanced release of IL-6, IL-8, CXCL1 and CCL2 of human myotubes upon 24 h of EPS by using cytokine antibody arrays (Raschke et al., 2013a). Whereas some factors have been already described as exercise-induced myokines, as IL-6, IL-8 and TNF (Steensberg et al., 2002; Pedersen and Febbraio, 2008) others were only described to be elevated in the plasma after a single bout of exercise in humans (CSF3 and CCL2) (Hirose et al., 2004; Paulsen et al., 2005). For other proteins no increase in plasma level could be determined but muscle protein levels are increased after exercise (CCL2 and IL-1B) (Malm et al., 2000; Hubal et al., 2008). Thus, based on our microarray analysis data and the determined levels of secreted peptides and proteins, we suggest EPS is capable to induce the expression and secretion of several cytokines and chemokines in human myotubes, which to some extent reflects *in vivo* situation.

However, the results revealed that myotubes obtained from different donors have an individual IL-6 and IL-8 response (mRNA expression and protein release) to EPS. Since we could exclude any differences in differentiation and fusion of the individual myotubes, one aim was to determine potential regulators affecting the individual exercise-induced interleukin-6 and 8 response. Therefore, the 12 myotubes obtained from different donors that were used in the microarray analysis were divided in a high IL-6/ IL-8 responder and a low responder group, and the differences in basal transcription investigated (Supplementary Figure II). Phospholipase PLA2GA, which is crucial for the hydrolysis of glycerophospholipids to free fatty acids and lysophospholipids (Murakami et al., 2011), might be such a candidate, with an enhanced basal expression in the high IL-6/IL-8 responder group. During EPS intracellular Ca^{2+} levels elevate, which is an important cofactor for this phospholipase (Murakami et al., 2011). Thus, it might be speculated that myotubes with higher *PLA2GA* expression, exhibit increased activity of this phospholipase upon EPS, resulting in higher levels of free fatty acids, which in the end lead to enhanced IL-6 expression and release (Weigert et al., 2004; Murakami et al., 2011; Sanchez et al., 2013). However, knockdown of the respective gene could clarify these speculations.

The physiological role of the exercise-induced cytokine response is only partially understood. The present knowledge was recently reviewed (Pedersen, 2011; Paulsen et al., 2012; Pillon et al., 2013). However, IL-6 is the best-studied myokine, involved in muscle tissue hypertrophy, satellite cell proliferation and myotube

formation (Serrano et al., 2008; Hoene et al., 2013; Zhang et al., 2013). LIF, member of the IL-6 cytokine family, functions in autocrine and/or paracrine fashion and induces satellite cell proliferation (Pedersen and Febbraio, 2012). IL-8 is an angiogenic-factor and thus might be involved in the training-induced muscle adaptations (Pedersen, 2011). CCL2 is described as a myokine involved in immune cell attraction and maintenance of the inflammatory phase in injured muscles (Sun et al., 2009).

Since the importance of myokines in the beneficial effects of exercise increased, during the last years several new myokines were described, in particular NAMPT (Costford et al., 2010), SPARC (Aoi et al., 2013), IL-15 (Tamura et al., 2011), myonectin (Seldin et al., 2012) and irisin (Bostrom et al., 2012). However, transcripts of *SPARC*, *IL-15*, *CTRP15/FAM132B* (myonectin) and *FNDC5* (irisin) were detected in the whole genome transcriptome analysis but not induced by 24 h of EPS. On the one hand, this might be due to the fact that other factors, e.g. hormones and fatty acids are necessary for the transcription activation or that repeated bouts of exercise are needed for the induction as described for irisin (Bostrom et al., 2012). On the other hand, it might be that not the muscle cell per se is the source for the elevated protein levels found in plasma after exercise. Additionally, genes with a fast and transient activation might be missed due to 24 h of EP-stimulation. Furthermore, not the expression of a respective gene but the translation or cleavage could occur during EPS. For example, during mechanical stretching of C2C12 myotubes, SPARC secretion was not paralleled by enhanced transcription but enhanced translation (Aoi et al., 2013). However, we observed an increased *NAMPT* gene expression in EP-stimulated human myotubes but no increased protein release. This proposes that NAMPT has an intracellular regulatory function during exercise, well in accordance with an *in vivo* study that showed increased *NAMPT* expression in skeletal muscle upon exercise (Costford et al., 2010).

In vivo, the muscle cytokine response is dependent on the mode and intensity of the exercise bout. Low-intensity exercise protocols induce a rather local protein expression of cytokines as IL-6, without any systemic alterations (Rosendal et al., 2005), whereas exercise protocols including downhill running, eccentric action of the leg or arm muscles and resistance training result in a solid cytokine response in the exercising muscle and also a higher systemic levels (Paulsen et al., 2012). In general, latter finding is explained by the fact that exercise-induced muscle damage is accompanied by activated infiltration of immune cells leading to a solid cytokine expression and release from muscle fibers and immune cells. Furthermore, muscle damage induces the release of creatine kinase into the plasma. Here, we provide evidence that EP-stimulated human myotubes are indeed capable to express and

secrete a variety of chemokines and cytokines without the simultaneous release of creatine kinase indicating no severe muscle cell damage. This indicates that the skeletal muscle cell per se is able to secrete cytokines without immune cells and thus may contribute to the local and systemic cytokine response more than generally assumed. Nevertheless, one limitation of the experiments performed in this study is that the presence of other cells than myotubes could not be completely excluded, but the cell culture conditions make the proliferation and survival of immune cells unlikely.

4.1.4 EPS-induced signaling pathways

Endurance exercise, e.g. cycling or running, leads to an increased activation of the mitogen activated protein kinases ERK1/2, p38 MAPK and JNK in the skeletal muscle of humans (Aronson et al., 1997; Aronson et al., 1998; Widegren et al., 1998; Yu et al., 2001). However, upon EPS these activations were only partially overlapping since no increased phosphorylation of p38 MAPK was detected, neither by our own nor by other EPS studies (Nedachi et al., 2008; Nedachi et al., 2009; Lambernd et al., 2012; Whitham et al., 2012). During one-leg cycling p38 is also activated in the resting leg, suggesting that contraction is not the exclusive stimulus for p38 activation (Widegren et al., 1998). In contrast, ERK1/2 and JNK phosphorylation was only induced in the exercising leg (Aronson et al., 1997; Aronson et al., 1998). Thus, it might be speculated that either EPS conditions (intensity and duration) are not sufficient for the activation of p38 MAPK or that other systemic factors, which activate p38 MAPK, are missing in this cell culture model.

In humans, activation of NFκB in skeletal muscle was shown as increased DNA binding activity and decreased IkBα protein levels or nuclear localization of NFκB after cycling (Tantiwong et al., 2010), resistance (Vella et al., 2012) or eccentric exercise (Hyldahl et al., 2011). Here, we provide evidence that 24 h of EPS is capable to enhance NFκB activity, which is blunted with the addition of the ERK1/2 inhibitor U0126. Additionally, this inhibitor decreased EPS-induced expression of NFκB–target gene *IL-8* after both 4 h and 24 h of EPS. This was also in accordance with a previous report, where U0126 inhibitor was applied to Electric pulse-stimulated isolated rat muscle (Ho et al., 2005), proposing a role for ERK1/2 in the contraction-induced NFκB activation.

Altogether, the EPS conditions used in this study activate several signaling pathways also known from *in vivo* exercise studies.

4.1.5 Advantages of the improved EPS protocol

Based on the previous discussion, the EPS protocol was further developed for a second project with myotubes obtained from insulin-sensitive and resistant donors.

It is known that the preparation of satellite cells from muscle biopsy obtained with percutaneous needle biopsy results in a cell mixture including minor amounts of other cell types as nerve cells, adipocytes and fibroblasts (Blau and Webster, 1981). However, it is not clear if cultivation of the myoblasts and myotubes leads to the loss of these additional cells. Nevertheless, the presence of these cells might influence the experimental outcome. Thus, in the second project, magnetic activated cell sorting (MACS) was included, resulting in an average enrichment of the myoblasts fraction for 20 %, which is in accordance with literature (Park et al., 2006).

The coating of the cell culture dishes with Matrigel resulted in a better and faster proliferation and differentiation (lab intern observation), which might be explained through the inclusion of growth factors, as TGF-β or EGF. Additionally, Matrigel provides an ECM-like and thus a more physiological surrounding, which might also influence proliferation and differentiation positively. However, a disadvantage is that the composition of Matrigel varies from batch to batch, which should be taken into account for future experiment.

The addition of fatty acids and L-carnitine enables the investigation of fatty acid induced molecular mechanisms and fatty acids intracellular fate, which will be discussed in section 4.2.1. *In vivo*, acute exercise increases lipolysis in adipose tissue resulting in increased plasma free fatty acids (Catoire et al., 2014), which are suggested to play a potential role in contraction-induced changes in skeletal muscle and thus were integrated in this developed EPS protocol.

Moreover, the EPS protocol was shortened to 8 h and a recovery phase of 16 h was included, since *in vivo* studies have been shown that the transcriptional response to an acute bout of exercise in skeletal muscle partially occurs during recovery phase (Mahoney et al., 2005; Neubauer et al., 2014).

We investigated *IL-6* and *PPARGC1A* mRNA expression in human myotubes stimulated with this improved EPS protocol, whereas *IL-6* showed highest expression directly after end of stimulation, while *PPARGC1A* further increased during recovery phase, which mimics *in vivo* situation. On the one hand, during knee-extensor exercise intramuscular *IL-6* mRNA levels peaked directly after end of exercise and decreased rapidly during recovery phase (Fischer et al., 2004). On the other hand, *PPARGC1A* reached maximal expression in the recovery phase in the human muscle after a single bout of exercise (Pilegaard et al., 2003) indicating that PGC1α is involved in long-term adaptations to exercise, e.g. mitochondrial biogenesis.

In summary, this improved EPS protocol provides new insights into intramuscular changes occurring post-exercise and might thus promote further understanding of exercise-induced long-term adaptations in the muscle.

4.1.6 Conclusion and future perspectives

In the beginning Electric pulse stimulation was only established for murine myotubes. However, we and others established EPS protocols for human primary myotubes (Lambernd et al., 2012; Nikolic et al., 2012; Scheler et al., 2013). These myotubes displayed altered metabolic properties, transcriptional response and myokine releases, which are all exercise-induced changes that are also observed *in vivo*. This confirms that EPS is a valuable tool for mimicking exercise *in vitro*. However, it has to be taken into account that in this model changes in systemic factors as hormones and metabolites induced by exercise *in vivo* could not be covered.

So far, this was the first EPS study using a whole genome transcriptome analysis for the investigation of EPS-induced changes in gene expression. Additionally, we were able to show that this *in vitro* exercise model is suitable to identify exercise-regulated myokines and that myotubes obtained from different muscle biopsy donors show an individual response to EPS. Thus in future studies, EPS may be applied to myotubes obtained from donors with different phenotypes (e.g. insulin sensitivity) to investigate altered molecular mechanisms in these groups.

4.2 EPS of myotubes obtained from donors with different insulin sensitivity

In this part of this thesis myotubes obtained from insulin-sensitive and resistant donors were investigated. In general we aimed to identify novel markers for insulin sensitivity and resistance and aspired to find pathomechanistic alterations including changes in lipid metabolism during basal and exercise conditions. For this study the improved EPS protocol including MACS, Matrigel coated dishes, altered EPS duration including recovery phase and the addition of fatty acids was used to accomplish a more physiological exercise situation. In a first targeted metabolomic analysis of the human myotube cell lysates acylcarnitine levels were determined.

4.2.1 Influence of EPS and insulin sensitivity on intracellular acylcarnitine pattern

Metabolic analysis of plasma and tissue reveals important metabolite patterns that indicate specific disease states and thus enable the investigation of chronic metabolic diseases, as type 2 diabetes or obesity (Bain et al., 2009). Especially, the investigation of acylcarnitines (AC), the esters of fatty acids obtained from incomplete β-oxidation, are frequently used for the detection of errors in fatty acid oxidation and other inborn defects of metabolism during newborn screening (Chace et al., 2003; Rinaldo et al., 2008).

Here, the intramyocellular acylcarnitine pattern of EP-stimulated human myotubes was investigated by targeted metabolomic profiling. Mainly even-chain acylcarnitine species ranging from C6 to C16 were detected that are obtained from incomplete β-oxidation. Two odd-chain species, in particular C3-AC and C5-AC, were detected, which are derived from amino acid breakdown. C4-AC can be produced either from fatty acid or amino acid catabolism. Acetylcarnitine (C2-AC) can be obtained from acetyl-CoA being the central product of the degradation of fatty acids, amino acids and glucose.

The results obtained in this study show that EPS does not increase β-oxidation since no enhanced ratio of acetylcarnitine to free carnitine (C2-AC/C0) was detected. CPT1, the enzyme mediating the rate-limiting step during β-oxidation by esterification of long-chain acyl-CoAs to acylcarnitines at the outer mitochondrial membrane and thus facilitating the uptake of fatty acids into mitochondria, showed also no increased activity (C16-AC/C0) upon 8 h of EPS. One explanation might be that increased acylcarnitines are shuttled out of the cells into the medium and thus no enhanced β-oxidation rate and CPT1-activtiy is determined, respectively. Additionally, human

myotubes have a rather glycolytic metabolism, thus fatty acid oxidation might only play a subordinated role in the energy production during EPS-induced contraction.

Of note, so far most studies concentrated on the measurement of acylcarnitines in the plasma; less is known about the changes occurring in skeletal muscle itself (Schooneman et al., 2014). Additionally, it could be shown that plasma acylcarnitine levels do not correlate with tissue levels (Hiatt et al., 1989; Burger et al., 2014). Lehmann and colleagues proposed that medium chain acylcarnitines are the predominant species elevated in plasma during moderate-intensity exercise (Lehmann et al., 2010). However, intramyocellular medium chain acylcarnitines were not elevated upon 8 h of EPS suggesting that the EPS protocol does not reflect moderate-intensity exercise or that intramuscular acylcarnitine patterns differ from plasma levels. In a recent study we could show that acylcarnitines accumulate in the supernatant of human myotubes resulting in a different pattern compared with the intracellular concentrations (Wolf et al., 2013). Moreover, a former study proposed that only high-intensity exercise increases intramuscular acylcarnitine levels, whereas low-intensity exercise induces no changes in carnitine metabolism (Hiatt et al., 1989). In future analysis the supernatant of EP-stimulated myotubes should be analyzed and the release of acylcarnitines investigated.

During recovery phase, the acylcarnitine levels of long, medium but especially short-chain AC increased during recovery phase, without any difference respective previous treatment (EPS or control). This can be explained by the fact that theses myotubes were longer exposed to the fatty acids in the medium and thus were able to take up more FA, which are then converted to acylcarnitines intracellular.

Many theories for the development of insulin resistance have been highlighted during the last years. One of these mechanisms is lipotoxicity: the increased fatty acid supply and simultaneous accumulation of lipids but especially lipid intermediates as diacylglycerol, ceramides, gangliosides in insulin-sensitive tissues, like skeletal muscle, results in decreased insulin response (Goodpaster and Kelley, 2002; Morino et al., 2006; Holland and Summers, 2008; Erion and Shulman, 2010). In another theory it was proposed that fatty acid oxidation rate overtakes tricarboxylic acid cycle (TCA), which causes increased levels of intermediate metabolites, e.g. acylcarnitines that may interfere with insulin sensitivity (Muoio and Koves, 2007; Koves et al., 2008; Muoio and Neufer, 2012). Our study proposed only a significant difference between IR-myotubes and IS-myotubes after acute EP-stimulation (8 h) in the acetylcarnitine to free carnitine ratio. Strikingly, the propionylcarnitine to carnitine ratio (C3-AC/C0) was increased in IR-myotubes at every condition, indicating a higher breakdown of branched-chain amino acids and odd-numbered LC-FA. However, C5-carnitine was also slightly decreased upon acute EP-stimulation in

IS-myotubes, indicating that propionylcarnitine might indeed be formed through C5-AC. Future analysis will show whether myotubes derived from insulin-resistant donors also have increased levels of branched-chain amino acids. Several studies proposed that branched-chain and aromatic amino acids correlate with present or future diabetes (Newgard et al., 2009; Fiehn et al., 2010; Wang et al., 2011). In concordance, enhanced levels of branched-chain amino acid derived C3-AC and C5-AC were found in the plasma of type 2 diabetic patients (Newgard et al., 2009; Mihalik et al., 2010).

Propionic aciduria (PA) and methylmalonic aciduria (MMA) are known defects in the breakdown of branched-chain amino acids as wells as odd-numbered fatty acids. Patients suffering from PA have a mutation in the gene encoding propionyl-CoA carboxylase, which converts propionyl-CoA to methylmalonyl-CoA, a precursor of succinyl-CoA, resulting in decreased uptake of propionyl-CoA into the TCA (Siliprandi et al., 1991). Often this disease comes along with respiratory chain deficiencies in various tissues including liver and skeletal muscle (de Keyzer et al., 2009) and reduced fatty acid oxidation (Siliprandi et al., 1991), which might in the end lead to hepatic steatosis (Siliprandi et al., 1991). Future examinations have to clarify the detailed mechanism how increased propionlycarnitines might influence β-oxidation and its impact on insulin resistance.

4.2.2 Conclusion and future perspectives

In summary, the EPS protocol used within this study induced no alterations in acylcarnitine composition in human primary myotubes. However, the investigation of IS- and IR-myotubes revealed a difference in propionylcarnitine to carnitine ratio. Further investigations, either by targeted or untargeted metabolomics, which are planed for future, aim to determine intramyocellular levels of fatty acids, lysophosphatidylcholines and amino acids and thus provide further information about the altered lipid metabolism due to decreased insulin sensitivity. However, the supernatant of these myotubes should also be analyzed for metabolites to obtain an overall picture.

So far, this is the first EPS study using human myotubes obtained from donors with different phenotypes, which investigates exercise-induced metabolomic changes and thus will hopefully provide a further example that EPS is a valuable tool for studying exercise-related mechanisms *in vitro.*

4.3 The muscle secretome

To identify novel exercise-induced myokines and myokines that are regulated differently between myotubes obtained from insulin-sensitive and insulin-resistant donors, the muscle cells secretome was analyzed by untargeted proteomic profiling via gel-free LC-MS/MS and gel-based 2D-DIGE MALDI-MS analysis.

The gel-free analysis method (Domon and Aebersold, 2006) allows the investigation of proteins on peptide level, having a high sensitivity, a large dynamic range for measurement and being independent of protein size, pI or hydrophobicity. A disadvantage of this method is that protein isoforms can hardly be distinguished.

2D gel based separation enables the analysis of intact proteins of up to 10000 protein spots on one gel (Zabel and Klose, 2009). It is the method of choice for checking sample quality by visualization and facilitates the investigation of protein isoforms and posttranslational modifications. However, this method has also several limitations concerning protein characteristics: (1) poor acquisition of very hydrophobic proteins and proteins with a molecular weight < 5 or > 200 kDa or pI < 3 or > 11; (2) limited sensitivity (Rabilloud et al., 2009). Thus it is beneficial to use a combination of both technologies to overcome the limitations of each method and hence facilitate an increased coverage of secreted proteins (Wohlbrand et al., 2013; Weigert et al., 2014).

In this study, myotubes from 6 different donors were EP-stimulated for 24 h (14 V, 5 Hz, 2 ms), which were grouped in an insulin-sensitive, lean group (ISI-MATS: 31.4 ± 5.3; BMI: 22.2 ± 1.4) and an insulin-resistant, moderately obese group (ISI-MATS: 8.7 ± 2.0; BMI: 30.4 ± 0.8). During stimulation, Fusion medium without FBS was used, since serum due to its complexity does interfere with secretome profiling. However, serum deprivation might induce cell lysis or membrane leakage (Villarreal et al., 2013).

The amount of proteins predicted as non-secreted by SignalP or SecretomeP database (Bendtsen et al., 2004; Petersen et al., 2011) and known as cytoplasmic proteins detected by both methods is rather high. On the one hand, it cannot be completely guaranteed that no cells were lysed upon EPS or serum deprivation. On the other hand, cytoplasmic proteins might be shuttled out of the cells via extracellular vesicles, like exosomes, containing miRNA, mRNA and also proteins and might thus contribute to the myotube secretome (Gyorgy et al., 2011; Le Bihan et al., 2012).

In the next part, data obtained by unbiased proteomic profiling will be discussed concerning the exercise-inducible effect and dependence on insulin sensitivity.

4.3.1 EPS-induced differences in myokine secretion

The data evaluation of the results obtained with LC-MS/MS analysis determined 170 significantly altered proteins in the supernatant of EP-stimulated myotubes of the six donors. With 2D-DIGE MALDI-MS/MS 165 significantly regulated spots were determined, whereof 76 spots are identified so far.

Of note, LC-MS/MS analysis revealed 7 collagens, in particular COL4A1, COL5A3, COL5A2, COL1A1, COL1A2, COL3A1 and COL8A1, which were decreased in the EPS-supernatant. In accordance, gel-based separation technique also identified two type I collagens (COL1A1, COL1A2) that were less abundant upon EPS. Strikingly, several spots were identified as COL1A1 (13 individual spots) and COL1A2 (10 individual spots) reflecting the variety of posttranslational modifications of collagens (Yamauchi and Sricholpech, 2012). Additionally, COL1A2 and POSTN were identified by several spots but one spot each was regulated in the reciprocal direction. One explanation might be that these spots reveal a special posttranslational modification, which is enhanced under the applied conditions.

Collagens are the major structural proteins in skeletal muscle extracellular matrix (ECM) building up a triple helix consisting of three polypeptide α-chains (Ricard-Blum and Ruggiero, 2005). Collagens of type I, III and V are clustered as fibrillar collagens, whereas type IV and VIII belong to the basement membrane associated collagens (Ricard-Blum and Ruggiero, 2005). The relative composition and amount of the different collagen types that build up the fibers influence the structure and organization of the matrix network and thus biomechanical properties of the tissue (Ricard-Blum and Ruggiero, 2005). Consequently, it is not surprising that during exercise collagens and other structural proteins are degraded and again regenerated, which results in ECM remodeling.

Despite that EP-stimulated myotubes revealed decreased extracellular collagen levels, transcription of these collagens was not altered in the previous performed microarray analysis. Therefore, it might be speculated that collagens are decreased through posttranslational mechanisms, in particular through degradation by matrix metallopeptidases (MMP). In concordance, the expression of *MMP-1* and *MMP-3* were significantly increased upon 24 h of EPS as determined in the microarray analysis. MMP-1 belongs to the family of collagenases, degrading whole collagen molecules, including type I, III and VIII collagens (Bramono et al., 2004). In contrast to that, MMP-3 belongs to the family of stromelysins, breaking down amongst others type III, IV and V collagens (Bramono et al., 2004). Thus, all collagens significantly altered in the supernatant upon EPS might be influenced by the protease activity of MMP-1, 3 or further regulated MMPs, respectively. In future experiments, MMP appearance and activity in the supernatant should be addressed either by targeted

proteomic analysis (BioPlex immunoassay using the MMP panel) or zymography, respectively.

ECM and its remodeling also in context with exercise-induced adaptations in skeletal muscle have been recently described (Kjaer, 2004; Gillies and Lieber, 2011). However, knowledge on exercise-induced collagen turnover and ECM remodeling is scarce. Additionally, most human studies focus on training-induced effects (Rullman et al., 2009; Urso et al., 2009). Here, we provide evidence that also a single bout of exercise induces ECM remodeling. Summing up, our study leads to the speculation that EPS-induced collagen breakdown facilitates ECM remodeling and thus exercise-induced adaptations.

Strikingly, SPARC and FSTL1 revealed decreased protein levels in EPS-supernatant. However, from *in vivo* studies it is known that both myokines are increased in the plasma after an acute bout of exercise (Aoi et al., 2013; Gorgens et al., 2013). Additionally, after 11 weeks of strength training also increased intramuscular mRNA levels of *FSTL1* and *SPARC* were found (Norheim et al., 2011) but *in vitro* studies showed no increased mRNA expression of these myokines after acute contraction (Aoi et al., 2013; Gorgens et al., 2013). Thus, so far, it is not clear whether the contraction-induced increase in plasma level is really due to an enhanced release from the muscle. Additionally, it might be speculated that EPS-myotubes release proteases, which breakdown these high abundant myokines or that the enzymatic activity of the present proteases is enhanced by EPS.

Despite COL1A1 and COL1A2 further proteins that were significantly altered in the supernatant upon EPS were identified by LC-MS/MS and 2D-DIGE MALDI-MS simultaneously (Table 23). All proteins identified by both techniques are regulated in the same direction validating the results obtained with the gel-free and gel-based separation technique, respectively. Additionally, every protein included in Table 23 despite phosphoserine aminotransferase (PSAT1), was also determined in another study profiling the secretome of human myotubes but in a contraction-independent approach (Hartwig et al., 2014b). Future studies will show if these novel contraction-induced myokines are also regulated on transcriptional level and if they are also regulated *in vivo*.

Table 23: Proteins that were identified by both separation techniques and significantly regulated upon EPS.

Protein ID	Name	Gene name	SP+/SP-/ NP	Ratio EPS/con	
				2D-DIGE	LC-MS
P07711	Cathepsin L1	CTSL1	SP+	2.30	2.56
Q9Y696	Chloride intracellular channel protein 4	CLIC4	SP-	0.63	0.75
P55291	Cadherin-15	CDH15	SP+	0.57	0.48
P22692	Insulin-like growth factor-binding protein 4	IGFBP4	SP+	0.56	0.52
Q12841	Follistatin-related protein 1	FSTL1	SP+	0.53	0.72
P08123	Collagen alpha-2(I) chain	COL1A2	SP+	0.52	0.51
Q96A32	Myosin regulatory light chain 2	MYLPF	SP-	0.49	0.53
Q99969	Retinoic acid receptor responder protein 2	RARRES2	SP+	0.49	0.82
P02452	Collagen alpha-1(I) chain	COL1A1	SP+	0.44	0.53
Q9Y617	Phosphoserine aminotransferase	PSAT1	NP	2.15	2.25
P67936	Tropomyosin alpha-4 chain	TPM4	NP	1.87	2.48
P23381	Tryptophan--tRNA ligase. cytoplasmic	WARS	NP	1.77	2.18
P23284	Peptidyl-prolyl cis-trans isomerase B	PPIB	NP	1.66	1.59
Q16555	Dihydropyrimidinase-related protein 2	DPYSL2	NP	1.59	2.03
P12277	Creatine kinase B-type	CKB	NP	0.62	0.79

Table shows protein ID, names and gene names of all significantly regulated proteins that had a fold change > 1.5x EPS vs. con in the 2D-DIGE MALDI-MS analysis and LC-MS/MS analysis (ratios EPS/con are indicated; $p < 0.05$). The upper part shows proteins predicted to be secreted via classical (SP+) or non-classical (SP-) secretion pathway, while lower part shows proteins that are predicted as not secreted (NP).

4.3.2 Insulin sensitivity of the myotube donors influence myokine secretion

Investigating the basal (control) supernatants of myotubes derived from donors with different insulin sensitivity, the most remarkable finding was the increased level of several subunits of the 20S proteasome core complex in the supernatant of IR-myotubes. Six subunits were significantly enriched as determined by LC-MS/MS, in particular PSMA2, PSMA4, PSMA6, PSMB4, PSMB5, PSMB6, whereas PSMA2 was also found by 2D-DIGE MALDI/MS (all predicted to be secreted by non-classical secretion pathway). Including the subunits that were predicted not to be secreted by SignalP and SecretomeP (Bendtsen et al., 2004; Petersen et al., 2011), 5 further subunits showed elevated extracellular levels with IR-myotubes (PSMA1, PSMA3, PSMA7, PSMB1, PSMB2, whereas PSMA7 was also found with 2D-DIGE MALDI/MS).

The 26S proteasome is a barrel shaped multi-protein complex, being the basic degradation machinery in eukaryotic cells. It consists of a 19S regulatory subunit,

identifying the proteins marked for proteasomal degradation and a 20S catalytic core complex, which performs proteolytic cleavage. Latter subunit is made up of four stacked heptameric rings: the two outer rings are composed of 7 different PSMA subunits, and the two inner rings of 7 different PSMB subunits (β1, β2 and β5 providing proteolytic activity) (Bochtler et al., 1999).

Well in concordance with the extracellular levels, IR-myotubes showed a trend towards an increase in intracellular 20S proteasome amount as determined by ELISA. However, 20S proteasome was not increased in the respective supernatants. In future experiments, the intracellular as well as extracellular amount of each proteasomal subunit should be determined by western blot. Additionally, the proteasomal activity in IR-myotubes should be investigated.

In vivo, several studies describe a link between type 2 diabetes and increased intracellular proteasomal activity in skeletal muscle as recently reviewed (Workeneh and Bajaj, 2013). In mice, insulin deficiency leads to decreased phosphatidylinositol 3-kinase (PI3K) activity, decreasing the level of phosphorylated Akt, and thus the inhibition of the expression of specific E3 ubiquitin ligases resulting in increased protein turnover and proteasome activity in the muscle (Wang et al., 2006). Thus, it might be speculated that IR-myotubes have beneath their increased 20S proteasome amount also enhanced activity. It is still unclear whether human myotubes obtained from insulin-resistant donors really reflect donors' phenotype and show impaired insulin signaling (Thompson et al., 1996; Krutzfeldt et al., 2000). However, the PI3K-Akt pathway should be further investigated in IR-myotubes. Accelerated intracellular proteasome quantity might be one explanation for the increased extracellular level of proteasomal subunits in IR-myotubes.

Additionally, increased levels of 20S proteasome were found in human serum (Wada et al., 1993), which were described as circulating proteasomes (c-proteasomes). These seem to be elevated in plasma of patients suffering from several diseases including cancer, autoimmune diseases, liver cirrhosis, hepatitis and fatty liver (Wada et al., 1993; Dutaud et al., 2002; Egerer et al., 2002). Hence, it might be speculated that c-proteasomes are also increased in the insulin-resistant state or during type 2 diabetes. Our findings described here, have to be further verified in a larger cohort, since only three different myotubes per group were included in this study, and afterwards *in vivo*.

In accordance with our study, all subunits of the 20S proteasome have been recently identified in the muscle secretome of human myotubes (Hartwig et al., 2014b) and PSMB6 also in a contraction-dependent manner (Roca-Rivada et al., 2012). However, the purpose and function of muscle-released proteasomes or subunits have to be further investigated in future studies.

The simultaneous influence of EPS and insulin sensitivity on human myotubes secretome was only little. Due to the limited number of altered proteins, no general hypothesis could be introduced. However, significantly altered spots on the 2D-gels will be further analyzed by a more sensitive MS-based technique, which will hopefully increase the number of annotated proteins.

Of note, EPS-induced cytokines and chemokines as determined by targeted BioPlex immunoassay were not found in this unbiased secretome profiling. These myokines are rather low abundant but have high biological effectivity and therefore are of high importance. It seems that the sensitivity of LC-MS/MS and 2D-DIGE MALDI-MS is not sufficient to record these proteins. Thus, it might be useful to enrich these low abundant proteins, e.g. by ProteoMiner, prior analysis.

4.3.3 Conclusion and future perspectives

The secretome profiling performed in this study revealed a general overview of the variety of proteins released by primary human myotubes. We identified several proteins that have not been described in the context of exercise so far. In future studies these have to be further verified and investigated to gain insights into their potential role in exercise-induced adaptations. Additionally, the proteins that were differently regulated between IS-myotubes and IR-myotubes might provide novel insights in the pathomechanism of insulin resistance. Of note, several proteins were identified by LC-MS/MS and 2D-DIGE MALDI-MS but most of the proteins were only identified by one method. Thus, a combination of both methods is indeed advisable to obtain a broad range of proteins. However, the sample number in this study is rather low so that results obtained here should be further verified by other experiments, e.g. ELISA, western blot or on transcriptional level. Additionally, it might be useful to confirm potential new myokines in human plasma.

Altogether, we found several new contraction-released myokines and changes in the secretome of human myotubes obtained from donors with different insulin sensitivity, which provides a valuable starting position for future analysis.

4.4 Final remarks

The results obtained within this thesis could verify the importance of Electric pulse stimulation as *in vitro* exercise model to study molecular mechanisms of exercise-induced alteration in glucose and fatty acid metabolism, gene expression and protein secretion as observed *in vivo*. The model has been further developed and might provide broader insights into contraction-induced adaptations in the skeletal muscle, which are of particular interest when investigating myotubes obtained from donors with different phenotypes, e.g. insulin resistance, type 2 diabetes or non-response to exercise intervention. With the application of EPS, future studies might provide insights in novel pathways important for the gene regulation of myokines, as well as exercise-induced changes in the muscle secretome.

5. Appendix

5.1 Supplementary figures
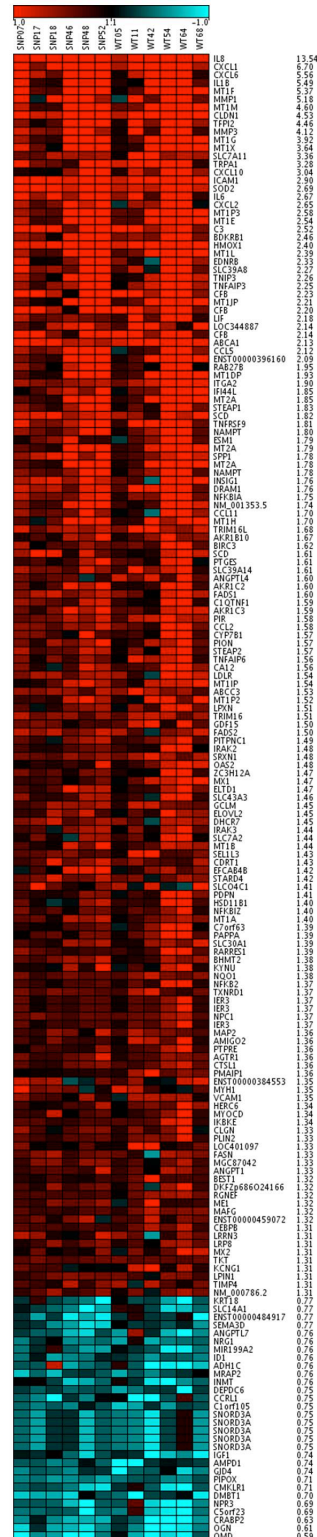
Supplementary Figure I: Heatmap of the 183 significantly regulated probe sets comparing EPS-myotubes with con-myotubes (FDR < 10 %).
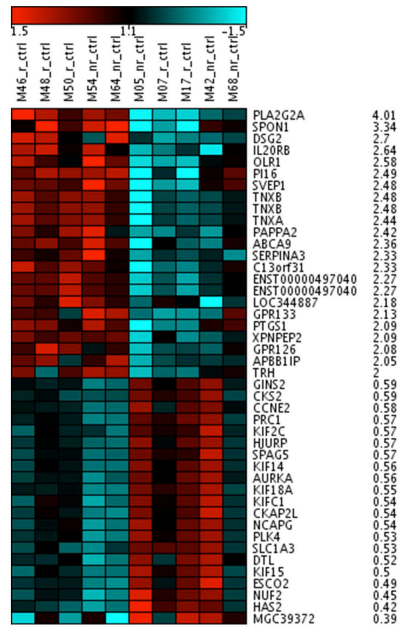
Supplementary Figure II: Heatmap of the top 45 regulated probe sets comparing basal secretion of *IL-8* high and low responder.

5.2 Supplementary tables

Supplementary Table I: Proteins that differ significantly in the supernatant of myotubes after 24 h of EPS vs. con obtained by LC-MS/MS analysis.

Protein ID	Gene name	Ratio EPS/con	Pval	SP+/SP-/NP
P42224	STAT1	2.76	0.0088	SP-
P07711	CTSL1	2.56	0.0087	SP+
Q14192	FHL2	2.55	0.0050	SP-
P67936	TPM4	2.48	0.0339	SP-
P41250	GARS	2.44	0.0035	SP+
Q8NBP7	PCSK9	2.40	0.0165	SP+
P17655	CAPN2	2.31	0.0100	SP-
P68371	TUBB4B	2.08	0.0231	SP-
Q5JP53	TUBB	2.08	0.0280	SP-
P60842	EIF4A1	2.05	0.0491	SP-
F5GX07	REXO2	1.89	0.0082	SP-
P15848	ARSB	1.85	0.0039	SP+
P13489	RNH1	1.83	0.0007	SP-
Q13162	PRDX4	1.81	0.0087	SP+
Q9Y678	COPG1	1.77	0.0158	SP-
Q96AY3	FKBP10	1.76	0.0174	SP+
F8W1R7	MYL6	1.75	0.0408	SP-
Q86UY0	TXNDC5	1.74	0.0110	SP+
P53396	ACLY	1.74	0.0038	SP-
Q76M96	CCDC80	1.67	0.0342	SP+
M0QZH0	RCN3	1.65	0.0492	SP-
Q8NHP8	PLBD2	1.63	0.0006	SP-
P30040	ERP29	1.63	0.0129	SP+
E7ETU9	PLOD2	1.60	0.0043	SP+
P23284	PPIB	1.59	0.0369	SP-
P09936	UCHL1	1.59	0.0268	SP-

B2R5P6	TXNRD1	1.54	0.0028	SP-
P45877	PPIC	1.53	0.0238	SP+
G5EA52	PDIA3	1.53	0.0329	SP+
P30044	PRDX5	1.51	0.0161	SP-
Q9H488	POFUT1	1.51	0.0439	SP+
Q96CX2	KCTD12	1.49	0.0058	SP-
Q969H8	C19orf10	1.49	0.0021	SP+
Q6IBS0	TWF2	1.45	0.0017	SP-
P16152	CBR1	1.44	0.0431	SP-
P15289	ARSA	1.43	0.0055	SP+
P10599	TXN	1.43	0.0239	SP-
P16930	FAH;DKFZp686F13224	1.43	0.0233	SP-
P26599	PTBP1	1.43	0.0326	SP-
O15145	ARPC3	1.42	0.0226	SP-
Q13126	MTAP	1.42	0.0298	SP-
P21291	CSRP1	1.41	0.0226	SP-
Q15113	PCOLCE	1.40	0.0427	SP+
P07858	CTSB	1.40	0.0058	SP+
Q8NBJ7	SUMF2	1.40	0.0488	SP+
P28838	LAP3	1.40	0.0090	SP-
Q9NYU2	UGGT1	1.39	0.0197	SP+
P61158	ACTR3	1.39	0.0164	SP-
P22234	PAICS	1.39	0.0170	SP-
B7Z4K6	DNASE2	1.38	0.0049	SP+
P42126	ECI1;DCI	1.37	0.0058	SP-
Q06323	PSME1	1.36	0.0446	SP-
O75874	IDH1	1.34	0.0185	SP-
P00338	LDHA	1.34	0.0155	SP-
Q9Y265	RUVBL1	1.33	0.0499	SP-
P49189	ALDH9A1	1.32	0.0015	SP-
P09211	GSTP1	1.32	0.0196	SP-
P63261	ACTG1	1.30	0.0177	SP-
Q9NR45	NANS	1.30	0.0280	SP-
P00367	GLUD1;GLUD2	1.30	0.0308	SP-
Q15404	RSU1	1.30	0.0239	SP-
Q96IU4	ABHD14B	1.29	0.0122	SP-
P54687	BCAT1	1.29	0.0192	SP-
P61160	ACTR2	1.28	0.0066	SP-
P04406	GAPDH	1.27	0.0063	SP-
Q07954	LRP1	1.26	0.0157	SP+
P06733	ENO1	1.26	0.0246	SP-
P17931	LGALS3	1.25	0.0461	SP-
Q13228	SELENBP1	1.24	0.0192	SP-
H0YD13	CD44	1.24	0.0193	SP+
Q5TD07	NQO2	1.24	0.0385	SP-
P62826	RAN	1.23	0.0120	SP-
P08107	HSPA1A	1.22	0.0064	SP-
B4DLR2	FAP	1.22	0.0448	SP-
P10768	ESD	1.21	0.0081	SP-
H7C3P4	GNS	1.20	0.0009	SP-
P60174	TPI1	1.20	0.0429	SP-
P09960	LTA4 h	1.19	0.0374	SP-
Q9Y646	CPQ	1.19	0.0392	SP+

P62140	PPP1CB;PPP1CC;PPP1CA	1.18	0.0456	SP-
Q14914	PTGR1	1.17	0.0428	SP-
P40121	CAPG	1.16	0.0331	SP-
O75083	WDR1	1.15	0.0345	SP-
P22314	UBA1	1.15	0.0473	SP-
Q92520	FAM3C	1.15	0.0279	SP-
Q9BZK7	TBL1XR1;TBL1Y;TBL1X	0.87	0.0231	SP-
Q09028	RBBP4;RBBP7	0.87	0.0075	SP-
P00352	ALDH1A1	0.87	0.0405	SP-
Q9UBQ7	GRHPR	0.86	0.0470	SP-
P40123	CAP2	0.85	0.0229	SP-
P13591	NCAM1	0.84	0.0003	SP+
Q13308	PTK7	0.84	0.0314	SP+
P34096	RNASE4	0.82	0.0440	SP+
Q99969	RARRES2	0.82	0.0296	SP+
P30566	ADSL	0.81	0.0364	SP-
Q13219	PAPPA	0.80	0.0243	SP+
Q8IXJ6	SIRT2	0.79	0.0476	SP-
Q9Y4K0	LOXL2	0.79	0.0427	SP+
Q15819	UBE2V2	0.79	0.0321	SP-
P12277	CKB	0.79	0.0303	SP-
P41222	PTGDS	0.79	0.0457	SP-
Q6ZMU5	TRIM72	0.78	0.0045	SP-
Q9BXJ0	C1QTNF5	0.78	0.0426	SP+
P25391	LAMA1	0.78	0.0273	SP+
Q68BL7	OLFML2A	0.78	0.0046	SP+
Q6FHJ7	SFRP4	0.77	0.0177	SP+
G3V5X6	HNRNPC;HNRNPCL1	0.77	0.0182	SP-
H0YM81	ACAN	0.77	0.0102	SP+
P24043	LAMA2	0.76	0.0163	SP+
P50895	BCAM	0.76	0.0125	SP+
P13497	BMP1	0.75	0.0211	SP+
Q9Y696	CLIC4	0.75	0.0157	SP-
P43121	MCAM	0.75	0.0095	SP+
P12829	MYL4	0.75	0.0034	SP-
P14649	MYL6B	0.74	0.0316	SP-
E7ERV9	ASAH1	0.73	0.0001	SP-
Q92743	HTRA1	0.72	0.0345	SP+
Q9NTK5	OLA1	0.72	0.0219	SP-
Q9H4D0	CLSTN2	0.72	0.0103	SP+
Q12841	FSTL1	0.72	0.0054	SP+
Q7Z7G0	ABI3BP	0.71	0.0166	SP+
P63000	RAC1;RAC3	0.71	0.0028	SP-
Q00688	FKBP3	0.71	0.0398	SP-
Q53GG5	PDLIM3	0.71	0.0124	SP-
P55058	PLTP	0.69	0.0348	SP+
P08476	INHBA	0.69	0.0090	SP+
Q9BUD6	SPON2	0.67	0.0067	SP+
P05090	APOD	0.67	0.0181	SP+
P24592	IGFBP6	0.67	0.0337	SP+
P49746	THBS3	0.67	0.0108	SP+
F8W717	EML1	0.66	0.0070	SP-
Q6UXB8	PI16	0.66	0.0183	SP+

Q92626	PXDN	0.65	0.0167	SP+
O75112	LDB3	0.65	0.0055	SP-
Q96KG7	MEGF10	0.64	0.0333	SP+
P07093	SERPINE2	0.64	0.0035	SP+
P02462	COL4A1	0.63	0.0211	SP+
Q7Z7M0	MEGF8	0.62	0.0011	SP+
Q8IX30	SCUBE3	0.60	0.0225	SP+
Q13203	MYBPH	0.60	0.0083	SP-
P25940	COL5A3	0.60	0.0010	SP+
P05556	ITGB1	0.60	0.0331	SP+
Q8WUJ3	KIAA1199	0.60	0.0351	SP+
B3KW70	MFAP5;MAGP2	0.59	0.0079	SP+
A1L4 h1	SSC5D	0.59	0.0318	SP+
P48740	MASP1	0.58	0.0092	SP-
Q93063	EXT2	0.57	0.0083	SP-
B1ALD9	POSTN	0.56	0.0029	SP+
P05997	COL5A2	0.56	0.0139	SP+
P52943	CRIP2	0.53	0.0127	SP-
P02452	COL1A1	0.53	0.0130	SP+
Q96A32	MYLPF	0.53	0.0049	SP-
Q86SR1	GALNT10	0.53	0.0229	SP-
P22692	IGFBP4	0.52	0.0043	SP+
Q13642	FHL1	0.52	0.0062	SP-
P19237	TNNI1	0.51	0.0180	SP-
P08123	COL1A2	0.51	0.0054	SP+
Q641Q3	METRNL	0.50	0.0129	SP+
O75462	CRLF1	0.50	0.0042	SP+
Q6QEF8	CORO6	0.49	0.0029	SP-
P55291	CDH15	0.48	0.0003	SP+
P02461	COL3A1	0.46	0.0039	SP+
P27658	COL8A1	0.46	0.0039	SP+
P07355	ANXA2;ANXA2P2	0.43	0.0067	SP-
Q86XX4	FRAS1	0.42	0.0010	SP+
F5H7N9	MFGE8	0.39	0.0126	SP+
P04083	ANXA1	0.31	0.0016	SP-
P08133	ANXA6	0.28	0.0292	SP-
E7ENM0	ELN	0.26	0.0040	SP+
E7EPW4	TNNT2	0.22	0.0469	SP-
Q9BS40	LXN	2.87	0.0086	NP
O75369	FLNB	2.49	0.0020	NP
Q9Y617	PSAT1	2.25	0.0028	NP
P11413	G6PD	2.24	0.0003	NP
P23381	WARS	2.18	0.0025	NP
Q14195	DPYSL3	2.07	0.0043	NP
O15143	ARPC1B	2.07	0.0029	NP
Q16555	DPYSL2	2.03	0.0040	NP
P21333	FLNA	1.93	0.0064	NP
P13797	PLS3	1.84	0.0045	NP
Q96TA1	FAM129B	1.74	0.0033	NP
P26639	TARS	1.69	0.0072	NP
P29401	TKT	1.63	0.0002	NP
P48444	ARCN1	1.60	0.0225	NP
Q07960	ARHGAP1	1.60	0.0427	NP

O43776	NARS	1.51	0.0069	NP
Q5VTE0	EEF1A1P5;EEF1A1	1.51	0.0390	NP
Q5TA02	GSTO1	1.51	0.0443	NP
C9JBI3	PSPH	1.50	0.0247	NP
P36871	PGM1	1.50	0.0089	NP
P14550	AKR1A1	1.48	0.0085	NP
O15144	ARPC2	1.42	0.0344	NP
Q9Y490	TLN1	1.41	0.0314	NP
P09382	LGALS1	1.39	0.0306	NP
P46940	IQGAP1	1.39	0.0137	NP
P45974	USP5	1.36	0.0298	NP
P46821	MAP1B	1.35	0.0203	NP
Q96G03	PGM2	1.35	0.0410	NP
Q16658	FSCN1	1.34	0.0012	NP
Q92598	HSPH1	1.28	0.0245	NP
O00299	CLIC1	1.26	0.0290	NP
P12814	ACTN1	1.26	0.0375	NP
Q15181	PPA1	1.25	0.0249	NP
P46926	GNPDA1	1.25	0.0296	NP
Q96KP4	CNDP2	1.24	0.0342	NP
O94760	DDAH1	1.24	0.0239	NP
B7Z1R5	ATP6V1A	1.23	0.0329	NP
P18206	VCL	1.15	0.0228	NP
P06744	GPI	1.13	0.0443	NP
P00558	PGK1	1.10	0.0357	NP
P15121	AKR1B1	0.87	0.0034	NP
Q96C23	GALM	0.82	0.0072	NP
P00488	F13A1	0.81	0.0014	NP
Q13263	TRIM28	0.79	0.0390	NP
Q8WZ422	TTN	0.74	0.0018	NP
P13929	ENO3	0.73	0.0334	NP
D6R9P3	HNRNPAB	0.72	0.0347	NP
H3BPE1	MACF1	0.72	0.0108	NP
O00499-9	BIN1	0.70	0.0288	NP
O75635	SERPINB7	0.69	0.0392	NP
Q01844	EWSR1	0.64	0.0115	NP
E9PAV3	NACA	0.63	0.0062	NP
Q15124	PGM5	0.62	0.0127	NP
O75882	ATRN	0.61	0.0322	NP
P06732	CKM	0.60	0.0025	NP
Q16394	EXT1	0.59	0.0204	NP
B7Z9G5	C1orf58;BROX	0.56	0.0000	NP
O14964	HGS	0.56	0.0031	NP

Table shows Uniprot ID (Protein ID) and annotated gene names. Pval is calculated by 2-way ANOVA. SP+: protein is secreted via classical secretion pathway (determined by SignalP database); SP-: protein is secreted via non-classical secretion pathway (determined by SignalP and SecretomeP database). NP: protein is described as non-secreted (determined by Secretome P database).

Supplementary Table II: Proteins that differ significantly between the control supernatant of myotubes obtained from insulin-sensitive and resistant donors obtained by LC-MS/MS analysis.

Protein ID	Gene name	Ratio IR/IS	Pval	SP+/SP-/NP
P30050	RPL12	9.36	0.01746	SP-
P39060-2	COL18A1	3.66	0.00819	SP+
P35052	GPC1	3.31	0.00209	SP+
P03956	MMP1	2.99	0.00053	SP+
P28070	PSMB4	2.45	0.03992	SP-
P17655	CAPN2	2.42	0.04970	SP-
Q15019	41884	2.34	0.03346	SP-
Q9HB71	CACYBP	2.21	0.04090	SP-
Q8IX30	SCUBE3	2.19	0.01113	SP+
P25787	PSMA2	2.13	0.01323	SP-
H0YMZ1	PSMA4	1.83	0.04700	SP-
P28072	PSMB6	1.78	0.03961	SP-
P60900	PSMA6	1.77	0.04096	SP-
P28074	PSMB5	1.73	0.04942	SP-
P19237	TNNI1	1.70	0.02105	SP-
Q08257	CRYZ	1.67	0.00581	SP-
Q9UHD1	CHORDC1	1.66	0.04733	SP-
P42330	AKR1C3	1.59	0.01371	SP-
P68032	ACTC1;ACTA2;ACTG2; ACTA1	1.58	0.00005	SP-
P25398	RPS12	1.56	0.02178	SP-
E9PQ56	PUF60	1.51	0.02228	SP-
E7ERV9	ASAH1	1.51	0.00005	SP-
Q9ULV4	CORO1C	1.50	0.03663	SP-
P63244	GNB2L1	1.50	0.04131	SP-
P10909-4	CLU	1.49	0.01233	SP-
G3V5X6	HNRNPC;HNRNPCL1	1.48	0.01023	SP-
P09211	GSTP1	1.48	0.04194	SP-
Q15365	PCBP1	1.44	0.01923	SP-
P05090	APOD	1.41	0.02648	SP+
Q8WX93-8	PALLD	1.41	0.00719	SP-
P78539	SRPX	1.40	0.04964	SP+
P26641	EEF1G	1.40	0.00077	SP-
P62826	RAN	1.38	0.04966	SP-
P63261	ACTG1	1.37	0.02330	SP-
P04406	GAPDH	1.36	0.01258	SP-
H7C3P4	GNS	1.33	0.00047	SP-
Q9NTK5	OLA1	1.33	0.03656	SP-
P47755	CAPZA2	1.32	0.03709	SP-
Q8IXJ6-2	SIRT2	1.32	0.04010	SP-
Q8WUP2-3	FBLIM1	1.31	0.00033	SP-
P10253	GAA	1.29	0.03392	SP+
P63000	RAC1;RAC3	1.28	0.01982	SP-
H0YM81	ACAN	1.27	0.02473	SP+
P17661	DES	1.25	0.01226	SP-
Q92820	GGH	1.25	0.03511	SP+
P11142	HSPA8	1.24	0.04336	SP-
P27348	YWHAQ	1.24	0.03830	SP-
O60662	KLHL41	1.23	0.02814	SP-

P39059	COL15A1	1.19	0.04839	SP+
Q68BL8	OLFML2B	1.18	0.03068	SP+
Q86XX4-2	FRAS1	1.16	0.03255	SP+
Q9BXJ0	C1QTNF5	1.13	0.03618	SP+
P12829	MYL4	1.13	0.00379	SP-
P25940	COL5A3	1.13	0.00896	SP+
Q9UBP4	DKK3	1.11	0.02868	SP+
Q9BZK7	TBL1XR1;TBL1Y;TBL1X	1.09	0.03920	SP-
Q68BL7-2	OLFML2A	1.09	0.04291	SP+
Q8WX77	IGFBPL1	1.07	0.04092	SP+
Q02809	PLOD1	1.05	0.03500	SP+
P42126-2	ECI1;DCI	1.04	0.03613	SP-
Q09028-3	RBBP4;RBBP7	1.03	0.04032	SP-
P08107	HSPA1A	1.01	0.04318	SP-
P09960	LTA4 h	0.96	0.03128	SP-
Q9NZL9	MAT2B	0.95	0.04386	SP-
O75874	IDH1	0.94	0.03039	SP-
Q9ULA0	DNPEP	0.92	0.04553	SP-
Q01459	CTBS	0.89	0.04849	SP+
Q9Y646	CPQ	0.86	0.02364	SP+
Q969H8	C19orf10	0.85	0.02559	SP+
P13611	VCAN	0.84	0.02364	SP+
P07954-2	FH	0.84	0.02930	SP-
B4DLR2	FAP	0.83	0.02399	SP-
E9PCB6	NLN	0.82	0.03813	SP-
J3KQG4	GBA	0.82	0.04988	SP-
P13591-4	NCAM1	0.82	0.00083	SP+
P11279	LAMP1	0.81	0.03476	SP+
P12955	PEPD	0.79	0.04940	SP-
Q9H4A4	RNPEP	0.78	0.00313	SP-
P11717	IGF2R	0.78	0.02993	SP+
Q99969	RARRES2	0.77	0.01438	SP+
P09622	DLD	0.77	0.01341	SP-
O00534	VWA5A	0.76	0.01751	SP-
Q07954	LRP1	0.74	0.02920	SP+
Q92859-3	NEO1	0.74	0.03114	SP+
P15848	ARSB	0.73	0.02174	SP+
O95834	EML2	0.73	0.02383	SP-
Q9UM22	EPDR1;UCC1	0.71	0.01399	SP+
P25391	LAMA1	0.70	0.04863	SP+
O00462	MANBA	0.70	0.02980	SP+
P24043	LAMA2	0.69	0.04037	SP+
G3XAP6	COMP	0.68	0.04024	SP+
P07093-2		0.68	0.00471	SP+
B7Z2R9	LAMP2	0.66	0.01324	SP-
P35555	FBN1	0.65	0.01064	SP+
Q13642-1	FHL1	0.64	0.02292	SP-
Q6EMK4	VASN	0.64	0.01977	SP+
P23142-4	FBLN1	0.63	0.01417	SP+
P50454	SERPINH1	0.63	0.01089	SP+
Q6FHJ7	SFRP4	0.63	0.00329	SP+
P00749-2	PLAU	0.60	0.00220	SP+
P23142	FBLN1	0.59	0.01938	SP+

Q6QEF8-5	CORO6	0.58	0.03719	SP-
Q15293	RCN1	0.58	0.04402	SP+
Q6UXB8	PI16	0.57	0.03356	SP+
Q13219	PAPPA	0.56	0.01002	SP+
Q99715	COL12A1	0.55	0.00990	SP+
Q8WUJ3	KIAA1199	0.55	0.04263	SP+
P49746	THBS3	0.55	0.01206	SP+
P05997	COL5A2	0.53	0.04406	SP+
G3V3X5	LTBP2	0.53	0.01490	SP+
P28300	LOX	0.49	0.00234	SP+
Q12805-2	EFEMP1	0.47	0.00411	SP-
Q06828	FMOD	0.46	0.01305	SP+
P27658	COL8A1	0.42	0.00968	SP+
Q9BXP8	PAPPA2	0.32	0.00465	SP+
P05388	RPLP0;RPLP0P6	12.03	0.01704	NP
P11055	MYH3	2.89	0.01615	NP
Q99460-2	PSMD1	2.75	0.02676	NP
A8K8G0	HDGF	2.52	0.01548	NP
P25788-2	PSMA3	2.24	0.01434	NP
Q4J6C6-4	PREPL	2.15	0.01186	NP
P02545	LMNA	2.03	0.03666	NP
P20618	PSMB1	1.86	0.03263	NP
P25786	PSMA1	1.86	0.03164	NP
O14818	PSMA7	1.81	0.02587	NP
Q9UQ80	PA2G4	1.71	0.02107	NP
D6RGI3	41893	1.64	0.01460	NP
P00966	ASS1	1.63	0.03719	NP
B7Z2C3	PPM1F	1.59	0.02071	NP
P49721	PSMB2	1.57	0.04438	NP
H0Y3Y4	41889	1.53	0.01964	NP
P45974-2	USP5	1.44	0.03735	NP
Q04917	YWHAH	1.37	0.04137	NP
O00499-9	BIN1	1.35	0.04777	NP
B4DQJ8	PGD	1.35	0.00464	NP
P13639	EEF2	1.34	0.01486	NP
P46821	MAP1B	1.33	0.03887	NP
P20700	LMNB1	1.11	0.04241	NP
Q8WZ42-12	TTN	1.07	0.00693	NP
P33908	MAN1A1	0.61	0.03632	NP
Q6UX71-2	PLXDC2	0.60	0.00115	NP
O75635-2	SERPINB7	0.49	0.01194	NP

Table shows Uniprot ID (Protein ID) and annotated gene names. Pval is calculated by 2-way ANOVA. SP+: protein is secreted via classical secretion pathway (determined by SignalP database); SP-: protein is secreted via non-classical secretion pathway (determined by SignalP and SecretomeP database). NP: protein is described as non-secreted (determined by SecretomeP database).

Supplementary Table III: Proteins that differ significantly between the supernatant of myotubes obtained from insulin-sensitive and resistant donors upon EPS obtained by LC-MS analysis

Protein ID	Gene name	Ratio IR (EPS/con)/ IS (EPS/con)	Pval	SP+/SP-/NP
H0YM81	ACAN	1.90	0.0283	SP+
A6NLG9	BGN	1.33	0.0055	SP+
P68032	ACTC1;ACTA2;ACTG2;ACTA1	1.31	0.0129	SP-
O60687	SRPX2	1.25	0.0235	SP+
P12111	COL6A3	1.23	0.0343	SP+
H7C3P4	GNS	1.18	0.0491	SP-
Q7Z7M0	MEGF8	1.17	0.0084	SP+
Q12841	FSTL1	1.17	0.0382	SP+
Q09028	RBBP4;RBBP7	1.14	0.0436	SP-
P14543	NID1	1.14	0.0057	SP+
P13611	VCAN	1.11	0.0432	SP+
G3V5X6	HNRNPC;HNRNPCL1	1.11	0.0482	SP-
O95967	EFEMP2	1.10	0.0460	SP+
P55268	LAMB2	1.06	0.0379	SP+
Q7Z7G0	ABI3BP	1.04	0.0418	SP+
P26641	EEF1G	1.04	0.0034	SP-
Q9Y3A5	SBDS	1.03	0.0391	SP-
E9PQ56	PUF60	0.95	0.0110	SP-
P62826	RAN	0.95	0.0202	SP-
P54687	BCAT1	0.94	0.0470	SP-
P46108	CRK	0.93	0.0171	SP-
P13693	TPT1	0.93	0.0463	SP-
P61160	ACTR2	0.93	0.0303	SP-
P63244	GNB2L1	0.92	0.0123	SP-
P13591	NCAM1	0.91	0.0229	SP+
O75083	WDR1	0.90	0.0414	SP-
P13489	RNH1	0.90	0.0398	SP-
O00764	PDXK	0.89	0.0081	SP-
Q5TD07	NQO2	0.88	0.0352	SP-
E9PGT1	TSN	0.85	0.0349	SP-
Q13219	PAPPA	0.83	0.0203	SP+
P49189	ALDH9A1	0.83	0.0220	SP-
Q6IBS0	TWF2	0.81	0.0254	SP-
Q03154	ACY1;ABHD14A-ACY1	0.81	0.0441	SP-
Q9UJ70	NAGK	0.81	0.0500	SP-
P30044	PRDX5	0.80	0.0482	SP-
Q13630	TSTA3	0.79	0.0333	SP-
P42126	ECI1;DCI	0.75	0.0222	SP-
Q15181	PPA1	0.92	0.0246	NP
Q96KP4	CNDP2	0.90	0.0484	NP
P54136	RARS	0.89	0.0169	NP
P15121	AKR1B1	0.86	0.0323	NP
Q16658	FSCN1	0.86	0.0154	NP
O94760	DDAH1	0.84	0.0259	NP
B7Z9G5	C1orf58;BROX	0.84	0.0242	NP
P00558	PGK1	0.83	0.0067	NP

Q96C23	GALM		0.78	0.0070		NP
P30041	PRDX6		0.76	0.0488		NP
P36871	PGM1		0.71	0.0303		NP

Table shows Uniprot ID (Protein ID) and annotated gene names. Pval is calculated by 2-way ANOVA. SP+: protein is secreted via classical secretion pathway (determined by SignalP database); SP-: protein is secreted via non-classical secretion pathway (determined by SignalP and SecretomeP database). NP: protein is described as non-secreted (determined by Secretome P database).

Supplementary Table IV: Proteins that differ significantly in the supernatant of myotubes after 24 h of EPS vs. con obtained by 2D-DIGE MALDI-MS analysis.

Protein ID	Name	Gene name	Ratio EPS/con	Pval	No.	pH IEF	SP+/SP- /NP
Q15582	Transforming growth factor-beta-induced protein ig-h3	TGFBI	4.14	0.0089	3	6-9	SP+
P08670	Vimentin	VIM	3.72	0.0204	3	4-7	SP-
O95336	6-phosphogluconolactonase	PGLS	3.00	0.0375	1	4-7	SP-
P07711	Cathepsin L1	CTSL	2.30	0.0282	1	4-7	SP+
Q15063	Periostin	POSTN	1.79	0.0089	1	6-9	SP+
P08123	Collagen alpha-2(I) chain	COL1A2	1.52	0.0306	1	6-9	SP+
P28074	Proteasome subunit beta type-5	PSMB5	0.67	0.0487	1	6-9	SP-
P17661	Desmin	DES	0.65	0.0043	1	4-7	SP-
Q9Y696	Chloride intracellular channel protein 4	CLIC4	0.63	0.0010	1	4-7	SP-
P36955	Pigment epithelium-derived factor	SERPINF1	0.60	0.0011	2	4-7	SP+
Q06830	Peroxiredoxin-1	PRDX1	0.60	0.0329	1	6-9	SP-
P09486	SPARC	SPARC	0.60	0.0014	3	4-7	SP+
P55291	Cadherin-15	CDH15	0.57	0.0005	4	4-7	SP+
P22692	Insulin-like growth factor-binding protein 4	IGFBP4	0.56	0.0063	1	6-9	SP+
Q12841	Follistatin-related protein 1	FSTL1	0.53	0.0095	8	4-7	SP+
P08123	Collagen alpha-2(I) chain	COL1A2	0.52	0.0031	10	6-9	SP+
Q96A32	Myosin regulatory light chain 2	MYLPF	0.49	0.0081	2	4-7	SP-
Q99969	Retinoic acid receptor responder protein 2	RARRES2	0.49	0.0095	1	6-9	SP+
P02452	Collagen alpha-1(I) chain	COL1A1	0.44	0.0006	13	4-7	SP+
Q15063	Periostin	POSTN	0.36	0.0043	8	6-9	SP+
P30041	Peroxiredoxin-6	PRDX6	2.84	0.0446	1	4-7	NP
Q9Y617	Phosphoserine aminotransferase	PSAT1	2.15	0.0200	2	6-9	NP
P67936	Tropomyosin alpha-4 chain	TPM4	1.87	0.0024	1	4-7	NP
P23381	Tryptophan--tRNA ligase. cytoplasmic	WARS	1.77	0.0221	1	4-7	NP
P23284	Peptidyl-prolyl cis-trans isomerase B	PPIB	1.66	0.0186	1	6-9	NP
Q16555	Dihydropyrimidinase-	DPYSL2	1.59	0.0281	1	4-7	NP

	related protein 2						
P12277	Creatine kinase B-type	CKB	0.62	0.0104	1	4-7	NP
P35232	Prohibitin	PHB	0.42	0.0002	2	4-7	NP

Table shows all annotated proteins that had a fold change > 1.5x EPS vs. con and a p-value < 0.05. Uniprot ID (Protein ID) and annotated names and gene names are shown. Pval is calculated by students t-test. No.: Number of total spots found for this protein (shown is ratio of spot with highest fold change in one direction). pH IEF: pH scale of isolelectric focusing strips. SP+: protein is secreted via classical secretion pathway (determined by SignalP database); SP-: protein is secreted via non-classical secretion pathway (determined by SignalP and SecretomeP database). NP: protein is described as non-secreted (determined by SecretomeP database).

Supplementary Table V: Proteins that differ significantly in the control supernatant of myotubes obtained from insulin-sensitive and resistant donors obtained by 2D-DIGE MALDI-MS analysis.

Protein ID	Name	Gene name	Ratio IR/IS	Pval	No.	pH IEF	SP+/ SP-/NP
Q00688	Peptidyl-prolyl cis-trans isomerase FKBP3	FKBP3	1.70		1	6-9	SP-
P08670	Vimentin	VIM	1.56	0.0181	2	4-7	SP-
Q99969	Retinoic acid receptor responder protein 2	RARRES2	0.67		1	6-9	SP+
Q15063	Periostin	POSTN	0.67		1	6-9	SP+
P02452	Collagen alpha-1(I) chain	COL1A1	0.66	0.0276	3	4-7	SP+
Q00689	Peptidyl-prolyl cis-trans isomerase FKBP3	FKBP3	0.59		1	6-9	SP-
P08123	Collagen alpha-2(I) chain	COL1A2	0.56		1	6-9	SP+
P50454	Serpin H1	SERPINH1	0.54		3	6-9	SP+
Q13642	Four and a half LIM domains protein 1	FHL1	0.41		1	6-9	SP-
P21291	Cysteine and glycine-rich protein 1	CSRP1	0.65		1	6-9	NP
P13929	Beta-enolase	ENO3	0.67		1	6-9	NP
P06744	Glucose-6-phosphate isomerase	GPI	0.60		2	6-9	NP
P02545	Prelamin-A/C	LMNA	1.70		1	6-9	NP
P25787	Proteasome subunit alpha type-2	PSMA2	1.67		1	6-9	NP
O14818	Proteasome subunit alpha type-7	PSMA7	1.56		1	6-9	NP

Table shows all annotated proteins that had a fold change > 1.5x IR vs. IS (in the con-supernatant samples). p-value could be calculated only for pH 4-7 since only two gels with con samples of IS-myotubes were ran. Uniprot ID (Protein ID) and annotated names and gene names are shown. Pval is calculated by students t-test. No.: Number of total spots with a fold change > 1.5x found for this protein (shown is spot with highest fold change in one direction). pH IEF: pH scale of isolelectric focusing strips. SP+: protein is secreted via classical secretion pathway (determined by SignalP database); SP-: protein is secreted via non-classical secretion pathway (determined by SignalP and SecretomeP database). NP: protein is described as non-secreted (determined by SecretomeP database).

6. References

Aas, V., N.P. Hessvik, M. Wettergreen, A.W. Hvammen, S. Hallen, G.H. Thoresen, and A.C. Rustan. 2011. Chronic hyperglycemia reduces substrate oxidation and impairs metabolic switching of human myotubes. *Biochimica et biophysica acta*. 1812:94-105.

Ameln, H., T. Gustafsson, C.J. Sundberg, K. Okamoto, E. Jansson, L. Poellinger, and Y. Makino. 2005. Physiological activation of hypoxia inducible factor-1 in human skeletal muscle. *FASEB journal : official publication of the Federation of American Societies for Experimental Biology*. 19:1009-1011.

Anderson, R.J., K.E. Freedland, R.E. Clouse, and P.J. Lustman. 2001. The prevalence of comorbid depression in adults with diabetes: a meta-analysis. *Diabetes care*. 24:1069-1078.

Aoi, W., Y. Naito, T. Takagi, Y. Tanimura, Y. Takanami, Y. Kawai, K. Sakuma, L.P. Hang, K. Mizushima, Y. Hirai, R. Koyama, S. Wada, A. Higashi, S. Kokura, H. Ichikawa, and T. Yoshikawa. 2013. A novel myokine, secreted protein acidic and rich in cysteine (SPARC), suppresses colon tumorigenesis via regular exercise. *Gut*. 62:882-889.

Arany, Z., S.Y. Foo, Y. Ma, J.L. Ruas, A. Bommi-Reddy, G. Girnun, M. Cooper, D. Laznik, J. Chinsomboon, S.M. Rangwala, K.H. Baek, A. Rosenzweig, and B.M. Spiegelman. 2008. HIF-independent regulation of VEGF and angiogenesis by the transcriptional coactivator PGC-1alpha. *Nature*. 451:1008-1012.

Aronson, D., M.D. Boppart, S.D. Dufresne, R.A. Fielding, and L.J. Goodyear. 1998. Exercise stimulates c-Jun NH2 kinase activity and c-Jun transcriptional activity in human skeletal muscle. *Biochemical and biophysical research communications*. 251:106-110.

Aronson, D., M.A. Violan, S.D. Dufresne, D. Zangen, R.A. Fielding, and L.J. Goodyear. 1997. Exercise stimulates the mitogen-activated protein kinase pathway in human skeletal muscle. *The Journal of clinical investigation*. 99:1251-1257.

Austin, R.L., A. Rune, K. Bouzakri, J.R. Zierath, and A. Krook. 2008. siRNA-mediated reduction of inhibitor of nuclear factor-kappaB kinase prevents tumor necrosis factor-alpha-induced insulin resistance in human skeletal muscle. *Diabetes*. 57:2066-2073.

Bain, J.R., R.D. Stevens, B.R. Wenner, O. Ilkayeva, D.M. Muoio, and C.B. Newgard. 2009. Metabolomics applied to diabetes research: moving from information to knowledge. *Diabetes*. 58:2429-2443.

Baker, J.S., M.C. McCormick, and R.A. Robergs. 2010. Interaction among Skeletal Muscle Metabolic Energy Systems during Intense Exercise. *Journal of nutrition and metabolism*. 2010:905612.

Balsom, P.D., G.C. Gaitanos, B. Ekblom, and B. Sjodin. 1994. Reduced oxygen availability during high intensity intermittent exercise impairs performance. *Acta physiologica Scandinavica*. 152:279-285.

Bendtsen, J.D., L.J. Jensen, N. Blom, G. Von Heijne, and S. Brunak. 2004. Feature-based prediction of non-classical and leaderless protein secretion. *Protein engineering, design & selection : PEDS*. 17:349-356.

Blau, H.M., and C. Webster. 1981. Isolation and characterization of human muscle cells. *Proceedings of the National Academy of Sciences of the United States of America*. 78:5623-5627.

Bochtler, M., L. Ditzel, M. Groll, C. Hartmann, and R. Huber. 1999. The proteasome. *Annual review of biophysics and biomolecular structure*. 28:295-317.

Boppart, M.D., D. Aronson, L. Gibson, R. Roubenoff, L.W. Abad, J. Bean, L.J. Goodyear, and R.A. Fielding. 1999. Eccentric exercise markedly increases c-Jun NH(2)-terminal kinase activity in human skeletal muscle. *J Appl Physiol (1985)*. 87:1668-1673.

Bortoluzzi, S., P. Scannapieco, A. Cestaro, G.A. Danieli, and S. Schiaffino. 2006. Computational reconstruction of the human skeletal muscle secretome. *Proteins*. 62:776-792.

Bostrom, P., J. Wu, M.P. Jedrychowski, A. Korde, L. Ye, J.C. Lo, K.A. Rasbach, E.A. Bostrom, J.H. Choi, J.Z. Long, S. Kajimura, M.C. Zingaretti, B.F. Vind, H. Tu, S. Cinti, K. Hojlund, S.P. Gygi, and B.M. Spiegelman. 2012. A PGC1-alpha-dependent myokine that drives brown-fat-like development of white fat and thermogenesis. *Nature*. 481:463-468.

Bourlier, V., C. Saint-Laurent, K. Louche, P.M. Badin, C. Thalamas, I. de Glisezinski, D. Langin, C. Sengenes, and C. Moro. 2013. Enhanced glucose metabolism is preserved in cultured primary myotubes from obese donors in response to exercise training. *The Journal of clinical endocrinology and metabolism*. 98:3739-3747.

Bradford, M.M. 1976. A rapid and sensitive method for the quantitation of microgram quantities of protein utilizing the principle of protein-dye binding. *Analytical biochemistry*. 72:248-254.

Bramono, D.S., J.C. Richmond, P.P. Weitzel, D.L. Kaplan, and G.H. Altman. 2004. Matrix metalloproteinases and their clinical applications in orthopaedics. *Clinical orthopaedics and related research*:272-285.

Broholm, C., M.J. Laye, C. Brandt, R. Vadalasetty, H. Pilegaard, B.K. Pedersen, and C. Scheele. 2011. LIF is a contraction-induced myokine stimulating human myocyte proliferation. *J Appl Physiol (1985)*. 111:251-259.

Bruce, C.R., and D.J. Dyck. 2004. Cytokine regulation of skeletal muscle fatty acid metabolism: effect of interleukin-6 and tumor necrosis factor-alpha. *American journal of physiology. Endocrinology and metabolism*. 287:E616-621.

Burch, N., A.S. Arnold, F. Item, S. Summermatter, G. Brochmann Santana Santos, M. Christe, U. Boutellier, M. Toigo, and C. Handschin. 2010. Electric pulse stimulation of cultured murine muscle cells reproduces gene expression changes of trained mouse muscle. *PloS one*. 5:e10970.

Burger, N.B., K.E. Stuurman, E. Kok, T. Konijn, D. Schooneman, K. Niederreither, M. Coles, W.W. Agace, V.M. Christoffels, R.E. Mebius, S.A. van de Pavert, and M.N. Bekker. 2014. Involvement of neurons and retinoic acid in lymphatic development: new insights in increased nuchal translucency. *Prenatal diagnosis*.

Bustamante, M., R. Fernandez-Verdejo, E. Jaimovich, and S. Buvinic. 2014. Electrical stimulation induces IL-6 in skeletal muscle through extracellular ATP by activating Ca2+ signals and an IL-6 autocrine loop. *American journal of physiology. Endocrinology and metabolism*. 306:E869-882.

Calvo, J.A., T.G. Daniels, X. Wang, A. Paul, J. Lin, B.M. Spiegelman, S.C. Stevenson, and S.M. Rangwala. 2008. Muscle-specific expression of

PPARgamma coactivator-1alpha improves exercise performance and increases peak oxygen uptake. *J Appl Physiol (1985)*. 104:1304-1312.

Canto, C., Z. Gerhart-Hines, J.N. Feige, M. Lagouge, L. Noriega, J.C. Milne, P.J. Elliott, P. Puigserver, and J. Auwerx. 2009. AMPK regulates energy expenditure by modulating NAD+ metabolism and SIRT1 activity. *Nature*. 458:1056-1060.

Carey, A.L., G.R. Steinberg, S.L. Macaulay, W.G. Thomas, A.G. Holmes, G. Ramm, O. Prelovsek, C. Hohnen-Behrens, M.J. Watt, D.E. James, B.E. Kemp, B.K. Pedersen, and M.A. Febbraio. 2006. Interleukin-6 increases insulin-stimulated glucose disposal in humans and glucose uptake and fatty acid oxidation in vitro via AMP-activated protein kinase. *Diabetes*. 55:2688-2697.

Catoire, M., S. Alex, N. Paraskevopulos, F. Mattijssen, I. Evers-van Gogh, G. Schaart, J. Jeppesen, A. Kneppers, M. Mensink, P.J. Voshol, G. Olivecrona, N.S. Tan, M.K. Hesselink, J.F. Berbee, P.C. Rensen, E. Kalkhoven, P. Schrauwen, and S. Kersten. 2014. Fatty acid-inducible ANGPTL4 governs lipid metabolic response to exercise. *Proceedings of the National Academy of Sciences of the United States of America*. 111:E1043-1052.

Catoire, M., M. Mensink, M.V. Boekschoten, R. Hangelbroek, M. Muller, P. Schrauwen, and S. Kersten. 2012. Pronounced effects of acute endurance exercise on gene expression in resting and exercising human skeletal muscle. *PloS one*. 7:e51066.

Chace, D.H., T.A. Kalas, and E.W. Naylor. 2003. Use of tandem mass spectrometry for multianalyte screening of dried blood specimens from newborns. *Clinical chemistry*. 49:1797-1817.

Chalder, M., N.J. Wiles, J. Campbell, S.P. Hollinghurst, A.M. Haase, A.H. Taylor, K.R. Fox, C. Costelloe, A. Searle, H. Baxter, R. Winder, C. Wright, K.M. Turner, M. Calnan, D.A. Lawlor, T.J. Peters, D.J. Sharp, A.A. Montgomery, and G. Lewis. 2012. Facilitated physical activity as a treatment for depressed adults: randomised controlled trial. *Bmj*. 344:e2758.

Chan, M.H., A.L. Carey, M.J. Watt, and M.A. Febbraio. 2004. Cytokine gene expression in human skeletal muscle during concentric contraction: evidence that IL-8, like IL-6, is influenced by glycogen availability. *American journal of physiology. Regulatory, integrative and comparative physiology*. 287:R322-327.

Chinsomboon, J., J. Ruas, R.K. Gupta, R. Thom, J. Shoag, G.C. Rowe, N. Sawada, S. Raghuram, and Z. Arany. 2009. The transcriptional coactivator PGC-1alpha mediates exercise-induced angiogenesis in skeletal muscle. *Proceedings of the National Academy of Sciences of the United States of America*. 106:21401-21406.

Church, T.S., Y.J. Cheng, C.P. Earnest, C.E. Barlow, L.W. Gibbons, E.L. Priest, and S.N. Blair. 2004. Exercise capacity and body composition as predictors of mortality among men with diabetes. *Diabetes care*. 27:83-88.

Coggan, A.R., C.A. Raguso, A. Gastaldelli, L.S. Sidossis, and C.W. Yeckel. 2000. Fat metabolism during high-intensity exercise in endurance-trained and untrained men. *Metabolism: clinical and experimental*. 49:122-128.

Costford, S.R., S. Bajpeyi, M. Pasarica, D.C. Albarado, S.C. Thomas, H. Xie, T.S. Church, S.A. Jubrias, K.E. Conley, and S.R. Smith. 2010. Skeletal muscle NAMPT is induced by exercise in humans. *American journal of physiology. Endocrinology and metabolism*. 298:E117-126.

de Keyzer, Y., V. Valayannopoulos, J.F. Benoist, F. Batteux, F. Lacaille, L. Hubert, D. Chretien, B. Chadefeaux-Vekemans, P. Niaudet, G. Touati, A. Munnich, and P. de Lonlay. 2009. Multiple OXPHOS deficiency in the liver, kidney, heart, and skeletal muscle of patients with methylmalonic aciduria and propionic aciduria. *Pediatric research*. 66:91-95.

de Luna, N., E. Gallardo, M. Soriano, R. Dominguez-Perles, C. de la Torre, R. Rojas-Garcia, J.M. Garcia-Verdugo, and I. Illa. 2006. Absence of dysferlin alters myogenin expression and delays human muscle differentiation "in vitro". *The Journal of biological chemistry*. 281:17092-17098.

DeFronzo, R.A., E. Jacot, E. Jequier, E. Maeder, J. Wahren, and J.P. Felber. 1981. The effect of insulin on the disposal of intravenous glucose. Results from indirect calorimetry and hepatic and femoral venous catheterization. *Diabetes*. 30:1000-1007.

Diamant, M., E.E. Blaak, and W.M. de Vos. 2011. Do nutrient-gut-microbiota interactions play a role in human obesity, insulin resistance and type 2 diabetes? *Obesity reviews : an official journal of the International Association for the Study of Obesity*. 12:272-281.

Domon, B., and R. Aebersold. 2006. Mass spectrometry and protein analysis. *Science*. 312:212-217.

Dreyer, H.C., S. Fujita, J.G. Cadenas, D.L. Chinkes, E. Volpi, and B.B. Rasmussen. 2006. Resistance exercise increases AMPK activity and reduces 4E-BP1 phosphorylation and protein synthesis in human skeletal muscle. *The Journal of physiology*. 576:613-624.

Dutaud, D., L. Aubry, L. Henry, D. Levieux, K.B. Hendil, L. Kuehn, J.P. Bureau, and A. Ouali. 2002. Development and evaluation of a sandwich ELISA for quantification of the 20S proteasome in human plasma. *Journal of immunological methods*. 260:183-193.

Ebeling, P., H.A. Koistinen, and V.A. Koivisto. 1998. Insulin-independent glucose transport regulates insulin sensitivity. *FEBS letters*. 436:301-303.

Eckardt, K., S.W. Gorgens, S. Raschke, and J. Eckel. 2014. Myokines in insulin resistance and type 2 diabetes. *Diabetologia*.

Egan, B., and J.R. Zierath. 2013. Exercise metabolism and the molecular regulation of skeletal muscle adaptation. *Cell metabolism*. 17:162-184.

Egerer, K., U. Kuckelkorn, P.E. Rudolph, J.C. Ruckert, T. Dorner, G.R. Burmester, P.M. Kloetzel, and E. Feist. 2002. Circulating proteasomes are markers of cell damage and immunologic activity in autoimmune diseases. *The Journal of rheumatology*. 29:2045-2052.

Erion, D.M., and G.I. Shulman. 2010. Diacylglycerol-mediated insulin resistance. *Nature medicine*. 16:400-402.

Farmawati, A., Y. Kitajima, T. Nedachi, M. Sato, M. Kanzaki, and R. Nagatomi. 2013. Characterization of contraction-induced IL-6 up-regulation using contractile C2C12 myotubes. *Endocrine journal*. 60:137-147.

Febbraio, M.A., and B.K. Pedersen. 2002. Muscle-derived interleukin-6: mechanisms for activation and possible biological roles. *FASEB journal : official publication of the Federation of American Societies for Experimental Biology*. 16:1335-1347.

Fernandez-Gonzalo, R., T.R. Lundberg, L. Alvarez-Alvarez, and J.A. de Paz. 2014. Muscle damage responses and adaptations to eccentric-overload resistance exercise in men and women. *European journal of applied physiology*.

Fiehn, O., W.T. Garvey, J.W. Newman, K.H. Lok, C.L. Hoppel, and S.H. Adams. 2010. Plasma metabolomic profiles reflective of glucose homeostasis in non-diabetic and type 2 diabetic obese African-American women. *PloS one*. 5:e15234.

Fingerhut, R., W. Roschinger, A.C. Muntau, T. Dame, J. Kreischer, R. Arnecke, A. Superti-Furga, H. Troxler, B. Liebl, B. Olgemoller, and A.A. Roscher. 2001. Hepatic carnitine palmitoyltransferase I deficiency: acylcarnitine profiles in blood spots are highly specific. *Clinical chemistry*. 47:1763-1768.

Fischer, C.P. 2006. Interleukin-6 in acute exercise and training: what is the biological relevance? *Exercise immunology review*. 12:6-33.

Fischer, C.P., N.J. Hiscock, M. Penkowa, S. Basu, B. Vessby, A. Kallner, L.B. Sjoberg, and B.K. Pedersen. 2004. Supplementation with vitamins C and E inhibits the release of interleukin-6 from contracting human skeletal muscle. *The Journal of physiology*. 558:633-645.

Fluck, M. 2006. Functional, structural and molecular plasticity of mammalian skeletal muscle in response to exercise stimuli. *The Journal of experimental biology*. 209:2239-2248.

Frontera, W.R., and J. Ochala. 2014. Skeletal Muscle: A Brief Review of Structure and Function. *Calcified tissue international*.

Fujii, N., T. Hayashi, M.F. Hirshman, J.T. Smith, S.A. Habinowski, L. Kaijser, J. Mu, O. Ljungqvist, M.J. Birnbaum, L.A. Witters, A. Thorell, and L.J. Goodyear. 2000. Exercise induces isoform-specific increase in 5'AMP-activated protein kinase activity in human skeletal muscle. *Biochemical and biophysical research communications*. 273:1150-1155.

Fujita, H., T. Nedachi, and M. Kanzaki. 2007. Accelerated de novo sarcomere assembly by electric pulse stimulation in C2C12 myotubes. *Experimental cell research*. 313:1853-1865.

Funanage, V.L., S.M. Smith, and M.A. Minnich. 1992. Entactin promotes adhesion and long-term maintenance of cultured regenerated skeletal myotubes. *Journal of cellular physiology*. 150:251-257.

Gillies, A.R., and R.L. Lieber. 2011. Structure and function of the skeletal muscle extracellular matrix. *Muscle & nerve*. 44:318-331.

Goldstein, M.S. 1961. Humoral nature of the hypoglycemic factor of muscular work. *Diabetes*. 10:232-234.

Goodpaster, B.H., J. He, S. Watkins, and D.E. Kelley. 2001. Skeletal muscle lipid content and insulin resistance: evidence for a paradox in endurance-trained athletes. *The Journal of clinical endocrinology and metabolism*. 86:5755-5761.

Goodpaster, B.H., and D.E. Kelley. 2002. Skeletal muscle triglyceride: marker or mediator of obesity-induced insulin resistance in type 2 diabetes mellitus? *Current diabetes reports*. 2:216-222.

Gorgens, S.W., S. Raschke, K.B. Holven, J. Jensen, K. Eckardt, and J. Eckel. 2013. Regulation of follistatin-like protein 1 expression and secretion in primary human skeletal muscle cells. *Archives of physiology and biochemistry*. 119:75-80.

Grarup, N., C.H. Sandholt, T. Hansen, and O. Pedersen. 2014. Genetic susceptibility to type 2 diabetes and obesity: from genome-wide association studies to rare variants and beyond. *Diabetologia*. 57:1528-1541.

Guenard, F., Y. Deshaies, K. Cianflone, J.G. Kral, P. Marceau, and M.C. Vohl. 2013. Differential methylation in glucoregulatory genes of offspring born before vs.

after maternal gastrointestinal bypass surgery. *Proceedings of the National Academy of Sciences of the United States of America*. 110:11439-11444.

Gustafsson, T., A. Knutsson, A. Puntschart, L. Kaijser, A.C. Nordqvist, C.J. Sundberg, and E. Jansson. 2002. Increased expression of vascular endothelial growth factor in human skeletal muscle in response to short-term one-legged exercise training. *Pflugers Archiv : European journal of physiology*. 444:752-759.

Gustafsson, T., A. Puntschart, L. Kaijser, E. Jansson, and C.J. Sundberg. 1999. Exercise-induced expression of angiogenesis-related transcription and growth factors in human skeletal muscle. *The American journal of physiology*. 276:H679-685.

Gyorgy, B., T.G. Szabo, M. Pasztoi, Z. Pal, P. Misjak, B. Aradi, V. Laszlo, E. Pallinger, E. Pap, A. Kittel, G. Nagy, A. Falus, and E.I. Buzas. 2011. Membrane vesicles, current state-of-the-art: emerging role of extracellular vesicles. *Cellular and molecular life sciences : CMLS*. 68:2667-2688.

Handschin, C., J. Rhee, J. Lin, P.T. Tarr, and B.M. Spiegelman. 2003. An autoregulatory loop controls peroxisome proliferator-activated receptor gamma coactivator 1alpha expression in muscle. *Proceedings of the National Academy of Sciences of the United States of America*. 100:7111-7116.

Hartwig, S., S. Goeddeke, G. Poschmann, H.D. Dicken, S. Jacob, U. Nitzgen, W. Passlack, K. Stuhler, D.M. Ouwens, H. Al-Hasani, B. Knebel, J. Kotzka, and S. Lehr. 2014a. Identification of novel adipokines differential regulated in C57BL/Ks and C57BL/6. *Archives of physiology and biochemistry*. 120:208-215.

Hartwig, S., S. Raschke, B. Knebel, M. Scheler, M. Irmler, W. Passlack, S. Muller, F.G. Hanisch, T. Franz, X. Li, H.D. Dicken, K. Eckardt, J. Beckers, M.H. de Angelis, C. Weigert, H.U. Haring, H. Al-Hasani, D.M. Ouwens, J. Eckel, J. Kotzka, and S. Lehr. 2014b. Secretome profiling of primary human skeletal muscle cells. *Biochimica et biophysica acta*. 1844:1011-1017.

Haugen, F., F. Norheim, H. Lian, A.J. Wensaas, S. Dueland, O. Berg, A. Funderud, B.S. Skalhegg, T. Raastad, and C.A. Drevon. 2010. IL-7 is expressed and secreted by human skeletal muscle cells. *American journal of physiology. Cell physiology*. 298:C807-816.

Henningsen, J., K.T.G. Rigbolt, B. Blagoev, B.K. Pedersen, and I. Kratchmarova. 2010. Dynamics of the Skeletal Muscle Secretome during Myoblast Differentiation. *Molecular & Cellular Proteomics*. 9:2482-2496.

Hiatt, W.R., J.G. Regensteiner, E.E. Wolfel, L. Ruff, and E.P. Brass. 1989. Carnitine and acylcarnitine metabolism during exercise in humans. Dependence on skeletal muscle metabolic state. *The Journal of clinical investigation*. 84:1167-1173.

Hirose, L., K. Nosaka, M. Newton, A. Laveder, M. Kano, J. Peake, and K. Suzuki. 2004. Changes in inflammatory mediators following eccentric exercise of the elbow flexors. *Exercise immunology review*. 10:75-90.

Ho, R.C., M.F. Hirshman, Y. Li, D. Cai, J.R. Farmer, W.G. Aschenbach, C.A. Witczak, S.E. Shoelson, and L.J. Goodyear. 2005. Regulation of IkappaB kinase and NF-kappaB in contracting adult rat skeletal muscle. *American journal of physiology. Cell physiology*. 289:C794-801.

Hoene, M., R. Lehmann, A.M. Hennige, A.K. Pohl, H.U. Haring, E.D. Schleicher, and C. Weigert. 2009. Acute regulation of metabolic genes and insulin receptor

substrates in the liver of mice by one single bout of treadmill exercise. *The Journal of physiology*. 587:241-252.

Hoene, M., H. Runge, H.U. Haring, E.D. Schleicher, and C. Weigert. 2013. Interleukin-6 promotes myogenic differentiation of mouse skeletal muscle cells: role of the STAT3 pathway. *American journal of physiology. Cell physiology*. 304:C128-136.

Hoene, M., and C. Weigert. 2008. The role of interleukin-6 in insulin resistance, body fat distribution and energy balance. *Obesity reviews : an official journal of the International Association for the Study of Obesity*. 9:20-29.

Holland, W.L., and S.A. Summers. 2008. Sphingolipids, insulin resistance, and metabolic disease: new insights from in vivo manipulation of sphingolipid metabolism. *Endocrine reviews*. 29:381-402.

Hoppeler, H., O. Baum, G. Lurman, and M. Mueller. 2011. Molecular mechanisms of muscle plasticity with exercise. *Comprehensive Physiology*. 1:1383-1412.

Hu, F.B., M.J. Stampfer, C. Solomon, S. Liu, G.A. Colditz, F.E. Speizer, W.C. Willett, and J.E. Manson. 2001. Physical activity and risk for cardiovascular events in diabetic women. *Annals of internal medicine*. 134:96-105.

Hubal, M.J., T.C. Chen, P.D. Thompson, and P.M. Clarkson. 2008. Inflammatory gene changes associated with the repeated-bout effect. *American journal of physiology. Regulatory, integrative and comparative physiology*. 294:R1628-1637.

Huh, J.Y., V. Mougios, A. Kabasakalis, I. Fatouros, A. Siopi, Douroudos, II, A. Filippaios, G. Panagiotou, K.H. Park, and C.S. Mantzoros. 2014. Exercise-induced irisin secretion is independent of age or fitness level and increased irisin may directly modulate muscle metabolism through AMPK activation. *The Journal of clinical endocrinology and metabolism*:jc20141437.

Hurley, B.F., P.M. Nemeth, W.H. Martin, 3rd, J.M. Hagberg, G.P. Dalsky, and J.O. Holloszy. 1986. Muscle triglyceride utilization during exercise: effect of training. *J Appl Physiol (1985)*. 60:562-567.

Huss, J.M., R.P. Kopp, and D.P. Kelly. 2002. Peroxisome proliferator-activated receptor coactivator-1alpha (PGC-1alpha) coactivates the cardiac-enriched nuclear receptors estrogen-related receptor-alpha and -gamma. Identification of novel leucine-rich interaction motif within PGC-1alpha. *The Journal of biological chemistry*. 277:40265-40274.

Huxley, A.F., and R. Niedergerke. 1954. Measurement of muscle striations in stretch and contraction. *The Journal of physiology*. 124:46-47P.

Huxley, H., and J. Hanson. 1954. Changes in the cross-striations of muscle during contraction and stretch and their structural interpretation. *Nature*. 173:973-976.

Hyldahl, R.D., L. Xin, M.J. Hubal, S. Moeckel-Cole, S. Chipkin, and P.M. Clarkson. 2011. Activation of nuclear factor-kappaB following muscle eccentric contractions in humans is localized primarily to skeletal muscle-residing pericytes. *FASEB journal : official publication of the Federation of American Societies for Experimental Biology*. 25:2956-2966.

IDF. 2013. IDF Diabetes Atlas. International Diabetes Federation, Brussels, Belgium.

Issaq, H.J., Z. Xiao, and T.D. Veenstra. 2007. Serum and plasma proteomics. *Chemical reviews*. 107:3601-3620.

Jager, S., C. Handschin, J. St-Pierre, and B.M. Spiegelman. 2007. AMP-activated protein kinase (AMPK) action in skeletal muscle via direct phosphorylation of

PGC-1alpha. *Proceedings of the National Academy of Sciences of the United States of America*. 104:12017-12022.

Johnson, N.A., S.R. Stannard, and M.W. Thompson. 2004. Muscle triglyceride and glycogen in endurance exercise: implications for performance. *Sports Med*. 34:151-164.

Joost, H.G. 2014. Diabetes and cancer: Epidemiology and potential mechanisms. *Diabetes & vascular disease research : official journal of the International Society of Diabetes and Vascular Disease*.

Kahn, B.B., T. Alquier, D. Carling, and D.G. Hardie. 2005. AMP-activated protein kinase: ancient energy gauge provides clues to modern understanding of metabolism. *Cell metabolism*. 1:15-25.

Kahn, S.E., M.E. Cooper, and S. Del Prato. 2014. Pathophysiology and treatment of type 2 diabetes: perspectives on the past, present, and future. *Lancet*. 383:1068-1083.

Kahn, S.E., R.L. Prigeon, D.K. McCulloch, E.J. Boyko, R.N. Bergman, M.W. Schwartz, J.L. Neifing, W.K. Ward, J.C. Beard, J.P. Palmer, and et al. 1993. Quantification of the relationship between insulin sensitivity and beta-cell function in human subjects. Evidence for a hyperbolic function. *Diabetes*. 42:1663-1672.

Keller, C., A. Steensberg, H. Pilegaard, T. Osada, B. Saltin, B.K. Pedersen, and P.D. Neufer. 2001. Transcriptional activation of the IL-6 gene in human contracting skeletal muscle: influence of muscle glycogen content. *FASEB journal : official publication of the Federation of American Societies for Experimental Biology*. 15:2748-2750.

Kiens, B., and E.A. Richter. 1998. Utilization of skeletal muscle triacylglycerol during postexercise recovery in humans. *The American journal of physiology*. 275:E332-337.

Kjaer, M. 2004. Role of extracellular matrix in adaptation of tendon and skeletal muscle to mechanical loading. *Physiol Rev*. 84:649-698.

Kleinridders, A., H.A. Ferris, W. Cai, and C.R. Kahn. 2014. Insulin action in brain regulates systemic metabolism and brain function. *Diabetes*. 63:2232-2243.

Knowler, W.C., E. Barrett-Connor, S.E. Fowler, R.F. Hamman, J.M. Lachin, E.A. Walker, D.M. Nathan, and G. Diabetes Prevention Program Research. 2002. Reduction in the incidence of type 2 diabetes with lifestyle intervention or metformin. *The New England journal of medicine*. 346:393-403.

Koves, T.R., J.R. Ussher, R.C. Noland, D. Slentz, M. Mosedale, O. Ilkayeva, J. Bain, R. Stevens, J.R. Dyck, C.B. Newgard, G.D. Lopaschuk, and D.M. Muoio. 2008. Mitochondrial overload and incomplete fatty acid oxidation contribute to skeletal muscle insulin resistance. *Cell metabolism*. 7:45-56.

Krogh-Madsen, R., J.P. Thyfault, C. Broholm, O.H. Mortensen, R.H. Olsen, R. Mounier, P. Plomgaard, G. van Hall, F.W. Booth, and B.K. Pedersen. 2010. A 2-wk reduction of ambulatory activity attenuates peripheral insulin sensitivity. *J Appl Physiol (1985)*. 108:1034-1040.

Krssak, M., K.F. Petersen, R. Bergeron, T. Price, D. Laurent, D.L. Rothman, M. Roden, and G.I. Shulman. 2000. Intramuscular glycogen and intramyocellular lipid utilization during prolonged exercise and recovery in man: a 13C and 1H nuclear magnetic resonance spectroscopy study. *The Journal of clinical endocrinology and metabolism*. 85:748-754.

Krutzfeldt, J., C. Kausch, A. Volk, H.H. Klein, K. Rett, H.U. Haring, and M. Stumvoll. 2000. Insulin signaling and action in cultured skeletal muscle cells from lean healthy humans with high and low insulin sensitivity. *Diabetes*. 49:992-998.

Lambernd, S., A. Taube, A. Schober, B. Platzbecker, S.W. Gorgens, R. Schlich, K. Jeruschke, J. Weiss, K. Eckardt, and J. Eckel. 2012. Contractile activity of human skeletal muscle cells prevents insulin resistance by inhibiting pro-inflammatory signalling pathways. *Diabetologia*. 55:1128-1139.

Lauritzen, H.P., and J.D. Schertzer. 2010. Measuring GLUT4 translocation in mature muscle fibers. *American journal of physiology. Endocrinology and metabolism*. 299:E169-179.

Lawlor, D.A., and S.W. Hopker. 2001. The effectiveness of exercise as an intervention in the management of depression: systematic review and meta-regression analysis of randomised controlled trials. *Bmj*. 322:763-767.

Le Bihan, M.C., A. Bigot, S.S. Jensen, J.L. Dennis, A. Rogowska-Wrzesinska, J. Laine, V. Gache, D. Furling, O.N. Jensen, T. Voit, V. Mouly, G.R. Coulton, and G. Butler-Browne. 2012. In-depth analysis of the secretome identifies three major independent secretory pathways in differentiating human myoblasts. *Journal of proteomics*. 77:344-356.

Lehmann, R., X. Zhao, C. Weigert, P. Simon, E. Fehrenbach, J. Fritsche, J. Machann, F. Schick, J. Wang, M. Hoene, E.D. Schleicher, H.U. Haring, G. Xu, and A.M. Niess. 2010. Medium chain acylcarnitines dominate the metabolite pattern in humans under moderate intensity exercise and support lipid oxidation. *PloS one*. 5:e11519.

Lehr, S., S. Hartwig, D. Lamers, S. Famulla, S. Muller, F.G. Hanisch, C. Cuvelier, J. Ruige, K. Eckardt, D.M. Ouwens, H. Sell, and J. Eckel. 2012. Identification and validation of novel adipokines released from primary human adipocytes. *Molecular & cellular proteomics : MCP*. 11:M111 010504.

Lehr, S., J. Kotzka, H. Avci, B. Knebel, S. Muller, F.G. Hanisch, S. Jacob, C. Haak, F. Susanto, and D. Muller-Wieland. 2005. Effect of sterol regulatory element binding protein-1a on the mitochondrial protein pattern in human liver cells detected by 2D-DIGE. *Biochemistry*. 44:5117-5128.

Leick, L., P. Plomgaard, L. Gronlokke, F. Al-Abaiji, J.F. Wojtaszewski, and H. Pilegaard. 2010. Endurance exercise induces mRNA expression of oxidative enzymes in human skeletal muscle late in recovery. *Scandinavian journal of medicine & science in sports*. 20:593-599.

Lin, J., H. Wu, P.T. Tarr, C.Y. Zhang, Z. Wu, O. Boss, L.F. Michael, P. Puigserver, E. Isotani, E.N. Olson, B.B. Lowell, R. Bassel-Duby, and B.M. Spiegelman. 2002. Transcriptional co-activator PGC-1 alpha drives the formation of slow-twitch muscle fibres. *Nature*. 418:797-801.

Mahoney, D.J., G. Parise, S. Melov, A. Safdar, and M.A. Tarnopolsky. 2005. Analysis of global mRNA expression in human skeletal muscle during recovery from endurance exercise. *FASEB journal : official publication of the Federation of American Societies for Experimental Biology*. 19:1498-1500.

Malm, C., P. Nyberg, M. Engstrom, B. Sjodin, R. Lenkei, B. Ekblom, and I. Lundberg. 2000. Immunological changes in human skeletal muscle and blood after eccentric exercise and multiple biopsies. *The Journal of physiology*. 529 Pt 1:243-262.

McGee, S.L., E. Fairlie, A.P. Garnham, and M. Hargreaves. 2009. Exercise-induced histone modifications in human skeletal muscle. *The Journal of physiology*. 587:5951-5958.

Mehlig, K., I. Skoog, M. Waern, J. Miao Jonasson, L. Lapidus, C. Bjorkelund, S. Ostling, and L. Lissner. 2014. Physical activity, weight status, diabetes and dementia: a 34-year follow-up of the population study of women in Gothenburg. *Neuroepidemiology*. 42:252-259.

Mentzer, S.J., and M.A. Konerding. 2014. Intussusceptive angiogenesis: expansion and remodeling of microvascular networks. *Angiogenesis*. 17:499-509.

Michael, L.F., Z. Wu, R.B. Cheatham, P. Puigserver, G. Adelmant, J.J. Lehman, D.P. Kelly, and B.M. Spiegelman. 2001. Restoration of insulin-sensitive glucose transporter (GLUT4) gene expression in muscle cells by the transcriptional coactivator PGC-1. *Proceedings of the National Academy of Sciences of the United States of America*. 98:3820-3825.

Mihalik, S.J., B.H. Goodpaster, D.E. Kelley, D.H. Chace, J. Vockley, F.G. Toledo, and J.P. DeLany. 2010. Increased levels of plasma acylcarnitines in obesity and type 2 diabetes and identification of a marker of glucolipotoxicity. *Obesity (Silver Spring)*. 18:1695-1700.

Morino, K., K.F. Petersen, and G.I. Shulman. 2006. Molecular mechanisms of insulin resistance in humans and their potential links with mitochondrial dysfunction. *Diabetes*. 55 Suppl 2:S9-S15.

Muoio, D.M., and T.R. Koves. 2007. Lipid-induced metabolic dysfunction in skeletal muscle. *Novartis Foundation symposium*. 286:24-38; discussion 38-46, 162-163, 196-203.

Muoio, D.M., and P.D. Neufer. 2012. Lipid-induced mitochondrial stress and insulin action in muscle. *Cell metabolism*. 15:595-605.

Murakami, M., Y. Taketomi, H. Sato, and K. Yamamoto. 2011. Secreted phospholipase A2 revisited. *Journal of biochemistry*. 150:233-255.

Nedachi, T., H. Fujita, and M. Kanzaki. 2008. Contractile C2C12 myotube model for studying exercise-inducible responses in skeletal muscle. *American journal of physiology. Endocrinology and metabolism*. 295:E1191-1204.

Nedachi, T., H. Hatakeyama, T. Kono, M. Sato, and M. Kanzaki. 2009. Characterization of contraction-inducible CXC chemokines and their roles in C2C12 myocytes. *American journal of physiology. Endocrinology and metabolism*. 297:E866-878.

Neubauer, O., S. Sabapathy, K.J. Ashton, B. Desbrow, J.M. Peake, R. Lazarus, B. Wessner, D. Cameron-Smith, K.H. Wagner, L.J. Haseler, and A.C. Bulmer. 2014. Time course-dependent changes in the transcriptome of human skeletal muscle during recovery from endurance exercise: from inflammation to adaptive remodeling. *J Appl Physiol (1985)*. 116:274-287.

Newgard, C.B., J. An, J.R. Bain, M.J. Muehlbauer, R.D. Stevens, L.F. Lien, A.M. Haqq, S.H. Shah, M. Arlotto, C.A. Slentz, J. Rochon, D. Gallup, O. Ilkayeva, B.R. Wenner, W.S. Yancy, Jr., H. Eisenson, G. Musante, R.S. Surwit, D.S. Millington, M.D. Butler, and L.P. Svetkey. 2009. A branched-chain amino acid-related metabolic signature that differentiates obese and lean humans and contributes to insulin resistance. *Cell metabolism*. 9:311-326.

Newsholme, E., and T. Leech. 2010. Functional Biochemistry in Health and Disease. Wiley-Blackwell, Chichester.

Nielsen, J.N., C. Frosig, M.P. Sajan, A. Miura, M.L. Standaert, D.A. Graham, J.F. Wojtaszewski, R.V. Farese, and E.A. Richter. 2003. Increased atypical PKC activity in endurance-trained human skeletal muscle. *Biochemical and biophysical research communications*. 312:1147-1153.

Nieman, D.C., J.M. Davis, D.A. Henson, S.J. Gross, C.L. Dumke, A.C. Utter, D.M. Vinci, J.A. Carson, A. Brown, S.R. McAnulty, L.S. McAnulty, and N.T. Triplett. 2005. Muscle cytokine mRNA changes after 2.5 h of cycling: influence of carbohydrate. *Medicine and science in sports and exercise*. 37:1283-1290.

Nieman, D.C., D.A. Henson, L.L. Smith, A.C. Utter, D.M. Vinci, J.M. Davis, D.E. Kaminsky, and M. Shute. 2001. Cytokine changes after a marathon race. *J Appl Physiol (1985)*. 91:109-114.

Nikolic, N., S. Skaret Bakke, E. Tranheim Kase, I. Rudberg, I. Flo Halle, A.C. Rustan, G.H. Thoresen, and V. Aas. 2012. Electrical pulse stimulation of cultured human skeletal muscle cells as an in vitro model of exercise. *PloS one*. 7:e33203.

Norheim, F., T. Raastad, B. Thiede, A.C. Rustan, C.A. Drevon, and F. Haugen. 2011. Proteomic identification of secreted proteins from human skeletal muscle cells and expression in response to strength training. *American journal of physiology. Endocrinology and metabolism*. 301:E1013-1021.

Novak, M., L. Bjorck, K.W. Giang, C. Heden-Stahl, L. Wilhelmsen, and A. Rosengren. 2013. Perceived stress and incidence of Type 2 diabetes: a 35-year follow-up study of middle-aged Swedish men. *Diabetic medicine : a journal of the British Diabetic Association*. 30:e8-16.

Olfert, I.M., R.A. Howlett, P.D. Wagner, and E.C. Breen. 2010. Myocyte vascular endothelial growth factor is required for exercise-induced skeletal muscle angiogenesis. *American journal of physiology. Regulatory, integrative and comparative physiology*. 299:R1059-1067.

Olsen, R.H., R. Krogh-Madsen, C. Thomsen, F.W. Booth, and B.K. Pedersen. 2008. Metabolic responses to reduced daily steps in healthy nonexercising men. *JAMA : the journal of the American Medical Association*. 299:1261-1263.

Ordelheide, A.M., M. Heni, C. Thamer, F. Machicao, A. Fritsche, N. Stefan, H.U. Haring, and H. Staiger. 2011. In vitro responsiveness of human muscle cell peroxisome proliferator-activated receptor delta reflects donors' insulin sensitivity in vivo. *European journal of clinical investigation*. 41:1323-1329.

Ostrowski, K., C. Hermann, A. Bangash, P. Schjerling, J.N. Nielsen, and B.K. Pedersen. 1998. A trauma-like elevation of plasma cytokines in humans in response to treadmill running. *The Journal of physiology*. 513 (Pt 3):889-894.

Ostrowski, K., T. Rohde, S. Asp, P. Schjerling, and B.K. Pedersen. 2001. Chemokines are elevated in plasma after strenuous exercise in humans. *European journal of applied physiology*. 84:244-245.

Park, H., R. Bhalla, R. Saigal, M. Radisic, N. Watson, R. Langer, and G. Vunjak-Novakovic. 2008. Effects of electrical stimulation in C2C12 muscle constructs. *Journal of tissue engineering and regenerative medicine*. 2:279-287.

Park, Y.G., J.H. Moon, and J. Kim. 2006. A comparative study of magnetic-activated cell sorting, cytotoxicity and preplating for the purification of human myoblasts. *Yonsei medical journal*. 47:179-183.

Paulsen, G., H.B. Benestad, I. Strom-Gundersen, L. Morkrid, K.T. Lappegard, and T. Raastad. 2005. Delayed leukocytosis and cytokine response to high-force

eccentric exercise. *Medicine and science in sports and exercise*. 37:1877-1883.

Paulsen, G., U.R. Mikkelsen, T. Raastad, and J.M. Peake. 2012. Leucocytes, cytokines and satellite cells: what role do they play in muscle damage and regeneration following eccentric exercise? *Exercise immunology review*. 18:42-97.

Pedersen, B.K. 2009. The diseasome of physical inactivity--and the role of myokines in muscle--fat cross talk. *The Journal of physiology*. 587:5559-5568.

Pedersen, B.K. 2011. Muscles and their myokines. *The Journal of experimental biology*. 214:337-346.

Pedersen, B.K. 2012. Muscular interleukin-6 and its role as an energy sensor. *Medicine and science in sports and exercise*. 44:392-396.

Pedersen, B.K., and M.A. Febbraio. 2008. Muscle as an Endocrine Organ: Focus on Muscle-derived Interleukin-6. *Physiological Reviews*. 88:1379-1406.

Pedersen, B.K., and M.A. Febbraio. 2012. Muscles, exercise and obesity: skeletal muscle as a secretory organ. *Nature reviews. Endocrinology*. 8:457-465.

Pedersen, B.K., and C.P. Fischer. 2007. Beneficial health effects of exercise--the role of IL-6 as a myokine. *Trends in pharmacological sciences*. 28:152-156.

Pedersen, B.K., A. Steensberg, C. Fischer, C. Keller, P. Keller, P. Plomgaard, M. Febbraio, and B. Saltin. 2003. Searching for the exercise factor: is IL-6 a candidate? *Journal of muscle research and cell motility*. 24:113-119.

Petersen, E.W., A.L. Carey, M. Sacchetti, G.R. Steinberg, S.L. Macaulay, M.A. Febbraio, and B.K. Pedersen. 2005. Acute IL-6 treatment increases fatty acid turnover in elderly humans in vivo and in tissue culture in vitro. *American journal of physiology. Endocrinology and metabolism*. 288:E155-162.

Petersen, T.N., S. Brunak, G. von Heijne, and H. Nielsen. 2011. SignalP 4.0: discriminating signal peptides from transmembrane regions. *Nature methods*. 8:785-786.

Phillips, S.M., H.J. Green, M.A. Tarnopolsky, G.J. Heigenhauser, and S.M. Grant. 1996. Progressive effect of endurance training on metabolic adaptations in working skeletal muscle. *The American journal of physiology*. 270:E265-272.

Pilegaard, H., G.A. Ordway, B. Saltin, and P.D. Neufer. 2000. Transcriptional regulation of gene expression in human skeletal muscle during recovery from exercise. *American journal of physiology. Endocrinology and metabolism*. 279:E806-814.

Pilegaard, H., B. Saltin, and P.D. Neufer. 2003. Exercise induces transient transcriptional activation of the PGC-1alpha gene in human skeletal muscle. *The Journal of physiology*. 546:851-858.

Pillon, N.J., P.J. Bilan, L.N. Fink, and A. Klip. 2013. Cross-talk between skeletal muscle and immune cells: muscle-derived mediators and metabolic implications. *American journal of physiology. Endocrinology and metabolism*. 304:E453-465.

Pruchnic, R., A. Katsiaras, J. He, D.E. Kelley, C. Winters, and B.H. Goodpaster. 2004. Exercise training increases intramyocellular lipid and oxidative capacity in older adults. *American journal of physiology. Endocrinology and metabolism*. 287:E857-862.

Puigserver, P., J. Rhee, J. Lin, Z. Wu, J.C. Yoon, C.Y. Zhang, S. Krauss, V.K. Mootha, B.B. Lowell, and B.M. Spiegelman. 2001. Cytokine stimulation of

energy expenditure through p38 MAP kinase activation of PPARgamma coactivator-1. *Molecular cell*. 8:971-982.

Rabilloud, T., A.R. Vaezzadeh, N. Potier, C. Lelong, E. Leize-Wagner, and M. Chevallet. 2009. Power and limitations of electrophoretic separations in proteomics strategies. *Mass spectrometry reviews*. 28:816-843.

Rainer, J., F. Sanchez-Cabo, G. Stocker, A. Sturn, and Z. Trajanoski. 2006. CARMAweb: comprehensive R- and bioconductor-based web service for microarray data analysis. *Nucleic acids research*. 34:W498-503.

Raschke, S., K. Eckardt, K. Bjorklund Holven, J. Jensen, and J. Eckel. 2013a. Identification and validation of novel contraction-regulated myokines released from primary human skeletal muscle cells. *PloS one*. 8:e62008.

Raschke, S., M. Elsen, H. Gassenhuber, M. Sommerfeld, U. Schwahn, B. Brockmann, R. Jung, U. Wisloff, A.E. Tjonna, T. Raastad, J. Hallen, F. Norheim, C.A. Drevon, T. Romacho, K. Eckardt, and J. Eckel. 2013b. Evidence against a beneficial effect of irisin in humans. *PloS one*. 8:e73680.

Reaven, G.M. 1988. Banting lecture 1988. Role of insulin resistance in human disease. *Diabetes*. 37:1595-1607.

Rebbeck, R.T., Y. Karunasekara, P.G. Board, N.A. Beard, M.G. Casarotto, and A.F. Dulhunty. 2014. Skeletal muscle excitation-contraction coupling: who are the dancing partners? *The international journal of biochemistry & cell biology*. 48:28-38.

Ricard-Blum, S., and F. Ruggiero. 2005. The collagen superfamily: from the extracellular matrix to the cell membrane. *Pathologie-biologie*. 53:430-442.

Richardson, R.S., H. Wagner, S.R. Mudaliar, E. Saucedo, R. Henry, and P.D. Wagner. 2000. Exercise adaptation attenuates VEGF gene expression in human skeletal muscle. *American journal of physiology. Heart and circulatory physiology*. 279:H772-778.

Rinaldo, P., J.S. Lim, S. Tortorelli, D. Gavrilov, and D. Matern. 2008. Newborn screening of metabolic disorders: recent progress and future developments. *Nestle Nutrition workshop series. Paediatric programme*. 62:81-93; discussion 93-86.

Roca-Rivada, A., O. Al-Massadi, C. Castelao, L.L. Senin, J. Alonso, L.M. Seoane, T. Garcia-Caballero, F.F. Casanueva, and M. Pardo. 2012. Muscle tissue as an endocrine organ: comparative secretome profiling of slow-oxidative and fast-glycolytic rat muscle explants and its variation with exercise. *Journal of proteomics*. 75:5414-5425.

Rose, A.J., and M. Hargreaves. 2003. Exercise increases Ca2+-calmodulin-dependent protein kinase II activity in human skeletal muscle. *The Journal of physiology*. 553:303-309.

Rose, A.J., B. Kiens, and E.A. Richter. 2006. Ca2+-calmodulin-dependent protein kinase expression and signalling in skeletal muscle during exercise. *The Journal of physiology*. 574:889-903.

Rosendal, L., K. Sogaard, M. Kjaer, G. Sjogaard, H. Langberg, and J. Kristiansen. 2005. Increase in interstitial interleukin-6 of human skeletal muscle with repetitive low-force exercise. *J Appl Physiol (1985)*. 98:477-481.

Rovio, S., I. Kareholt, E.L. Helkala, M. Viitanen, B. Winblad, J. Tuomilehto, H. Soininen, A. Nissinen, and M. Kivipelto. 2005. Leisure-time physical activity at midlife and the risk of dementia and Alzheimer's disease. *The Lancet. Neurology*. 4:705-711.

Rowland, L.A., N.C. Bal, and M. Periasamy. 2014. The role of skeletal-muscle-based thermogenic mechanisms in vertebrate endothermy. *Biological reviews of the Cambridge Philosophical Society*.

Rullman, E., J. Norrbom, A. Stromberg, D. Wagsater, H. Rundqvist, T. Haas, and T. Gustafsson. 2009. Endurance exercise activates matrix metalloproteinases in human skeletal muscle. *J Appl Physiol (1985)*. 106:804-812.

Sachdev, S., and K.J. Davies. 2008. Production, detection, and adaptive responses to free radicals in exercise. *Free radical biology & medicine*. 44:215-223.

Saltin, B., and P.D. Gollnick. 1983. Skeletal muscle adaptability: significance for metabolism and performance. American Physiological Society, Bethesda.

Sanchez, J., Y. Nozhenko, A. Palou, and A.M. Rodriguez. 2013. Free fatty acid effects on myokine production in combination with exercise mimetics. *Molecular nutrition & food research*. 57:1456-1467.

Scheler, M., M. Hrabé de Angelis, H. Al-Hasani, H.U. Häring, C. Weigert, and S. Lehr. 2015. Methods for proteomics based analysis of the human muscle secretome using an in vitro exercise model. *Methods in Molecular Biology*:in press.

Scheler, M., M. Irmler, S. Lehr, S. Hartwig, H. Staiger, H. Al-Hasani, J. Beckers, M.H. de Angelis, H.U. Haring, and C. Weigert. 2013. Cytokine response of primary human myotubes in an in vitro exercise model. *American journal of physiology. Cell physiology*. 305:C877-886.

Schiaffino, S., and C. Reggiani. 2011. Fiber types in mammalian skeletal muscles. *Physiol Rev*. 91:1447-1531.

Schmid, D., and M.F. Leitzmann. 2014. Television viewing and time spent sedentary in relation to cancer risk: a meta-analysis. *Journal of the National Cancer Institute*. 106.

Schmutz, S., C. Dapp, M. Wittwer, M. Vogt, H. Hoppeler, and M. Fluck. 2006. Endurance training modulates the muscular transcriptome response to acute exercise. *Pflugers Archiv : European journal of physiology*. 451:678-687.

Schooneman, M.G., N. Achterkamp, C.A. Argmann, M.R. Soeters, and S.M. Houten. 2014. Plasma acylcarnitines inadequately reflect tissue acylcarnitine metabolism. *Biochimica et biophysica acta*. 1841:987-994.

Seldin, M.M., J.M. Peterson, M.S. Byerly, Z. Wei, and G.W. Wong. 2012. Myonectin (CTRP15), a Novel Myokine That Links Skeletal Muscle to Systemic Lipid Homeostasis. *The Journal of biological chemistry*. 287:11968-11980.

Serrano, A.L., B. Baeza-Raja, E. Perdiguero, M. Jardi, and P. Munoz-Canoves. 2008. Interleukin-6 is an essential regulator of satellite cell-mediated skeletal muscle hypertrophy. *Cell metabolism*. 7:33-44.

Shaw, C.S., S.O. Shepherd, A.J. Wagenmakers, D. Hansen, P. Dendale, and L.J. van Loon. 2012. Prolonged exercise training increases intramuscular lipid content and perilipin 2 expression in type I muscle fibers of patients with type 2 diabetes. *American journal of physiology. Endocrinology and metabolism*. 303:E1158-1165.

Siliprandi, N., F. Di Lisa, and R. Menabo. 1991. Propionyl-L-carnitine: biochemical significance and possible role in cardiac metabolism. *Cardiovascular drugs and therapy / sponsored by the International Society of Cardiovascular Pharmacotherapy*. 5 Suppl 1:11-15.

Silveira, L.R., H. Pilegaard, K. Kusuhara, R. Curi, and Y. Hellsten. 2006. The contraction induced increase in gene expression of peroxisome proliferator-

activated receptor (PPAR)-gamma coactivator 1alpha (PGC-1alpha), mitochondrial uncoupling protein 3 (UCP3) and hexokinase II (HKII) in primary rat skeletal muscle cells is dependent on reactive oxygen species. *Biochimica et biophysica acta.* 1763:969-976.

Sparks, L.M., C. Moro, B. Ukropcova, S. Bajpeyi, A.E. Civitarese, M.W. Hulver, G.H. Thoresen, A.C. Rustan, and S.R. Smith. 2011. Remodeling lipid metabolism and improving insulin responsiveness in human primary myotubes. *PloS one.* 6:e21068.

Stadler, G., J.C. Chen, K. Wagner, J.D. Robin, J.W. Shay, C.P. Emerson, Jr., and W.E. Wright. 2011. Establishment of clonal myogenic cell lines from severely affected dystrophic muscles - CDK4 maintains the myogenic population. *Skeletal muscle.* 1:12.

Staiger, H., A. Bohm, M. Scheler, L. Berti, J. Machann, F. Schick, F. Machicao, A. Fritsche, N. Stefan, C. Weigert, A. Krook, H.U. Haring, and M.H. de Angelis. 2013. Common genetic variation in the human FNDC5 locus, encoding the novel muscle-derived 'browning' factor irisin, determines insulin sensitivity. *PloS one.* 8:e61903.

Steensberg, A., M.A. Febbraio, T. Osada, P. Schjerling, G. van Hall, B. Saltin, and B.K. Pedersen. 2001. Interleukin-6 production in contracting human skeletal muscle is influenced by pre-exercise muscle glycogen content. *The Journal of physiology.* 537:633-639.

Steensberg, A., C. Keller, R.L. Starkie, T. Osada, M.A. Febbraio, and B.K. Pedersen. 2002. IL-6 and TNF-alpha expression in, and release from, contracting human skeletal muscle. *American journal of physiology. Endocrinology and metabolism.* 283:E1272-1278.

Steensberg, A., G. van Hall, T. Osada, M. Sacchetti, B. Saltin, and B. Klarlund Pedersen. 2000. Production of interleukin-6 in contracting human skeletal muscles can account for the exercise-induced increase in plasma interleukin-6. *The Journal of physiology.* 529 Pt 1:237-242.

Stouthard, J.M., J.A. Romijn, T. Van der Poll, E. Endert, S. Klein, P.J. Bakker, C.H. Veenhof, and H.P. Sauerwein. 1995. Endocrinologic and metabolic effects of interleukin-6 in humans. *The American journal of physiology.* 268:E813-819.

Sun, D., C.O. Martinez, O. Ochoa, L. Ruiz-Willhite, J.R. Bonilla, V.E. Centonze, L.L. Waite, J.E. Michalek, L.M. McManus, and P.K. Shireman. 2009. Bone marrow-derived cell regulation of skeletal muscle regeneration. *FASEB journal : official publication of the Federation of American Societies for Experimental Biology.* 23:382-395.

Tamura, Y., K. Watanabe, T. Kantani, J. Hayashi, N. Ishida, and M. Kaneki. 2011. Upregulation of circulating IL-15 by treadmill running in healthy individuals: is IL-15 an endocrine mediator of the beneficial effects of endurance exercise? *Endocrine journal.* 58:211-215.

Tantiwong, P., K. Shanmugasundaram, A. Monroy, S. Ghosh, M. Li, R.A. DeFronzo, E. Cersosimo, A. Sriwijitkamol, S. Mohan, and N. Musi. 2010. NF-kappaB activity in muscle from obese and type 2 diabetic subjects under basal and exercise-stimulated conditions. *American journal of physiology. Endocrinology and metabolism.* 299:E794-801.

Terzis, G., G. Georgiadis, G. Stratakos, I. Vogiatzis, S. Kavouras, P. Manta, H. Mascher, and E. Blomstrand. 2008. Resistance exercise-induced increase in

muscle mass correlates with p70S6 kinase phosphorylation in human subjects. *European journal of applied physiology*. 102:145-152.

Thayer, K.A., J.J. Heindel, J.R. Bucher, and M.A. Gallo. 2012. Role of environmental chemicals in diabetes and obesity: a National Toxicology Program workshop review. *Environmental health perspectives*. 120:779-789.

Thompson, D.B., R. Pratley, and V. Ossowski. 1996. Human primary myoblast cell cultures from non-diabetic insulin resistant subjects retain defects in insulin action. *The Journal of clinical investigation*. 98:2346-2350.

Thornalley, P.J., and M. Vasak. 1985. Possible role for metallothionein in protection against radiation-induced oxidative stress. Kinetics and mechanism of its reaction with superoxide and hydroxyl radicals. *Biochimica et biophysica acta*. 827:36-44.

Timmons, J.A., K. Baar, P.K. Davidsen, and P.J. Atherton. 2012. Is irisin a human exercise gene? *Nature*. 488:E9-10; discussion E10-11.

Trujillo, M.E., S. Sullivan, I. Harten, S.H. Schneider, A.S. Greenberg, and S.K. Fried. 2004. Interleukin-6 regulates human adipose tissue lipid metabolism and leptin production in vitro. *The Journal of clinical endocrinology and metabolism*. 89:5577-5582.

Tuomilehto, J., J. Lindstrom, J.G. Eriksson, T.T. Valle, H. Hamalainen, P. Ilanne-Parikka, S. Keinanen-Kiukaanniemi, M. Laakso, A. Louheranta, M. Rastas, V. Salminen, M. Uusitupa, and G. Finnish Diabetes Prevention Study. 2001. Prevention of type 2 diabetes mellitus by changes in lifestyle among subjects with impaired glucose tolerance. *The New England journal of medicine*. 344:1343-1350.

Turcotte, L.P., E.A. Richter, and B. Kiens. 1992. Increased plasma FFA uptake and oxidation during prolonged exercise in trained vs. untrained humans. *The American journal of physiology*. 262:E791-799.

Urso, M.L., J.R. Pierce, J.A. Alemany, E.A. Harman, and B.C. Nindl. 2009. Effects of exercise training on the matrix metalloprotease response to acute exercise. *European journal of applied physiology*. 106:655-663.

Vella, L., M.K. Caldow, A.E. Larsen, D. Tassoni, P.A. Della Gatta, P. Gran, A.P. Russell, and D. Cameron-Smith. 2012. Resistance exercise increases NF-kappaB activity in human skeletal muscle. *American journal of physiology. Regulatory, integrative and comparative physiology*. 302:R667-673.

Villarreal, L., O. Mendez, C. Salvans, J. Gregori, J. Baselga, and J. Villanueva. 2013. Unconventional secretion is a major contributor of cancer cell line secretomes. *Molecular & cellular proteomics : MCP*. 12:1046-1060.

Wada, M., M. Kosaka, S. Saito, T. Sano, K. Tanaka, and A. Ichihara. 1993. Serum concentration and localization in tumor cells of proteasomes in patients with hematologic malignancy and their pathophysiologic significance. *The Journal of laboratory and clinical medicine*. 121:215-223.

Wang, T.J., M.G. Larson, R.S. Vasan, S. Cheng, E.P. Rhee, E. McCabe, G.D. Lewis, C.S. Fox, P.F. Jacques, C. Fernandez, C.J. O'Donnell, S.A. Carr, V.K. Mootha, J.C. Florez, A. Souza, O. Melander, C.B. Clish, and R.E. Gerszten. 2011. Metabolite profiles and the risk of developing diabetes. *Nature medicine*. 17:448-453.

Wang, X., Z. Hu, J. Hu, J. Du, and W.E. Mitch. 2006. Insulin resistance accelerates muscle protein degradation: Activation of the ubiquitin-proteasome pathway by defects in muscle cell signaling. *Endocrinology*. 147:4160-4168.

Wei, M., L.W. Gibbons, J.B. Kampert, M.Z. Nichaman, and S.N. Blair. 2000. Low cardiorespiratory fitness and physical inactivity as predictors of mortality in men with type 2 diabetes. *Annals of internal medicine*. 132:605-611.

Weigert, C., K. Brodbeck, H. Staiger, C. Kausch, F. Machicao, H.U. Haring, and E.D. Schleicher. 2004. Palmitate, but not unsaturated fatty acids, induces the expression of interleukin-6 in human myotubes through proteasome-dependent activation of nuclear factor-kappaB. *The Journal of biological chemistry*. 279:23942-23952.

Weigert, C., A.M. Hennige, K. Brodbeck, H.U. Haring, and E.D. Schleicher. 2005. Interleukin-6 acts as insulin sensitizer on glycogen synthesis in human skeletal muscle cells by phosphorylation of Ser473 of Akt. *American journal of physiology. Endocrinology and metabolism*. 289:E251-257.

Weigert, C., R. Lehmann, S. Hartwig, and S. Lehr. 2014. The secretome of the working human skeletal muscle-A promising opportunity to combat the metabolic disaster? *Proteomics. Clinical applications*. 8:5-18.

Wensaas, A.J., A.C. Rustan, M. Just, R.K. Berge, C.A. Drevon, and M. Gaster. 2009. Fatty acid incubation of myotubes from humans with type 2 diabetes leads to enhanced release of beta-oxidation products because of impaired fatty acid oxidation: effects of tetradecylthioacetic acid and eicosapentaenoic acid. *Diabetes*. 58:527-535.

Whitham, M., M.H. Chan, M. Pal, V.B. Matthews, O. Prelovsek, S. Lunke, A. El-Osta, H. Broenneke, J. Alber, J.C. Bruning, F.T. Wunderlich, G.I. Lancaster, and M.A. Febbraio. 2012. Contraction-induced IL-6 gene transcription in skeletal muscle is regulated by c-jun terminal kinase/Activator protein -1. *The Journal of biological chemistry*.

WHO. 1999. Definition, diagnosis and classification of diabetes mellitus and its complications. Part 1: Diagnosis and classification of diabetes mellitus. World Health Organization, Geneva.

WHO. 2011. Global status report on noncommunicable diseases 2010. World Health Organization, Geneva.

WHO. 2013. Factsheet No 312. World Health Organization, Geneva.

Widegren, U., X.J. Jiang, A. Krook, A.V. Chibalin, M. Bjornholm, M. Tally, R.A. Roth, J. Henriksson, H. Wallberg-henriksson, and J.R. Zierath. 1998. Divergent effects of exercise on metabolic and mitogenic signaling pathways in human skeletal muscle. *FASEB journal : official publication of the Federation of American Societies for Experimental Biology*. 12:1379-1389.

Widegren, U., J.W. Ryder, and J.R. Zierath. 2001. Mitogen-activated protein kinase signal transduction in skeletal muscle: effects of exercise and muscle contraction. *Acta physiologica Scandinavica*. 172:227-238.

Widegren, U., C. Wretman, A. Lionikas, G. Hedin, and J. Henriksson. 2000. Influence of exercise intensity on ERK/MAP kinase signalling in human skeletal muscle. *Pflugers Archiv : European journal of physiology*. 441:317-322.

Wohlbrand, L., K. Trautwein, and R. Rabus. 2013. Proteomic tools for environmental microbiology--a roadmap from sample preparation to protein identification and quantification. *Proteomics*. 13:2700-2730.

Wojtaszewski, J.F., P. Nielsen, B.F. Hansen, E.A. Richter, and B. Kiens. 2000. Isoform-specific and exercise intensity-dependent activation of 5'-AMP-activated protein kinase in human skeletal muscle. *The Journal of physiology*. 528 Pt 1:221-226.

Wolf, M., S. Chen, X. Zhao, M. Scheler, M. Irmler, H. Staiger, J. Beckers, M.H. de Angelis, A. Fritsche, H.U. Haring, E.D. Schleicher, G. Xu, R. Lehmann, and C. Weigert. 2013. Production and release of acylcarnitines by primary myotubes reflect the differences in fasting fat oxidation of the donors. *The Journal of clinical endocrinology and metabolism*. 98:E1137-1142.

Workeneh, B., and M. Bajaj. 2013. The regulation of muscle protein turnover in diabetes. *The international journal of biochemistry & cell biology*. 45:2239-2244.

Wrzodek, C., J. Eichner, and A. Zell. 2012. Pathway-based visualization of cross-platform microarray datasets. *Bioinformatics*. 28:3021-3026.

Wu, Z., P. Puigserver, U. Andersson, C. Zhang, G. Adelmant, V. Mootha, A. Troy, S. Cinti, B. Lowell, R.C. Scarpulla, and B.M. Spiegelman. 1999. Mechanisms controlling mitochondrial biogenesis and respiration through the thermogenic coactivator PGC-1. *Cell*. 98:115-124.

Yamauchi, M., and M. Sricholpech. 2012. Lysine post-translational modifications of collagen. *Essays in biochemistry*. 52:113-133.

Yoon, J.H., K. Yea, J. Kim, Y.S. Choi, S. Park, H. Lee, C.S. Lee, P.G. Suh, and S.H. Ryu. 2009. Comparative proteomic analysis of the insulin-induced L6 myotube secretome. *Proteomics*. 9:51-60.

Yu, M., E. Blomstrand, A.V. Chibalin, A. Krook, and J.R. Zierath. 2001. Marathon running increases ERK1/2 and p38 MAP kinase signalling to downstream targets in human skeletal muscle. *The Journal of physiology*. 536:273-282.

Zabel, C., and J. Klose. 2009. High-resolution large-gel 2DE. *Methods Mol Biol*. 519:311-338.

Zhang, C., Y. Li, Y. Wu, L. Wang, X. Wang, and J. Du. 2013. Interleukin-6/signal transducer and activator of transcription 3 (STAT3) pathway is essential for macrophage infiltration and myoblast proliferation during muscle regeneration. *The Journal of biological chemistry*. 288:1489-1499.

Zhao, M., L. New, V.V. Kravchenko, Y. Kato, H. Gram, F. di Padova, E.N. Olson, R.J. Ulevitch, and J. Han. 1999. Regulation of the MEF2 family of transcription factors by p38. *Molecular and cellular biology*. 19:21-30.

Zurlo, F., K. Larson, C. Bogardus, and E. Ravussin. 1990. Skeletal muscle metabolism is a major determinant of resting energy expenditure. *The Journal of clinical investigation*. 86:1423-1427.

7. Figures

8. Tables

Acknowledgements

Ich danke allen Leuten, die zur Fertigstellung dieser Doktorarbeit beigetragen haben.

Ich möchte mich speziell bei Prof. Martin Hrabé de Angelis für das entgegengebrachte Vertrauen und die Unterstützung bedanken. Prof. Hans-Ulrich Häring möchte ich für die motivierenden Worte, das entgegengebrachte Interesse und die Möglichkeit der Promotion in seiner Arbeitsgruppe bedanken.

Besonders möchte ich mich auch bei meiner direkten Betreuerin Prof. Cora Weigert für die tolle Leitung und großartige Unterstützung bedanken, so wie bei ihrem Tübinger Kollegen Prof. Harald Staiger. Beide haben mit ihren Vorschlägen, Anmerkungen und der Motivase maßgeblich zu dem Erfolg dieser Arbeit beigetragen und für uns „Münchner" viele Stunden im Auto verbracht. Die Diskussionen mit ihnen waren immer inspirierend und lehrreich.

Außerdem möchte ich mich bei Prof. Philippe Schmitt-Kopplin bedanken, der durch seine konstruktive Kritik ein wesentlichen Beitrag während meiner Thesis Committee Meetings geleistet hat.

Vielen Dank auch an Prof. Martin Klingenspor, der sich bereit erklärt hat den Vorsitz der Prüfungskommission zu übernehmen und an Prof. Hans Hauner, der als 2. Prüfer involviert ist.

Ich möchte mich bei meinen ehemaligen Kollegen Christina und Anja bedanken, zusammen haben wir der Gruppe Translationale Diabetologie Leben eingehaucht. Ich habe viel durch euch gelernt, es war eine schöne Zeit!

Ein großen Dank auch an meine jetzigen Kollegen, Lucia und Bernd, die mich während der zweiten Hälfte der Doktorarbeit immer toll unterstützt haben.

Herzlile Dank au an moi Tübingr Kollegen, die mir mid Rad und Tad zur Seide schdanden. Speziell möchte ich mich hier bei Heike für ihre großartige technische Assistenz bedanken, bei Chrisi, der mir die Zeit auf diversen Kongressen versüßt hat und immer ein offenes Ohr hatte, wenn mal gerade was nicht so funktioniert hat und bei Miriam und Sabine, für hilfreiche wissenschaftliche Diskussionen.

Ohne die Zusammenarbeit mit diversen Kooperationspartnern aus München, Kopenhagen, Dalian und Düsseldorf wäre diese Arbeit nicht annähernd so vielseitig und spannend geworden. Besonders möchte ich mich hier bei Sonja und Stefan aus Düsseldorf bedanken, mit denen der Spaß neben der Wissenschaft nie zu kurz kam.

An dieser Stelle möchte ich auch dem Deutschen Zentrum für Diabetesforschung (DZD) danken, ohne deren finanzielle Unterstützung wären diverse Konferenzen,

Forschungsaufenthalte bei Kooperationspartnern und die damit verbundenen Projekte nur teilweise möglich gewesen.

Vielen Dank auch an die jetzigen und ehemaligen Kollegen des IEGs, die mich während der Anfertigung der Arbeit begleitet haben, immer für eine tolle Arbeitsatmosphäre gesorgt haben und mir bei experimentellen Problemen immer zur Hilfe eilten. Besonderer Dank gilt hier Martin I., Andras, Christian, Davide, Daniel, Nina und Micha.

Nicht zuletzt möchte ich meinen Freunden, meiner Familie, aber besonders meinen Eltern, Uli und Stephan, danken, die immer an mich geglaubt haben, mich unterstützt haben und jeder Zeit für mich da waren.

Abschließend möchte ich mich bei Lukas bedanken: Danke für deine unermüdliche Unterstützung, die helfenden Worte, das Korrekturlesen, die Verbesserungs-vorschläge und Ideen und dafür, dass du mich immer wieder aufgebaut hast, wenn es gerade mal nicht so gut lief. Schön, dass es dich gibt!

VIELEN DANK!